Bulletin of Romanian Chemical Engineering Society

1 2020

ISSN 2360-4697

Edited by SICR and Matrix Rom

The journal is included in the international database
INDEX COPERNICUS INTERNATIONAL

ISSN 2360-4697

Bulletin of Romanian Chemical Engineering Society

Volume 7 2020 Number 1

Contents

TRANSPORT PHENOMENA CHEMICAL ENGINEERING PARADIGM IN PROFESSOR LIVIU LITERAT ACTIVITY

Alexandru OZUNU*,

Babeș-Bolyai University, Faculty of Environmental Science and Engineering, Cluj-Napoca

Abstract. *The implementation of paradigm of unit operations and of paradigm of transfer phenomena to the chemical engineering education from Cluj was largely due to professor Liviu Literat. In this paper we try to show some of the aspects related to these paradigms to which the teacher dedicated work and love*.

Key words: unit operations paradigm, transport phenomena paradigm, chemical engineering, history, theoretical contributions

1. Introduction

The emergence and development of chemical engineering paradigms worldwide [1-3] has led to the restructuring of the system for organizing chemical engineering education in Romania, especially in the university centers of Bucharest, Cluj, Iasi and Timisoara, where this system of professional training dates back to 1938**.** In Cluj-Napoca, modern chemical engineering in higher education began at the Polytechnic Institute in the academic year 1971/72 for the establishment of a Faculty of Industrial Chemistry with specializations in Inorganic Substances Technology and Oxides Materials Technology. The role of Professor Liviu Literat is major, falling within both paradigms of chemical engineering – paradigm of the Unitary Operations, developed in Romania by Acad. Prof. Emilian Bratu, and the paradigm of Transfer Phenomena, which is being developed in the reference university centers in the country - Bucharest, Iași, Timișoara and Cluj. The main role of these component paradigms of Chemical Engineering in Romania was its integration in the country's economy. Cluj is thus distinguished by the need to develop the zonal chemical industry in the mentioned fields at the inception of chemical engineering. Thus it can be shown that Professor Liviu Literat, within these paradigms, through his education as an engineer and chemist, developed the concept of interdisciplinarity and transdisciplinarity in science and engineering through what will become the existing faculty in 2021 as the Faculty of Chemistry and Chemical Engineering.

*Corresponding author:alexandru.ozunu@ubbcluj.ro

The main achievements obtained by professor Literat are in the field of university book, treatises, monographs, studies of the history of sciences and education of which one can mention: General chemistry (1966, 1970, 1975); Transfer phenomena and equipment in chemical engineering- Transport Processes (1985); Operations and equipment in the Oxide Materials Industry (1994, 1995), etc., over 130 scientific articles published in specialized journals in the country and abroad, research contracts, grants, patents for inventions and innovations.

2. Short CV Professor L. Literat

Prof. Liviu Literat, at 85 Years, in a conference in senate of UBB Cluj

Liviu Literat, born on September 9, 1928, Vinţu de Jos, Alba County. Education: high school in Brasov, Fagaras and Cluj; higher education: at the Victor Babeş University of Cluj, Faculty of Chemistry (1947-1951), degree in physical chemistry (1951) and at the Bucharest Polytechnic Institute, Faculty of Industrial Chemistry; chemical engineer specializing in Inorganic Substances Technology (1963). Doctor of Chemistry in 1966 with the thesis *Physico-chemical study on non-stoichiometric reducing alumina.* Didactic and scientific activity at the Victor Babeş University of Cluj, becomes as preparator (1950), assistant (1951-1953), lecturer (1960), associate professor (1966) and is completed as professor (1972-1974) at the Polytechnic Institute of Cluj. The carrier continues as Professor (1974) and head of departments Organic Chemistry and Technology (1977-1985), Chemical Engineering (1990-1993), Chemical Engineering and Oxide Materials Science (1993-1995), at Babeş-Bolyai University, Faculty of Chemistry and Chemical Engineering. Professor Emeritus Consultant (since 1995).

3. Characteristics of Transport Phenomena Paradigm in vision of professor Liviu Literat

As young, professor Literat observed that for chemical engineers education the unit operations paradigm successfully brought: a) a core of chemical engineering curriculum, based on unit operations, stoichiometry and thermodynamics, b) an useful principle to organize knowledge, c) an inspiration for research to fill in the gaps in knowledge. It observed that this paradigm was offered to graduates chemical engineers a good toolbox to solve processing problems in oil distillation, petrochemical, fertilizers, new polymers, etc. With all these special findings He enthusiastically adheres to *nothing in chemical engineering without transfer phenomena, without differential equations and without mathematical models*, elements that express the essence of transfer phenomena paradigm in chemical engineering and which was crystallized between 1960 -1970 [4,5].

The activity of Professor Literat is subscribed to the directions of this paradigm as well as to the scientific interdisciplinarity of chemical engineering, expressed through many achievements, among which we mention:

- Scientific activity in the field of physical chemistry, materials science and chemical engineering,
- Fundamental, experimental and applied research in physical chemistry of frontier phenomena (heterogeneous catalysis, sorption, extraction, solid phase reactions),
- Significant contributions to the kinetics of processes with mass variation (theory, modeling, experimental procedures and installations, computational programs),
- Applications to the study of interface processes and nanosystems (Investigation of porous solids by kinetic measurements of sorption (1973),
- Automatic device for registration and exploring program of adsorption isotherms (2000),
- Computerized recording of the settling curves,
- Application to the classification of the powdery systems (2001).

We also show that he synthesized and studied a class of new refractory oxide compounds (alumina) with deviation from stoichiometry (absolute priority), bringing unique information to the theory and concept of stoichiometry for nanometric oxide systems. For theory of transport and property transfer phenomena he established 12 new similarity criteria and criterion equations for electric charge carriers by molecular and convective mechanism, stationary and transient. Contributions to the technique of chemical, punctual, qualitative and

quantitative analysis (with electronic microsound) of microphases in composite systems are newer or older professor participation to the explosive field of composite development.

4. Transport Phenomena Paradigm in chemical engineering courses (didactic activities) of Professor Liviu Literat

According the spirit of the transfer phenomena paradigm to teaching and to organization teaching structure of chemical engineering in Cluj Napoca, the Professor activities [6-8] can be presented as follows:
Important Chemical Engineering Development Data at Babeș-Bolyai University

- I. The first stage (1971-1974) belongs to Cluj Polytechnic Institute
- II. The second stage (from 1974 - present) continues in the Babeş- Bolyai University, where several periods of administrative and organizational evolution are distinguished.
- 1977 - The head of the Department of Organic Chemistry and Technology (DOCT) is appointed Prof. Liviu Literat. From his position, he acts for the establishment of the Organic Substances Technology (TSO).
- 1990 - The Department of Chemical Engineering (Chief of the Department, Prof. Liviu Literat).
- 1990 - The Specialization Section (Engineers) of Oxidation Materials Science and Engineering (SIMO) (initiator Prof. L. Literat)
- 1991 - 20th Anniversary of Chemical Engineering Education in Cluj-Napoca (Jubilee Symposium, September 19-22, 1991).
- 1992 - The Faculty of Chemistry and Chemical Engineering was established.
- 1992 - The Department of Chemical Engineering also includes the Science and Engineering of Oxide Materials profile and is named the Department of Chemical Engineering and Oxide Materials Science (Chief of the department: Prof. Liviu Literat).
- 1995 - The Department of Chemical Engineering and Oxide Material Science initiates and becomes a founding member of the Chemical Engineering Society of Romania (SIChR), Branch President Prof. Liviu Literat and Vice-President of the National Leadership Council .
- 1995 - Professor Liviu Literat retires and becomes a consultant professor.
- 1997 - Official participation in the 60th anniversary of chemical engineering at the “Gh. Asachi” Technical University, Iasi, 23.10.1997.
- 2001 - The National Symposium “30 Years of Chemical Engineering in Cluj-Napoca”, organized by the Department of Chemical Engineering and Oxidation Science, takes place (6-9 September).

- 2004 – Prof. Liviu Literat is elected honorary member of the Academy of Technical Sciences of Romania (ASTR), Chemical Engineering Section.
- 2006 - National Chemical Engineering Symposium dedicated to the 35th anniversary of the Chemical Engineering education in Cluj-Napoca, (July 3, Cluj-Napoca).

5. Some photos with prof. Liviu Literat and books

Prof. Liviu Literat at his 90th birthday celebration together with Acad. Ioan Aurel Pop, the Rector of BBU and Pr.Prof. Ioan Chirila, the Senat BBU President, in Aula Magna

Prof. Liviu Literat surrounded by a group of friends at a meeting with the National Society of Environmental Science and Engineering in Bistrița

Throughout this short history, I have had the privilege of mixing my existence with the life of this institution from the beginning until today. I saw it grow and assert itself. I wish it a life without death and I urge the younger colleagues to watch over her future which depends on their work, will, wisdom and struggles." (Liviu Literat, The History of Chemical Engineering Education at the celebration of 20th year in Cluj-Napoca, 1991)

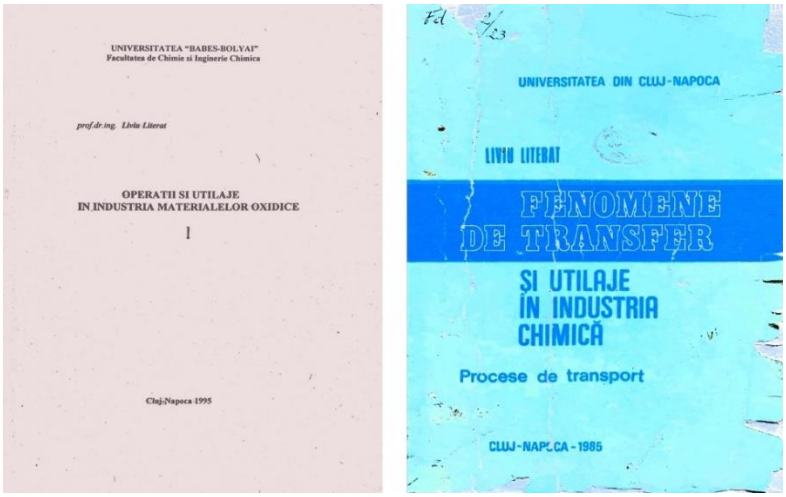

Books for the students by Professor Literat

6. Conclusions

The paper presents data specific to the activity of Professor Liviu Literat regarding the development of chemical engineering at the universities of Cluj Napoca. Particular attention is paid to the implementation in this development of transfer phenomena paradigm of chemical engineering. In fact, the paper is a tribute to the professor and his long activity in the field of chemical engineering.

REFERENCES

[1] Reynolds T. S., Forman J. C., Resen, L., (Eds), *75 Years of Progress: A History of the American Institute of Chemical Engineers 1908-1983*, American Institute of Chemical Engineers (1983).
[2] Scriven E.L., *On the Emergence and Evolution of Chemical Engineering*, Advances in Chemical Engineering, 16,3, 207-2017, 1991.
[3] Woinaroschi A., *The Paradigms of Chemical Engineering*, AGIR Bulletin, 1, 9-16, 2015.
[4] Byron R. Bird, Waren E. Stewart, Edwin N. Lightfoot, *Transport Phenomena*, Wiley,1960.
[5] Neal Russell Amundson, *Mathematical Methods in Chemical Engineering*, Prentice Hall, 1966.
[6] Literat l., *45 Years of Chemical Engineering in the University City of Cluj-Napoca 1971-2016: Landmarks on the Establishment, Development and Affirmation of Chemical Engineering*

Education in the Universitary City of Cluj-Napoca, Studia UBB Chemia, LXII, 4, Tom II, 7-18, 2017.

[7] Literat L., *From the History of Chemical Engineering Education in Cluj-Napoca*, in Monographic Breviary, 1971-1991, Anniversary Symposium '20 Years of Chemical Engineering Education in the University City of Cluj-Napoca', 19 – 22 September 1991, Babeş-Bolyai University, Faculty of Chemistry and Industrial Chemistry, Chair of Chemical Engineering, 1991, p.24-29. Editor L. Literat (in Romanian language).

[8] A. Ozunu, *Words in Honor of Prof. Emerit Dr.Ing Liviu Literat at 92 Years*, Presentation at SICHEM 2020, 9/17/20, Polytechnic University of Bucharest, Romania.

CHEMICAL ENGINEERING PARADIGMS IN PROFESSOR EMIL DANCIU ACTIVITY

Tiberiu Dinu DANCIU*

University ”Politehnica” of Bucharest, Chemical and Biochemical Engineering Department, Romania

Abstract. *The implementation of unit operations, transfer phenomena, and furthermore, transport phenomena analogy paradigms to the chemical engineering education from UPB is among major contributions of the professor Emil Danciu. This paper briefly remembers few aspects of the continuously teaching activity of the beloved and respected professor*.

Keywords: transport phenomena analogy paradigm, unit operations paradigm, chemical engineering history, teaching engineering

1. Introduction

The emergence and development of chemical engineering paradigms worldwide [1-2] had led to the restructuring of the system for organizing chemical engineering education in Romania, especially in the university centres of Bucharest, Cluj, Iași, and Timișoara, where this system of professional training dates back to 1938. The paradigm of the Unit Operations, first developed in Romania by Acad. Prof. Emilian Bratu, and the paradigm of Transfer Phenomena, which is being developed later in the same reference university centres in the country, were only first major steps. Next levels in developing chemical engineering as a science were done also by Prof. Bratu, together with his first line of disciples (i.e., his Ph.D. students, covering all major domains of interest in chemical engineering: R. Mihail, E. Ruckenstein, I. Teoreanu, O. Floarea, R. Tudose, Z. Gropșian, O. Smigelschi, D. Suciu, E. Danciu). These steps were Chemical Reaction Engineering, Transfer Intensification, Advanced (and later Computerized) Calculus in Chemical Engineering, Transport Phenomena Analogy, Integration of Processes. After Prof. Bratu retreat, his above disciples, being now professors of Chemical Engineering, continued to teach, research, discover, and develop the domain – new directions, new publications, new books, and first of all, a lot of new generations of students who, at their turn, evolve to academic positions – in Bucharest, or in Romania, or worldwide. This article contains a shortly description of the activity of Prof. Emil Danciu, one of these first line teachers.

*Corresponding author: tiberiu.danciu@upb.ro

2. Short CV

Emil Danciu is born on February 23, 1929, Alba Iulia, Alba County. He is a Romanian engineer. Education: first levels in Alba Iulia, baccalaureate at former "Mihai Viteazul" high school, higher education at the University Politehnica of Bucharest, Faculty of Industrial Chemistry (1948-1953), degree as chemical engineer specializing Macromolecular Technology (1953). Ph.D. in the field named then "Processes and Apparatus" (say, Chemical Engineering), 1966, with the thesis entitled "Liquid Vapor Equilibrium. Correlation of Experimental Data and their Use in Conducting Chemical Processes", under the supervision of Prof. Emilian Bratu.

He has carried out a rich activity of fundamental and applied research, both at various institutes or research centers and within the Chemical and Biochemical Engineering (CBE) Department, materialized in over 50 contracts and over 50 published papers, countless scientific papers and 10 patents.

The most remarkable aspect of his activity, however, is teaching: he spent over 55 years in school, going through all stages of his university career (preparator since 1951, assistant since 1953, head of works since 1970, associate professor since 1973, professor since 1980, Ph.D. supervisor since 1993). Author of 7 textbooks, leader of 4 doctoral theses, he was also the head of CBE department for over 10 years, but also of the Chemical Engineering Society of Romania, since its establishment in 1995, being its first president.

Fig.1. Prof. Emil Danciu at his 85th anniversary

Diploma
de merit
759

se conferă Tov. Danciu N. Emil
absolvent al Facultății de Chimie industrială
Secția Chimie organică dela Institutul
Politehnic din București
care, prin hotărîrea Comisiei pentru examenul de Stat
din sesiunea februarie anul 1953,
a fost declarat inginer
în specialitatea ~~Macromoleculară~~

București 8 iunie 1954
(Locul și data)

PREȘEDINTELE
Comisiei pentru examenul de Stat
RECTOR,
SECRETAR,
Nr. 149

Fig.2. His diploma of merit

3. Contribution to Transport Phenomena Analogy Paradigm

Prof. Emil Danciu was the first in Romania who insert this chapter in his lectures, held at sophomore level, at the former Tools and Chemical Process Engineering Faculty, since 1978 (called then Technical Thermodynamics). Later in 1985, the first Romanian printed university course, mentioning and explaining the analogy, called Chemical Engineering Basics, was published in UPB, based on then latest prestigious books and monographies [3-11].

Prof. Danciu most beloved field in chemical engineering was undoubtedly heat transfer and heat exchangers (especially those with fins) – he solved countless contract problems for such devices in Romania, Syria, Iraq, Jordan, Turkey.

Also, prof. Danciu (already at his retreat) has major contributions in developing, after some reorganizations in 2005, the new directions of study in UPB, Chemical Processes Engineering and Biochemical Processes Engineering (merged later in the present bachelor's degree program of Engineering and Informatics in Chemical and Biochemical Processes, held at Faculty of Applied Chemistry and Materials' Science).

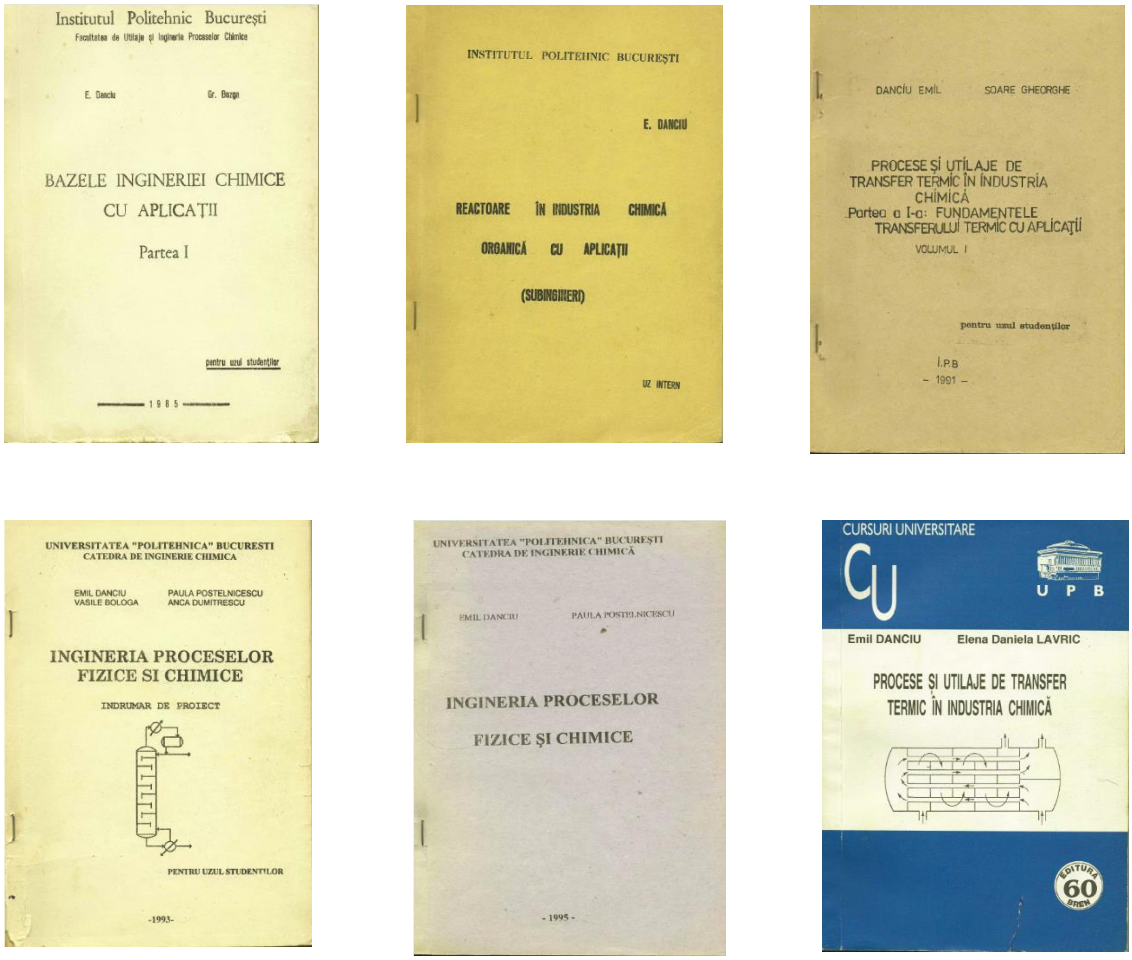

Fig. 3. Textbooks for student use published by Prof. Emil Danciu

4. Analogy Paradigm in all activities of Prof. Danciu

According to the spirit of the transport phenomena analogy paradigm, the Professor researching and teaching activities could be summarized as follows:

- starting with 1951, he worked as a preparator and then as a scientific referent, within the Institute of Physics of the Romanian Academy, the Physical Chemistry section, the Electrophoresis laboratory. Here he carried out research in the field of colloids, under the leadership of Acad. Ilie Murgulescu, until 1954;
- after graduating in 1952, he worked as a preparator and then as an assistant in the Department of Procedures and Apparatus, under the leadership of Acad. Emilian Bratu, who was his mentor and Ph.D. supervisor;
- in parallel, under the leadership of Acad. Costin D. Nenițescu, was employed at the Research Center for Organic Chemistry of the Romanian Academy, between 1959 and 1967, reaching the position of head of sector. Unfortunately, certain medical problems put an end to this activity, and after 1967, the year in which he defended his Ph.D. thesis, he worked exclusively within;
- the collaboration with these research and education giants has materialized in 3 patents and 8 publications, all in the fields of early development of researcher Emil Danciu: polymers, copolymers, adhesives, etc., at the border between organic and macromolecular chemistry;
- his research activity took an important turn in 1967: although he always remained faithful to organic and macromolecular chemistry (another 7 patents, but also numerous works), his main direction of action became chemical engineering, especially liquid-vapor equilibria (over 20 publications);
- he brought all the experimental skill, intuition, and patience learned in organic chemistry research, which he harmoniously combined with the physical-mathematical models he had mastered since collaborating with the masters of physical chemistry;
- within the Department of Chemical Engineering, he formed and led a team of Technical Thermodynamics; textbooks for students appear successively (written as a single author or in collaboration, as shown above), with important contributions especially in the field of analogy of transfer phenomena;
- perhaps his most important activity was mentoring – many students crossed the threshold of his modest office in room A212 – for all he had words of support, valuable advice and, above all, solutions to their problems. Today, leading personalities in various fields of scientific, public, or business life, all remember the kindness of Prof. Danciu.

*Corresponding author: tiberiu.danciu@upb.ro

Some photos will sustain precisely the last above point – with many opportunities, Prof. Danciu was in the middle of his former students, for graduation festivities or anniversary reunions:

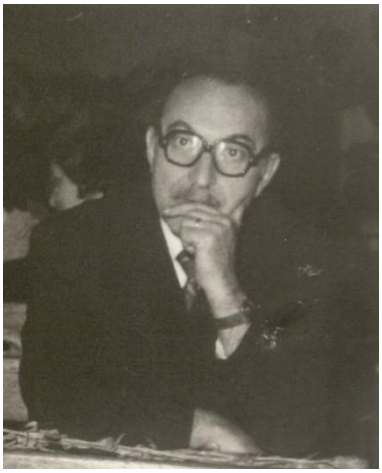

Fig.4. Prof. Danciu in 1984

Fig. 5. Prof. Danciu in 2013

Fig. 6. Prof. Danciu in 2019, after his 90th anniversary, with some former students from the Tools and Chemical Processes Engineering (UIPCh) faculty, at their 35 years graduation reunion

REFERENCES

[1] Woinaroschy A., *The Paradigms of Chemical Engineering*, AGIR Bulletin, 1, 9-16, 2015.
[2] Furter E.D. (ed), *History of Chemical Engineering*, in Advances in Chemistry, vol. 190, ACS, 1980.
[3] Henley E.I., Rosen E.M., *Material and Energy Balance Computations*, Wiley, 1969.
[4] Bird R.B., Stewart W.E., Lightfoot E.N., *Transport Phenomena*, Wiley,1960.
[5] Amundson N.R., *Mathematical Methods in Chemical Engineering*, Prentice Hall, 1966.

[6] Smith J.M., van Ness H.C., *Introduction to Chemical Engineering Thermodynamics*, McGraw-Hill, 1975.
[7] Reid C.R., Prausnitz M.I., Sherwood K.T., *The Properties of Gases and Liquids*, McGraw-Hill, 1977.
[8] Myers A.L., Seider W.D., *Introduction to Chemical Engineering and Computer Calculations*, Prentice Hall, 1976.
[9] Himmelblau D.M., Bischoff K., *Process Analysis and Simulation. Deterministic Systems*, Wiley, 1968.
[10] Fulford G.T., Pei D.C.T., *A Unified Approach to the Study of Transfer Processes*, IEC, **61**, 47 (1969).
[11] Bennett C.O., Myers J.E., *Momentum, Heat, and Mass Transfer*, McGraw-Hill, 1974.

TRANSPORT PHENOMENA CHEMICAL ENGINEERING PARADIGM IN PROFESSOR OCTAVIAN FLOAREA ACTIVITY

Tanase DOBRE*,

Politehnica University of Bucharest, Faculty Applied Chemistry and Materials Science, Chemical and Biochemical Engineering Department, Bucharest

Abstract. *The implementation of paradigm of unit operations and of paradigm of transfer phenomena to the chemical engineering education from Bucharest was largely due to some professors*[1]*, among which Professor Octavian Floarea has a leading place. This paper try to show some aspects related to these paradigms to which the professor he showed them dedication, work and love.*

Key words: unit operations paradigm, transport phenomena paradigm, chemical engineering, history, theoretical contributions

1. Introduction

In technical or humanistic education, the formulation of one didactic study program is in accordance with the specific scientific evolution respect to the concrete reporting field. And this evolution is materialized evolutionarily by paradigms [2-3], which for a given case represent a framework containing all the commonly accepted views about a subject, conventions about what direction research should take and how it should be performed. The issues and evolution of chemical engineering paradigms worldwide [4-6] has led to the restructuring of the system for organizing chemical engineering education in Romania, firstly in Politehnica University of Bucharest, where this system of professional training dates back to 1938 [7], and form here to Cluj, Iasi and Timisoara. With reference to implementation of Unit Operations paradigm, in the chemical engineering education in Politehnica University od Bucharest (and from here in all other universities of our country), it is unanimously accepted that it was done under the influence of professors Costin Nenitescu, Emilian Bratu and Serban Solacolu [7]. The curricula structure for departments of Inorganic Substances Technology (TSA), Organic Substances Technology (TSO), Silicates and Oxide Compounds Technology (TSCO), Carbochemistry (CCh) and then, after 1966, Macromolecular Compounds Technology (TCM), resumed schematically in Fig. 1 [8], is in fact an agreement, at the time of 1950-1965 years, of the three mentioned professors.

Corresponding author: tanase.dobre@upb.ro

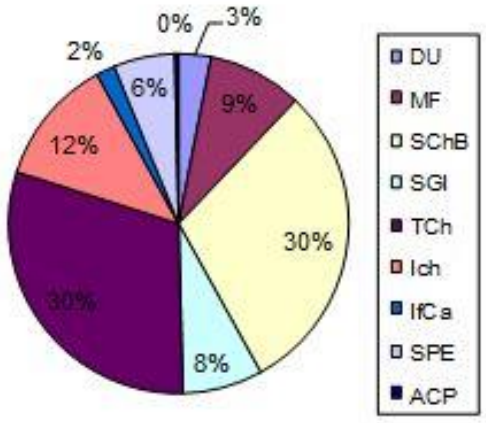

DU - Foreign Language, Psychology, Sports; MF: Mathematics, Physics; SChB: General Chemistry, Inorganic Chemistry, Analytical Chemistry, Physical Chemistry, Organic Chemistry, Reactions Mechanisms, Specific Laboratories; SGI: Mechanics and resistance, Machine parts, Electrical engineering and Electronics, Automation; TCh: General Chemical Technology, Electrochemistry and Corrosion, Organic Chemical Technology, Organic Dyes, Drug Technology, Organic Intermediates; ICh: Operations and processes for chemical industry, Chemical reactors, Design applications; SPE: Philosophy, Scientific Socialism, Political Economy, Chemical enteprises management; IfCa: Designs computation , ACP: Production design and research

Fig.1 Participation of discipline groups in the training curriculum of the chemical engineer at the Polytechnic University of Bucharest (1964,case of TSO specialization)

The new current given by the paradigm of transfer phenomena in chemical engineering education finds, immediately after 1960, in the Faculty of Industrial Chemistry from the Polytechnic University of Bucharest, many followers, young heads of works and doctoral students. At that time, inside of actual department of Chemical and Biochemical Engineering (former Department of Procedures and Apparatus for Industrial Chemistry), under the guidance of Professor Emilian Bratu, they became extremely active, along with Raul Mihail, Floarea Octavian, Smigelschi Octavian, Ely Ruckenstein, Jinescu Gheorghita and Gheorghe Iordache (Fig. 2)

Fig.2 Some of the members of the former Department of Procedures and Apparatus with Prof. Emilian Bratu on May 1, 1963 (from right to left: Ely Ruckenstein, Smighelschi Octavian, Floarea Octavian, Prof. Emilian Bratu, Nastase Gheorghita, Iordache Gheorghe).

At Faculty of Industrial Chemistry from UPB the strong restructuring of chemical engineers curricula, related to 1972- 1976 years, when the share of Chemical Engineering subjects increased from 12% (see Fig. 1) up to 25%,was the direct influence of the paradigm of transport phenomena. This restructuring had Professor Octavian Floarea, as faculty dean, in the leader role. Now the concept of unit operations was extended or enhanced through this increased attention paid to transport phenomena. Now the knowledge in the branch of chemical reactors becomes basic scientific part of chemical engineering and process modelling and process optimisation begin to obtain important role in engineering training for process design and process operation. The current of this restructuring also changed the title of the faculty which becomes the Faculty of Chemical Engineering. He quickly arrived in Iasi, Cluj and Timisoara, university centres where we had specializations in chemical engineers training.
It is unanimously known that the requirements of the Romanian chemical industry determined the appearance, in UPB, in 1978, of Equipment and Chemical Process Engineering Faculty (UIPCh in Romanian abbreviation), for which Professor Floarea, together with all members of the Chemical Engineering Department (former Procedures and Apparatus in the Chemical Industry Department), served in the first line. He was the first dean of this faculty (1978-1983) and we can say that he contributed decisively in defining the specialization of chemical engineer with extensive mechanical knowledge. This specialization was supported by a curriculum extremely rich in chemical engineering (Chemical Engineering Fundaments, Momentum Transfer, Heat Transfer, Mass Transfer, Chemical Reactors, Biochemical Reactors, Processes Optimization, Processes Modelling, Experiences Programming, Computers in Chemical Engineering) and mechanical engineering (Mechanics Fundaments, Materials Resistance, Design and Construction of Chemical Equipment, Devices Installation in Chemical Factories). This didactic curriculum is entirely found in its inside perceptions on transfer phenomena paradigm of chemical engineering.

2. Short CV Professor O. Floarea

Floarea Octavian was born in14.06.1929, Gradini, Olt district. After graduating from Ioniţă Asan High School in Caracal, he attended the courses of the Polytechnic Institute in Bucharest, obtaining in 1955, with a merit diploma the title of engineer in the specialty of Organic Industries. In 1963 he defended his doctoral thesis on hydrodynamics and mass transfer in absorption columns.

He carried out a rich didactic activity within the Polytechnic Institute of Bucharest (now Politehnica University of Bucharest) (assistant (1958), head of works (1964), associate professor (1967), respectively professor (1974)) teaching courses of Operations and Equipment in Chemical Engineering, Transfer Phenomena in Chemical Industry, Chemical Engineering, Mass Transfer Operations. Since 1979 he has taught, at the former Faculty of Chemical Process Machinery and Engineering, the course of Mass Transfer Processes, of his own conception and development, which is materialized in the manual Mass Transfer Processes and Specific Equipment (1984), the first of this profile in the country. As dean of the Faculty of Chemical Engineering (1971-1981), head of the Department of Chemical Engineering (1982-1987) and then Secretary of State in the Ministry of Education (1985-1990) he makes a meritorious contribution to the development of chemical engineering education. Achieves outstanding results in scientific research in key areas of chemical engineering (mechanism of transport and property transfer processes, intensification of mass transfer, modeling and simulation of mass transfer processes, heat and impulse, interaction of chemical and physical process kinetics, interfacial phenomena) , which are materialized in over 150 articles, 10 specialized books, 7 patents and countless scientific communications. To these are added important research topics for engineering and chemical industry, which were developed in the 31 doctoral theses conducted in scientific range of Procedures and Apparatus in Chemical Industry and Chemical Process Engineering.

3. Characteristics of Transport Phenomena Paradigm in vision of professor Octavian Floarea

As a young assistant, Octavian Floarea comes to Professor Bratu's team, at Procedures and Apparatus, where he begins to work in the spirit of unit operations, as organizing system in chemical engineering education. We show thus that: i) the first laboratory work he carried out, starting practically from scratch, was the work *Characterization of the drying dynamics of granular materials* (1957), in which he uses the psychrometric method as a solution to determine the momentary moisture loss of solid material; ii) together with his young colleagues (Octavian Smigelschi, Eli Ruckenstein, Ion Teoreanu), the activity carried out at the management of projects and seminars of discipline of *Procedures and Apparatus in Chemical Industry* is quickly noticed; iii) following the opening in UPB (1959) of the cycle of doctoral studies, he becomes a doctoral candidate under the leadership of professor Emilian Bratu, with a topic related to the mass transfer in columns with plates. The arrival of the young assistant to the new current that was opening up in chemical engineering probably began in 1960 when he received a scholarship from the Romanian state to

complete his doctoral thesis at the Institute of Machinery and Equipment for Chemical Industry in Moscow. Get in touch here with the new current in chemical engineering. Here he met for the first time, in the Russian version, the Phenomena Transport book of Bird, Steward and Lightfoot [9]. Also, here he finishes a very good doctoral thesis (*On hydrodynamics and mass transfer in absorption columns with plates*, scientific leader prof. Solomakha P.G) quoted in the famous book Gas Absorption by Ramm V.I (Fig. 3)

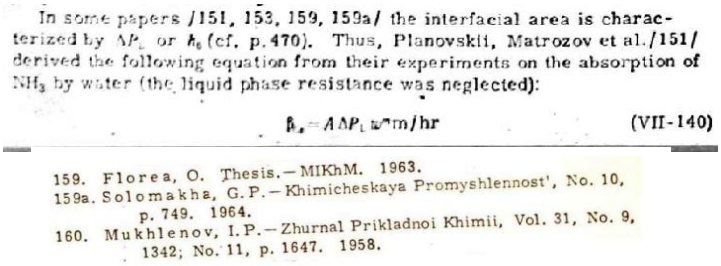

In some papers /151, 153, 159, 159a/ the interfacial area is characterized by ΔP_L or h_L (cf. p. 470). Thus, Planovskii, Matrozov et al./151/ derived the following equation from their experiments on the absorption of NH_3 by water (the liquid phase resistance was neglected):

$$\beta_L = A\Delta P_L \text{ cm/hr} \qquad \text{(VII-140)}$$

159. Florea, O. Thesis.—MIKhM. 1963.
159a. Solomakha, G.P.—Khimicheskaya Promyshlennost', No. 10, p. 749. 1964.
160. Mukhlenov, I.P.—Zhurnal Prikladnoi Khimii, Vol. 31, No. 9, 1342; No. 11, p. 1647. 1958.

Fig. 3 Facsimile from Ramm V.I., *Absoprtion of Gases*, Science, Jerusalem, 1969

Returning to the Department of Chemical Engineering (1964), he joined with Processes Intensification, a new research direction, which was born here. In fact, this research direction from department, at that time, was a consequence of intense access of transfer phenomena paradigm in training of the chemical engineering specialist. Also, during this time, together with his colleague and friend Octavian Smigelschi, he completed, in 1966, the manual *Calculus of Operations and Equipment for Chemical Industry* (Fig. 4). This book was taken as a special teaching material in all university centers where chemical engineers were trained. At the same time, the book was served as a manual for technological design of chemical equipment by all the profile design units in Romania. The structure of the manual and the widespread use of modeling and numerical solving is in the spirit of the paradigm of transfer phenomena that required *nothing in chemical engineering without transfer phenomena, without differential equations and without mathematical models*.

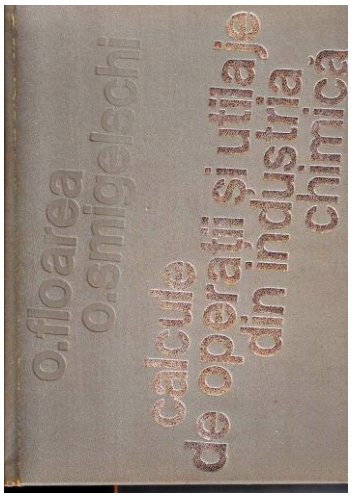

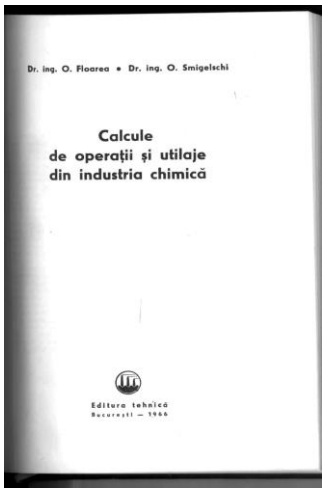

Fig. 4 Cover and dust jacket of the manual *Calculus of Operations and Equipment for Chemical Industry*, Floarea O.,Smigelschi O., Ed. Tehnica, Bucharest 1966.

4. Transport Phenomena Paradigm in chemical engineering courses (didactic activities) of Professor Octavian Floarea

According the spirit of the transfer phenomena paradigm reported to teaching and to organization teaching structure of chemical engineering in Politehnica University of Bucharest, the Professor activities can be presented as follows:

1. He restructured and renewed, from its fundaments, the course of Processes and Apparatus in Chemical Industry, which thus becomes the course Transfer Phenomena and Specific Equipment in Chemical Industry (1974). The major contributions, of special scientific value, brought with this course (1975-1977) are mentioned: I) the presentation of transfer phenomena equations as a case resulting from the laws of conservation, transport and transfer of property; II) the introduction of new contributions for the characterization of the turbulent transport of momentum; III) presentation of the hydrodynamic boundary layer and its characterization equations, as a motivation of the resistance brought by it to interphase transfer of moment, heat and mass; IV) expressing of partial heat and mass transfer coefficient on a scientific basis; V) detailed presentation of the theoretical and experimental methods for determining the partial heat and mass transfer coefficient; VI) the use of mathematical modeling as method for characterizing the specific unit operations on basis of momentum, heat and respectively physical species (mass) transfer. This course, which had a continuous dynamic until 1990, was taken over and used by all those who worked with Professor Floarea and pursued a teaching career in chemical engineering.

Fig.5. Chemical engineering books published in the Chemical Engineering Series

2. With the publication of the book *Intensive Processes in Interphase Transfer Operations*, co-authored with Jinescu Gheorghita, opens in the field of national publications the series Chemical Engineering (Fig. 5), where he keeps a leading place
3. He strongly involved (1983-1987) the Mass Transfer team from the Chemical Engineering department in the capitalization of Calimani sulfur ore (Fig. 6). In this sense, systematic theoretical, experimental and industrial implementation studies were performed on the flow, melting, separation and release of sulfur from autoclaved sulfur concentrate suspensions (2 patents), respectively on recovery by combustion, with air deficit or excess of concentrates and crude sulfur ore (1 patent)

Fig. 6. View from 1985 of sulfur ore caries (sulfur concentration in ore 12-16%) from the Calimani massif.

4. In Mass Transfer Laboratory activity he supported and guided (1980-1990), pioneering studies in directions: I) use of the mobile packed bed to intensify the absorption and rectification operation, II) intensification of the transfer processes by pulsating the contacting phases, III) identification and quantitative characterization of elementary processes at formation, displacement and release of bubbles and droplets under controlled Marangoni effect , IV) modeling of transport processes characteristic of heat pipes, with and without capillary structure, V) promotion of fluidized bed of particles with immobilized activated sludge as solution for anaerobic fermentation of waters with high organic load. In connection with these research directions, some Professor Floarea's PhD candidates manage to complete their doctoral theses (Mihaela Mihai - 1985, Dobre Tanase-1985).
5. He promoted chemical engineering at the Didactic and Pedagogical Publishing House where he published, as first author, *Operations and*

Equipment in the Chemical Industry - Problem Collection (1980) and *Mass Transfer Processes and Specific Equipments* (1984), textbooks in which the basic ideea of transfer phenomena paradigm is strongly present.

6. Immediately after 1990, he supported, by admission to doctoral studies and by completion of these, many candidates with activity in chemical engineering education; among others, he completes the doctoral theses Romulus Dima (UPB, Chemical Engineering - 1991) Lucian Rusnac (UP Timisoara, Chemical Engineering - 1994), Gheorghe Juncu (UPB, Chemical Engineering - 1995), Raluca Isopescu (UPB, Chemical Engineering - 1997), Marta Stroescu (UPB, Chemical Engineering - 1997), Rodica Ceclan (UPB,Chemical Engineering-1997), Anicuta Stoica (UPB, Chemical Engineering -1997), Iosif Nagy (UPB, Chemical Engineering, 1998).

Despite the punctual thematic diversity of the topics approached in the above mentioned works, in the theses whose completion was mentioned as well, as in others not reported, the professor keeps, in the guided activity, the major subjects of chemical engineering that consecrated him: modeling chemical processes and biochemical, enhancement of mass and heat transfer, new advanced separation solutions with or without unconventional methods, interface and neighborhood processes, surface effects and their role in mass and heat transfer

Conclusions

The paper presents data specific to the activity of Professor Floarea Octavian regarding the development of chemical engineering at University “Politehnica” of Bucharest. Particular attention is paid to the implementation in this development of transfer phenomena paradigm of chemical engineering. In fact, the paper is a tribute to the professor and his long activity in the field of chemical engineering.

REFERENCES

[1] Floarea O., *Response to the SICR honorary diploma at the age of 85*, SICHEM 2014, September 16-17, 2014.
[2] Gage N. L., *The paradigm wars and their aftermath: A historical sketch of research on teaching since 1989*. Educational Researcher, 18(7), 4-10, 1989.
[3] Thomson E.M., Brewster A.D., *Faculty Behavior in Low-Paradigm versus High-Paradigm Disciplines*, Research in Higher Education, 8,169-175,1978.
[4] Reynolds T. S., Forman J. C., Resen, L.,(Ed) *75 Years of Progress: A History of the American Institute of Chemical Engineers 1908-1983*, American Institute of Chemical Engineers ,1983.
[5] Scriven E.L., *On the Emergence and Evolution of Chemical Engineering*, Advances in Chemical Engineering, 16,3, 207-2017, 1991
[6] Woinaroschi A., *The Paradigms of Chemical Engineering*, AGIR Bulletin, 1, 9-16, 2015.

[7] Ecaterina Andronescu, *Two hundred years of chemical engineering education at Politehnica University of Bucharest*, Presentation at the opening of SICHEM 2018, September 16-17, 2018.
[8] Dobre T., *Education, Personal Training for Chemical Industries, Research and Development*, 331-365, in Ivanus Gh (Ed), Pages from History of Romanian Industry-Chemical, Petrochemical and Petroleum, Agir House, 2014.
[9] Byron R. Bird, Waren E. Stewart, Edwin N. Lightfoot, *Transport Phenomena*, Wiley,1960.

PROFESSOR RAUL MIHAIL - 100 YEARS SINCE BIRTH

Grigore BOZGA*
University "Politehnica" of Bucharest, Chemical and Biochemical Engineering Department, Romania

Through his overall didactic and scientific work, our former professor Raul Mihail (1920-1985) brought pioneering contributions to the development of the *Chemical Reactors (Chemical Reaction Engineering*) discipline in Romanian higher education and to the creation of a teaching and research school in this field, which placed him into the gold gallery of the Polytechnic Institute (actual Politehnica University) of Bucharest professors. His contributions to the development of chemical engineering education and research in Romania have already been presented in other homage papers, published by his former students and collaborators [1-3]. Now, at a century since his birth, it is an honor and a moral duty for those who knew him, to evoke again his work and personality, a model for the younger generations.

In this short paper, it will be brought to attention an episode in the evolution of chemical engineering education in Romania, one that took place in the period 1955-1960, during which the foundations were laid for the discipline Chemical Reactors, in the currently existing structure, an episode in which professor Mihail played a key role.

Prior to 1960, in Romanian faculties of Industrial Chemistry (existing within the Polytechnic Institutes of Bucharest, Timișoara and Iași), the elements of chemical reactor analysis and design were taught within the discipline *Special Apparatus and Installations* (in Romanian *Aparate și Instalații Speciale*), according to specific curricula for each faculty. The aim of this discipline was to complement the knowledge taught at the discipline *Unit Operations in Chemical Industry*, with specific topics for the main branches of chemical industry. Although significant weight was allocated to chemical reactors analysis and design issues, it also included the presentation of other apparatus (for transport of materials, feed of reactors, storage, processing of plastics and rubber etc.) along with specific complements of chemical technology.

*Corresponding author:g_bozga@chim.upb.ro

Professor Raul Mihail (in the first row, seating), at a graduation ceremony in 1983, with professors Octavian Smigelschi (who is addressing to the students) and Gheorghița Jinescu. In the second row, the last one on the right, prof. Alexandru Stefan (partially visible).

A priority of the economic policy at that time was the development of a national chemical industry, by its own efforts, putting an important focus on research, process development and design activities. Professor Mihail was directly involved in these chemical researches and design activities (at ICECHIM and IPROCHIM Bucharest), in parallel with his teaching activity (see details in [1]).

Realizing the important role of the reaction step in chemical process performance and, consequently, the importance of rigorous design and operation of chemical reactors, the specialists of the field pointed out the necessity of systematic training of chemical engineering students in this matter. In this context, the Ministry of Education and Culture organized a national-level analysis of the discipline *Special Apparatus and Installations*, with the participation of specialists from universities and chemical engineering design. The debates on this subject were hosted in the pages of the journal Revista de Chimie, in the years 1959 and 1960 [4-6]. From the various opinions regarding the topics of analysis, design and operation of chemical reactors and their teaching systematization, two alternatives were outlined: (i) by adopting the criteria of *physical state of the reaction mixture* (reactions in gas phase; reactions in homogeneous liquid phase; reactions in heterogeneous systems of different types: gas-liquid, liquid-liquid, catalytic gas-solid, non-catalytic gas-solid etc.) and the *constructive type of the reactor*, and (ii) the organization of chemical reactors topics using the criterion of the *fundamental chemical processes* they serve for (reactors for nitration, hydrolysis, sulfonation, oxidation, etc.) [4,5]. From the data presented in the cited papers, published by Revista de Chimie, one can see the important role of Professor Mihail in the formulation of the first alternative mentioned above, and his involvement in supporting it with various scientific and technical arguments. In his interventions, he showed that, considering the progress of theoretical knowledge regarding the

kinetics and thermodynamics of the physical and chemical phenomena taking place in the chemical reactors, as well as the practical experience accumulated in their design and operation up to that date, "*The Special Apparatus discipline aims to expose the theory and the constructive principles of the reaction vessels, or, as they are called, chemical reactors*". Professor Mihail emphasized also the basic principle followed in the reactor design: "*Considering that a reaction carried out in industrial conditions is a summation of physical stages (diffusion, heat transfer) with chemical stages (the reaction itself), often there have been solved systems of simultaneous equations that describe each of the mentioned steps; as a result, the main parameters underlying the design of the reactors were obtained* ".

Amongst the other opinions presented, it is worth mentioning that of Nicolae Petrescu, a design specialist, associate professor of the Processes and Apparatus Department (now the Chemical and Biochemical Engineering department) of Polytehnic Institute Bucharest (PIB), with experience in teaching the *Special Apparatus and Installations* subjects [6]. N. Petrescu sustained the first criteria presented above and proposed to teach exclusively chemical reactor topics, within the analyzed discipline, recommending to be named "*Reactors for chemical industry*" (organic and inorganic).

Finally, after a concluding intervention of Professor Emilian Bratu, Head of the Processes and Apparatus Department of PIB, there were adopted the criteria of physical state of reaction mixture and the constructive type of the reactor [6]. The topics and teaching systematization of chemical reactors subjects proposed by Professor Mihail, were innovative, not having been used in prior published works. The proposed content matches that adopted predominantly in the monographs on this subject published in the following period and it continues to be used in the teaching of this discipline.

Professor Mihail was recognized for his broad intellectual horizons, his rigor in the use of the time and a well-balanced exigency in rapport with the students. He was appreciated also for his fine spirit of observation, subtlety and sense of humor, an elegant style of expression and writing, modesty and naturalness in behavior.

In addition to celebrating a distinguished professor of our university, the centenary Raul Mihail is a new opportunity to emphasize the moral values guiding the activity of a professor and the importance of the vocation, for this profession of high social responsibility.

REFERENCES

[1] Muntean, O., Raul *Mihail Fondatorul Şcolii de Reactoare Chimice din Romania* (1920-1985), Revista de Chimie, 56(11), 1995, p.1069.

[2] Postelnicescu, P., *In Memoriam. Profesorul Raul Mihail*, Buletinul S. Ch. R., nr. 1, 2015, p.4.

[3] *Maria G., Profesor Raul Mihail - fondatorul școlii de Reactoare Chimice din România*, Revista de Chimie, 2020, to be published.
[4] * *Dezbaterea Publică Privind o Serie de Probleme din Conținutul Învățământului Superior Chimic*, Revista de Chimie, 10(11), 1959, p. 630.
[5] * *Ministerul Învățământului și Culturii, Programa Cursului de Aparate și Instalații Speciale în Industriile Organică și Anorganică pentru Facultățile de Chimie Industrială*, Revista de Chimie, 10(11), 1959, p. 654.
[6] * *Discuție Publică cu Privire la Cursul de "Aparate și Instalații Speciale",* Revista de Chimie, 11(4), 1960, p. 223.
`

ON SOME CASES OF MASS TRANSFER KINETICS IN MECHANICALLY STIRRED TANKS

Cristian RADUCANU[1], Silviu PRODAN [1,a], Andreea BURLACU [1,a], Ovidiu BISOC [1,a], Tanase DOBRE[1,2*]

[1]University Politehnica of Bucharest, Chemical and Biochemical Engineering Department, 1-7, Gheorghe Polizu street, 011061, Bucharest, Romania,
[2]Romanian Technical Sciences Academy, 26 Dacia Bld., Bucharest Romania,
[a] 3th year Bachelor student in Chemical Engineering

Abstract: *Solid-liquid, liquid-liquid and gas-liquid stirred vessels are widely used in many chemical, biochemical and food process industry operations. Mechanically agitated vessels appear to be the most used equipments in development of industrial procedures related with the above mentioned branches. From the mass transfer point of view three cases are fundamentals: i) mass transfer from a suspended particle (bubble, drop) to a liquid continuous phase, ii) mass transfer from a phase fixed on surface to a liquid continuous phase, iii) mass transfer from the wall to a liquid continuous phase. The present paper focuses on the last two cases. First part of the paper analyzes, by experimental way with data processing, mass transfer kinetics from a fixed sample of benzoic acid to water and sugar solutions, vigorously mixed with an open turbine device. In the second part of paper the sample of acid benzoic is fixed on the wall of tank and the liquid media is agitated with a turbo-dispersive device, which produces inside of tank an air-liquid dispersion. In both cases the dependence of mass transfer coefficient and correspondent Sherwood number upon process factors was given.*

Keywords: mass transfer, mechanically mixed medium, fixed particle in mixing stream, mass transfer at walls, criterial relationships.

1. Introduction

Mechanically agitated vessels are widely used in chemical engineering systems because they play an important role in enhancing mass and heat transfer between a solid and liquid phase. Improved mixing is of great importance for liquid-to-liquid and liquid-to-solid systems, and it can be used for a variety of purposes, *e.g.*, homogenisation of physical properties and composition, prevention of stratification or deposition of suspended particles, for improved rates of heat, mass transfer and chemical reaction [1.2]. While looking at figure 1, which shows a sketch with functionalities of such reactor, it is not difficult to anticipate the special mechanical problems (alignment of the shaker shaft, shaft sealing, sealing of the lid and manholes, etc.) imposed by such a machine type, especially when operating is under medium or high pressure.

*Corresponding author: tanase.dobre@upb.ro

Mass transfer between solid additions and bulk liquid is frequently present in several operations, especially in solid dissolving and crystallization [3-5]. To enhance the rate of mass transfer from the solid to the surrounding liquid, the liquid mixing or submerged gas injections have commonly been applied. This is so as the dissolution process is typically boundary layer mass transfer controlled and therefore convection plays important role in influencing the associated rate. It is now well known that the turbulent circulatory flow fields, induced during stirring practices, considerably affects the rate of the dissolution or mass transfer processes. Naturally therefore, it is important to know what extent the rate of dissolution is influenced by key operating variables, such as the gas flow rate or others parameters characterizing the liquid mixing. At this time in gas liquid reactions the most common reactors are gas-liquid contactors with mechanically mixing. In the microbial cells culture with these bioreactor type the cells can be considered as solid phase. However, their density is near to water density, reducing the terminal settling velocity and they are often neglected when considering only the hydrodynamics of bioreactors. Especially in bulk enzyme and chemical production, the reactor volumes may be several hundred cubic meters, and the efficiency of gas liquid mass transfer and bulk mixing becomes an important design parameter [6-8]. Stirred tank reactors (STR) with height to diameter ratio (H/D) above 2 are common in large scale industrial processes and, therefore, they are often equipped with multiple impellers.

From the mass transfer point of view three cases are fundamentals: i) mass transfer from a suspended particle (bubble, drop) to liquid continuous phase, ii) mass transfer from a phase fixed on surface to liquid continuous phase, iii) mass transfer from the wall to liquid continuous phase. For a long time the case of mass transfer from suspended particles in liquid, gas-liquid dispersion or suspension has been given special attention, many innovative aspects being brought in this case [9-12]. Mass transfer from a fixed particle to the reactor stream is important in order to characterize processes such as catalysis, corrosion reactions, etc. which take place on rigidly mounted surfaces inside the reactor [13]. The same problem arises for the case of mass transfer from the reactor wall to the agitated environment inside it [14, 15]. Considering the variables that determine the kinetics of mass transfer from the wall or from a fixed particle to a mixed medium (figure 2) it leads, for mass transfer coefficient (kl), to the general relation (1).

Here, together with the geometric quantities, identifiable in figure 2, it is shown that the physical quantities that control the mass transfer process are: n- stirrer speed, ρ – liquid environment density, η - liquid environment dynamic viscosity – superficial tension of liquid environment, D_A –diffusion coefficient of transferred species in liquid environment.

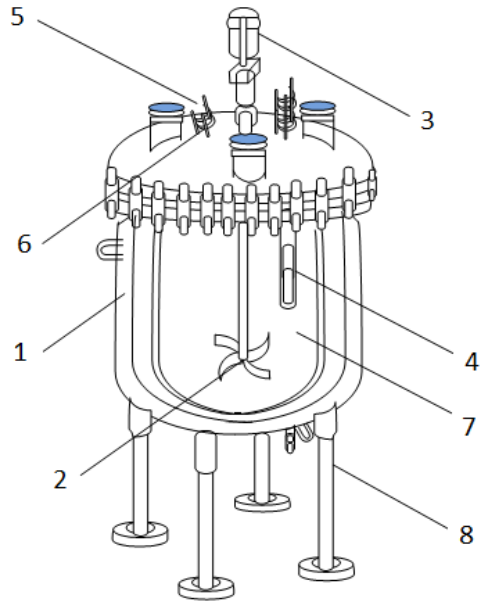

Fig 1. Sketch of a mechanically stirred reactor: 1- jacket pressure rating, 2- impellers for different level mixing, 3- mixer drive, 4- baffle with sensor temperature, 5- handhole with protection, 6- top head nozzle, 7- interior corrosion protection, 8- protection legs for seismic and wind conditions.

$$k_l = f(d, D, H, h, b, n, \rho, \eta, \sigma, D_A) \tag{1}$$

The dimensional analysis applied for cases in question finds that the kinetics of their corresponding mass transfer is given by relation (2), where in *Re*, *We* criteria (3) the characteristic length is the stirrer diameter d:

$$Sh = f\left(Re, We, Sc, \frac{D}{d}, \frac{H}{d}, \frac{h}{d}, \frac{b}{d}\right) \tag{2}$$

$$Sh = \frac{k_l\, d}{D_A} \qquad Re = \frac{nd^2\rho}{\eta} \quad Sc = \frac{\eta}{\rho D_A} \quad We = \frac{n^2\rho d^3}{\sigma} \tag{3}$$

The goal of this study is to determine the effects of the hydrodynamic and operating parameters on mass transfer coefficient from a fixed sample from benzoic acid, which is posted in zone of vigorously mixed liquid with an open centrifugal stirrer and respectively on the wall when the mixing is produced with a turbo-dispersive device.

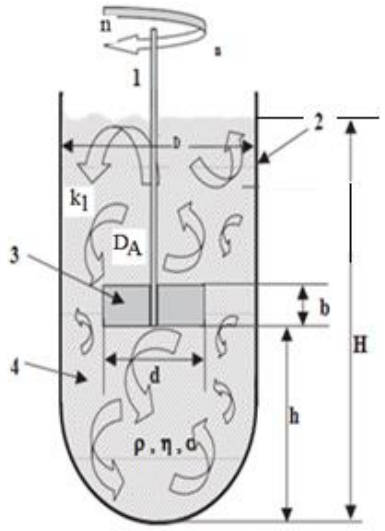

Fig 2. Schematic representation for dimensional analysis of mass transfer from a wall to a stirred liquid:
1- shaft of the stirrer, 2- mixer body, 3- paddle of the stirrer, 4- working environment.

2. Equipment, materials and methods

For measuring mass transfer coefficient from a fixed solid in mixed media it was used: i) a device model of cylindrical reservoir with controlled mixing and heating (see figure 3) of dissolving environment, ii) precision mechanically micrometer for establishing of geometric dimensions of sample and iii) precision balance for measurement of dissolved mass from sample in a selected time. The diameter of cylindrical reservoir of mixing unit was 120 mm. The stirrer used is an open centrifugal type having diameter of 50 mm, 6 paddles of 8 mm width and 8 mm of the shaft diameter. The position of the stirrer with respect to the vessel bottom of was kept the same, in all measurements, at h/d = 1. The position of the acid benzoic sample was at the middle of liquid environment height and of distance from the stirrer shaft and reservoir wall. Water and water sugar solution was used as liquid environment. Water and sugar solutions with a sugar content of 0.25 kg_{sg}/kg_{sol} and 0.5 kg_{sg}/ kg_{sol} were used as working medium. The use of sugar solutions was chosen as method for important modification of working environment viscosity. The agitator speed (n), working temperature (t) and sugar concentration (c_{zh}) in the working environment were chosen as process factors. Consequently, the experimental research was organized according to a factorial plan 2^3 where the dimensionless factors [16] with the inferior and superior level of factors as follow: n - 50 and 100 rpm, t - 20 and 40 ^{0}C, c_{zh} - 0 and 0.5 kg_{sg}/kg_{sol}.

The dimensionless agitator speed, temperature and sugar concentration are expressed as it is shown by relation (4)

$$x_1 = \frac{n-100}{50} \qquad x_2 = \frac{t-30}{10} \qquad x_3 = \frac{c_{sg}-0.25}{0.25} \tag{4}$$

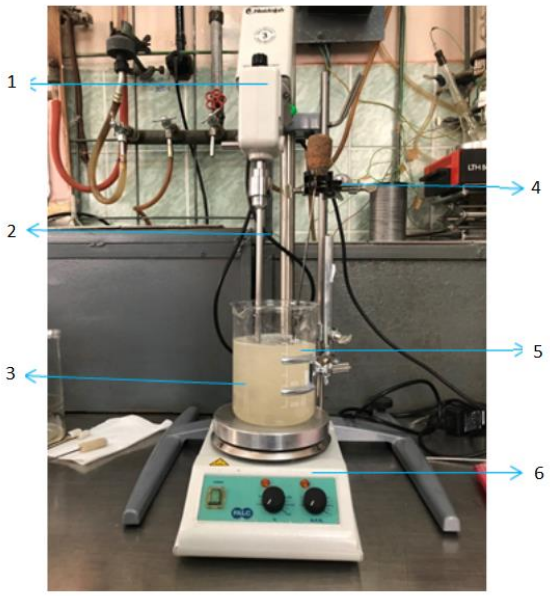

Fig 3. Laboratory experimental device for mass transfer analysis from a fixed solid to a mechanically mixed working solution: 1- rotation velocity controller; 2- mixer axe; 3- Berzelius 1 L glass, 4- holder for sample fixing; 5- cylindrical sample of benzoic acid; 6- heating system with controlled temperature.

For the dependence of benzoic acid saturation concentration in water and sugar solutions, concentration that determines the driving force of interphase transfer, data from the literature were adopted (table 1). For the expression of benzoic acid diffusion coefficient in water and sugar solutions, Wilke and Chang relation was used, where for viscosity the data from table 2 were used [16].

Table 1

Solubility data for acid benzoic (g_{ba}/kg_{sol}) in sugar solutions at temperature range 25-65 ^{0}C

Temperature ^{0}C / Sugar conc. kg_{sg}/kg_{sol}	25	35	45	55	65
0	2.86	4.14	5.95	8.42	11.87
0.2	2.56	3.76	5.48	7.55	10.67
0.4	2.16	3.29	4.88	6.55	8.99
0.6	1.71	2.55	4.08	5.39	7.75

In an experiment of mass transfer coefficient determination, where the values of process factors are fixed, the mass loss of the sample in a time interval is measured. Each experiment is replicated at least 3 times so that experimental sample handling errors are minimized.

Table 2

Viscosity of sugar solutions (cP) at temperature range 25-65 ^{0}C

Temperature ^{0}C Sugar conc. kg_{sg}/kg_{sol}	25	35	45	55	65
0	0.89	0.71	0.59	0.51	0.43
0.2	1.97	1.51	1.20	0.97	0.81
0.4	6.22	4.41	3.26	2.51	1.99
0.6	567	34.1	21.3	14.1	9.87

In all experiment for mass transfer from a fixed form to a mixed sugar solutions the benzoic acid (Reactivul - Chimpar S.A Romania) was cylindrical shaped to a rigid baguette so as to build the sample holder (see figure 1). So the experimental procedure for this mass transfer case contains the following sequences: 1) verify the position of centrifugal stirrer in cylindrical reservoir in order to h/D = 1; 2) fill water or sugar solution in cylindrical reservoir (Berzelius glass) to have H = 18 cm (H/D =1.5); 3) take benzoic acid cast, dip it in water, squeeze in paper towel, weigh it on electronic balance, measure its length and radius using Vernier caliper (electronic caliper); 4) select the stirrer rotation speed and the temperature and wait for steady state temperature; 5) put the sample in mixed liquid in geometric position above specified; 6) after 10 min take the sample from mixed media, squeeze in paper towel and weight and measure the radius and if is needed and the length of benzoic cylinder sample; 8) Plot the graph during experiment itself and get it signed; the sequence is repeated 3 times; 7) fill in the measured data in file with experiments plan (matrix of factorial plan) of process analysis.

From each experiment from the matrix of factorial plan the flow rate of dissolved benzoic acid (n_{bai}) was computed using relations (5)-(7), the transfer area at current time ($A_{\tau i}$) and current mass transfer coefficient (k_{lmi}). For c_S^* were used values from table 1.

$$n_{bai} = \frac{(m_{f\tau i} - m_{i0})}{\tau_i} \tag{5}$$

$$A_{\tau i} = 2\pi R_{\tau i} L_{\tau i} \tag{6}$$

$$k_{lmi} = \frac{n_{bai}}{A_{\tau i} c_S^*} \tag{7}$$

In the case of experimental analysis of mass transfer from reactor wall to the mixed liquid, it was decided to perform agitation with a turbo-dispersive device (IKA Ultraturax dispersor) and to use water as working liquid. Now, air-water dispersion becomes agitated in the reactor. Its gas holdup being measurable by measuring the increase in volume compared to water. For water as a working liquid, it was found that the gas holdup depends on rotating speed of disperser, on

the geometric simplexes d/D and h/D and even on the temperature, which modifies the viscosity of the water (figure 4).

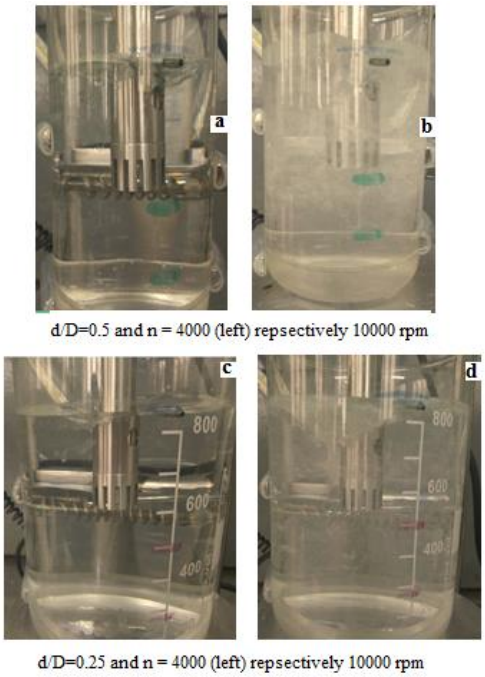

Fig 4. Gas holdup at water stirring with IKA ultraturax dispersor (t= 25 ^{0}C, a-ε = 0.05 m^3/m^3, b-ε = 0.35 m^3/m^3, c-ε = 0.03 m^3/m^3, d-ε = 0.25 m^3/m^3).

Consequently, the mass transfer coefficient, as a process-dependent variable, will depend on 4 factors that also influence gas holdup of dispersion under agitation (device speed, temperature, simplex d/D and simpelex h/D). The benzoic acid sample used in this case was a plate one with a width of no more than 3 cm, on which benzoic acid was deposited, which is fixed on the wall of the mixing vessel.

Table 3

Example of data collected in one experiments for mass transfer from the wall

Experiment number 1: n= 4000, t- 20, h/D= 0.5 , d/D= 0.25, τ_e = 10 min				
	0	1	2	3
m [g]	8.53	8.43	8.34	8.19
l [mm]	23.37	23.32	23.25	23.15
L [mm]	81.38	81.24	81.18	80.94
A [mm^2]	1901.85	1894.52	1887.44	1873.76

The experimental procedure is similar to the one above presented. The minimal experimental program has organized for a process with 4 independent factors.

Table 3 shows data set collected in an experiment (experiment number 1 here). In data processing the mass transfer area is corrected in respect to gas holdup in working environment (8).

$$A_{\tau i} = (1-\epsilon) l L \tag{8}$$

3. Data processing and results

As shown in the introductory part, the paper aim is to succeed in expressing the kinetics of mass transfer, for each of the two cases, in a concrete form of the general relation (2). This aim could be attained by the proper processing of primary experimental data. The large volume of data actually involves the use of an automatic calculation procedure. Here is explained and exemplified this processing with data from table 4, which refers to the case of transfer from a fixed particle in environment with mechanical stirring. The procedure for this data processing contains the following steps:

1. Import table 4 from Excel in Matchad;
2. Import of the data from Table 2 and process it to get the relationship (9), which shows the benzoic acid solubility versus c_{zh} and t;

$$c_S^* = c_S^*(t, c_{sg}) = c_{sAB}(t, c_{zh}) = 1.204(1 - c_{zh}^{1.95})\, exp\left(0.695 \frac{t}{20}\right) \tag{9}$$

3. Select from imported Excel file data for first experiment, which give values of process

factors and the state of mass and dimension of sample, and compute mass transfer

coefficient, as in the bellow example: $\text{Data}_1 := \text{submatrix}(\text{Data}, 1, 3, 5, 11)$,

$$\text{Data}_1 = \begin{pmatrix} 34.62 & 34.5 & 15.16 & 15.05 & 32.33 & 32.24 & 10 \\ 34.5 & 34.38 & 15.05 & 15 & 32.24 & 32.15 & 10 \\ 34.38 & 34.21 & 15 & 14.88 & 32.15 & 32.1 & 10 \end{pmatrix} \quad n_{A1} := \frac{\left(\text{Data}_1^{\langle 0 \rangle} - \text{Data}_1^{\langle 1 \rangle}\right)}{\text{Data}_1^{\langle 6 \rangle} \cdot 60},$$

$t := \text{Data}_{1,2}$

$$c_{zh} := \text{Data}_{1,3} \quad A := 3.14 \frac{\left(\text{Data}_1^{\langle 2 \rangle} + \text{Data}_1^{\langle 3 \rangle}\right) \cdot \left(\text{Data}_1^{\langle 4 \rangle} + \text{Data}_1^{\langle 5 \rangle}\right)}{4} \cdot 10^{-6}$$

$$k_{l1} := \frac{n_{A1}}{A \cdot C_{sAB}(t, c_{zh})} \qquad k_{l1} = \begin{pmatrix} 1.82 \times 10^{-5} \\ 1.82 \times 10^{-5} \\ 2.578 \times 10^{-5} \end{pmatrix}, \quad i := 0, 1 .. 2 \quad k_{l1m} := \frac{\sum_{i=0}^{2} k_{l1_i}}{3}, \quad k_{l1m} = 2.1\ 10^{-5}$$

m/s

Table 4

Primary experimental data for dissolving fixed benzoic acid sample in sugar solutions under stirring

	n rpm	t °C	c_{sg} kg/kg		m_i g	m_f g	d_i mm	d_f mm	h_i mm	h_f mm	τ_i, min
				1	34.62	34.5	15.16	15.05	32.33	32.24	10
				2	34.5	34.38	15.05	15	32.24	32.15	10
1	50	20	0	3	34.38	34.21	15	14.88	32.15	32.1	10
				1	32	31.76	15.04	14.7	32.37	31.44	10
				2	31.76	31.48	14.7	14.53	31.44	31.25	10
2	150	20	0	3	31.48	31.35	14.53	14.14	31.25	31.16	10
				1	30.84	30.2	14.17	13.17	30.54	29.53	10
				2	30.2	29.69	13.17	12.36	29.53	28.64	10
3	50	40	0	3	29.69	29.33	12.36	12.03	28.64	27.87	10
				1	24.84	24.44	15.23	14.92	53.53	53.25	10
				2	24.44	22.22	14.92	14.56	53.25	52.63	10
4	150	40	0	3	22.22	21.8	14.56	14.39	52.63	51.67	10
				1	34.98	34.84	15.41	15.33	32.9	32.81	10
				2	34.84	34.73	15.33	15.3	32.81	32.43	10
5	50		0	3	34.73	34.62	15.3	15.16	32.43	32.33	10
				1	23.88	23.65	15.64	15.21	46.63	45.53	10
				2	23.65	23.42	15.21	15.15	45.53	45.49	10
6	100		0	3	23.42	23.18	15.15	14.79	45.49	45.34	10
				1	30.24	29.91	15.15	14.92	52.79	50.46	10
				2	29.91	29.66	14.92	14.78	50.46	50.24	10
7	150		0	3	29.66	29.41	14.78	14.64	50.24	50.16	10
				1	31.35	31.2	14.14	13.9	31.16	31.08	10
				2	31.2	31.02	13.9	13.62	31.08	30.53	10
		t ct.-									
8	200	20	0	3	31.02	30.82	13.62	13.38	30.53	30.44	10
				1	23.49	23.33	14.44	14.26	51.68	51.3	10
				2	23.33	23.19	14.26	14.02	51.3	50.23	10
9	50	40	0.5	3	23.19	23.13	14.02	13.9	50.23	50.02	10
				1	29.33	29.32	14.81	14.73	49.4	49.12	10
				2	29.32	29.18	14.73	14.64	49.12	48.62	10
10	150	40	0.5	3	29.18	29.10	14.64	14.38	48.62	48.2	10
				1	29.10	29.09	14.38	14.15	48.2	48.18	10
				2	29.09	29.06	14.15	14.11	48.18	48	10
11	50	20	0.5	3	29.06	29.03	14.11	14.03	48	47.8	10

				1	29.03	29.02	14.03	13.92	47.8	47.52	10
				2	29.02	29.01	13.92	13.74	47.52	47.31	10
12	150	20	0.5	3	29.01	29	13.74	13.19	47.31	47.07	10

4. In order to have all values of mass transfer coefficient in the matrix of factorial experiments, repeat the sequence 3 for all experiments from Excel imported file;

5. Fill with k_l values the matrix of the factorial experiment (MG) and add here columns with density of the liquid phase, viscosity of the liquid phase (see table 2), diffusion coefficient of benzoic acid in the liquid phase and the mixer speed:

$$MG := \begin{pmatrix} 1 & -1 & -1 & -1 & 0.021 & 0.001 & 1000 & 10^{-9} & 50 \\ 2 & 1 & -1 & -1 & 0.035 & 0.001 & 1000 & 10^{-9} & 150 \\ 3 & -1 & 1 & -1 & 0.049 & 0.0007 & 989 & 1.2\cdot10^{-9} & 50 \\ 4 & 1 & 1 & -1 & 0.048 & 0.0007 & 989 & 1.2\cdot10^{-9} & 150 \\ 5 & -1 & 1 & 1 & 0.00825 & 0.003 & 1040 & 0.7\cdot10^{-9} & 50 \\ 6 & 1 & 1 & 1 & 0.0053 & 0.003 & 1040 & 0.7\cdot10^{-9} & 150 \\ 7 & -1 & -1 & 1 & 0.0034 & 0.006 & 1044 & 0.45\,10^{-9} & 50 \\ 8 & 1 & -1 & 1 & 0.00452 & 0.006 & 1044 & 0.45\,10^{-9} & 150 \end{pmatrix}$$

6. Uses the MG matrix for application of statistical procedure which identify the parameters of mass transfer coefficient dependence upon dimensionless factors of the process (10)

$$k_l = \beta_0+\beta_1x_1+ \beta_2x_2+ \beta_3x_3+ \beta_{12}x_1x_2+ \beta_{13}x_1x_3+ \beta_{23}x_2x_3+ \beta_{123}x_1x_2x_3 \quad (10)$$

7. Find a solution to test the significance of coefficients from relation (10) and display the obtained result (11)

$$k_l = 2.13\ 10^{-5} + 5\ 10^{-6}x_1 + 6.25\ 10^{-6}x_2 - 1.669\ 10^{-5}x_3 - 4.09\ 10^{-6}x_2x_3 \quad (11)$$

8. Use the MG matrix and the values of factors for each experiment to calculate the numbers *Sh*, *Re* and *Sc*;

9. Accept the dependence $Sh = cRe^mSc^n$ and minimize, to determine *c*, *m*, and *n*, the mean square deviation between experimental *Sh* and compute *Sh* values (12):

$$F(c,m,n) = \sum_{i=1}^{i=8}(Sh_i - cRe_i{}^mSc_i{}^n) \quad (12)$$

10. Displays the obtained dependency *Sh* vs. *Re* and *Sc* (13):

$$Sh = 0.033\, Re^{0.981} Sc^{0.05} \tag{13}$$

Even if the second case of investigated transfer, namely mass transfer from the vessel wall to the air-liquid dispersion under agitation, contains other process factors (stirrer speed, working temperature, geometric simplex d/D, geometric simplex h/D), the above procedure for experimental data processing remains valid. It specifies that in this case one experiment was not replicate and the sample was exposed to stirred water-air dispersion for 30 min. Here it cannot neglect the presence of benzoic acid in dispersion. Consequently the experimental values for mass transfer coefficient was obtained with relation (14), where c_l is the mean benzoic acid concentration in dispersion, during of one experiment.

$$k_{lmi} = \frac{n_{bai}}{A_{\tau i}(c_S^* - c_l)} \tag{14}$$

In this case the proposed relation for the dependence *Sh* number versus process factors has the form (15), where s_{g1} is the ratio d/D and s_{g2} is h/D.

$$Sh = \alpha Re^{\beta} Sc^{\gamma} {s_{g1}}^{\delta} {s_{g2}}^{\varepsilon} \tag{15}$$

$$M_R := \begin{pmatrix}
1 & 4000 & 20 & 0.5 & 0.25 & 8.53 & 7.63 & 1885 & 0.4 & 0.05 \\
2 & 4000 & 20 & 0.25 & 0.25 & 7.65 & 6.98 & 1964 & 0.55 & 0.05 \\
3 & 4000 & 40 & 0.5 & 0.25 & 6.83 & 5.69 & 1901 & 0.72 & 0.05 \\
4 & 4000 & 40 & 0.25 & 0.25 & 7.90 & 7.24 & 1830 & 0.95 & 0.05 \\
5 & 10000 & 20 & 0.5 & 0.25 & 9.15 & 8.41 & 1790 & 0.35 & 0.25 \\
6 & 10000 & 20 & 0.25 & 0.25 & 7.85 & 7.32 & 1380 & 0.45 & 0.25 \\
7 & 10000 & 40 & 0.5 & 0.25 & 8.41 & 7.35 & 1650 & 1.05 & 0.25 \\
8 & 10000 & 40 & 0.25 & 0.25 & 7.35 & 6.94 & 1550 & 1.42 & 0.25 \\
9 & 4000 & 20 & 0.5 & 0.5 & 12.96 & 12.53 & 1565 & 0.51 & 0.11 \\
10 & 4000 & 20 & 0.25 & 0.5 & 9.71 & 9.54 & 1548 & 0.75 & 0.11 \\
11 & 4000 & 40 & 0.5 & 0.5 & 9.07 & 8.70 & 1450 & 0.35 & 0.11 \\
12 & 4000 & 40 & 0.25 & 0.5 & 9.49 & 9.07 & 1501 & 0.71 & 0.11 \\
13 & 10000 & 20 & 0.5 & 0.5 & 8.79 & 8.25 & 1452 & 0.31 & 0.34 \\
14 & 10000 & 20 & 0.25 & 0.5 & 8.25 & 7.85 & 1423 & 0.61 & 0.34 \\
15 & 10000 & 40 & 0.5 & 0.5 & 8.70 & 7.70 & 1403 & 1.01 & 0.34
\end{pmatrix}$$

All the experimental data for k_l calculation, and hence the corresponding values for *Sh* number, are in the matrix M_R. In order, from left to right, the columns of this matrix contain the following data: stirrer device speed (*n* in rpm), working temperature (*t* in ^{0}C) , value of simplex s_{g1}, value of simpex s_{g2}, mass of the initial benzoic acid sample (m_{i0} in g), mass of the benzoic acid sample after 30 minutes of contact (m_{fti} in g), value of the interphase contact surface ($A_{\tau i}$ in mm^2), average concentration of benzoic acid in the water-air dispersion (c_1 in g/l), gas fraction of dispersion (ε). Table 5 contains the computed data needed for minimization of functional $F(\alpha,\beta,\gamma,\delta,\varepsilon)$ that will gives us the values we are looking for $\alpha,\beta,\gamma,\delta$ and respectively ε.

Table 5

Computed values for dimensionless number from relation (14)

$k_l =$

	0
0	$1.121\cdot10^{-5}$
1	$8.983\cdot10^{-6}$
2	$6.97\cdot10^{-6}$
3	$4.262\cdot10^{-6}$
4	$9.007\cdot10^{-6}$
5	$6.763\cdot10^{-6}$
6	$7.017\cdot10^{-6}$
7	$2.991\cdot10^{-6}$
8	$5.65\cdot10^{-6}$
9	$2.537\cdot10^{-6}$
10	$2.084\cdot10^{-6}$
11	$2.562\cdot10^{-6}$
12	$6.454\cdot10^{-6}$
13	$5.531\cdot10^{-6}$
14	$6.554\cdot10^{-6}$
15	$3.507\cdot10^{-6}$

$Sh_l =$

	0
0	240.275
1	192.491
2	298.712
3	182.664
4	193.007
5	144.913
6	300.722
7	128.206
8	121.081
9	54.36
10	89.302
11	109.798
12	138.294
13	118.53
14	280.884
15	150.289

$Re_d =$

	0
0	$6\cdot10^4$
1	$6\cdot10^4$
2	$1.2\cdot10^5$
3	$1.2\cdot10^5$
4	$1.5\cdot10^5$
5	$1.5\cdot10^5$
6	$3\cdot10^5$
7	$3\cdot10^5$
8	$6\cdot10^4$
9	$6\cdot10^4$
10	$1.2\cdot10^5$
11	$1.2\cdot10^5$
12	$1.5\cdot10^5$
13	$1.5\cdot10^5$
14	$3\cdot10^5$
15	$3\cdot10^5$

$Sc_l =$

	0
0	714.286
1	714.286
2	357.143
3	357.143
4	714.286
5	714.286
6	357.143
7	357.143
8	714.286
9	714.286
10	357.143
11	357.143
12	714.286
13	714.286
14	357.143
15	357.143

$s_{g1} =$

	0
0	0.5
1	0.25
2	0.5
3	0.25
4	0.5
5	0.25
6	0.5
7	0.25
8	0.5
9	0.25
10	0.5
11	0.25
12	0.5
13	0.25
14	0.5
15	0.25

$s_{g2} =$

	0
0	0.25
1	0.25
2	0.25
3	0.25
4	0.25
5	0.25
6	0.25
7	0.25
8	0.5
9	0.5
10	0.5
11	0.5
12	0.5
13	0.5
14	0.5
15	0.5

$$F(\alpha,\beta,\gamma,\delta,\varepsilon)\sum_{i=0}^{i=15}\left(Sh_{li}-\alpha {Re_{di}}^{\beta}{Sc_i}^{\gamma}{s_{g1i}}^{\delta}{s_{g2i}}^{\varepsilon}\right) \quad (16)$$

The identification of the coefficients *a* $\alpha,\beta,\gamma,\delta$ and respectively ε makes the mass transfer kinetics relation (16) to have the concrete expression (17):

$$Sh = 0.047{Re_d}^{0.725}Sc^{0.254}{s_{g1}}^{0.645}{s_{g2}}^{0.505} \quad (17)$$

Looking on the above relation, it should be noted that the present paper has obtained the criterial relationships (13) and (17), which are considered important in design of reactors with mechanical mixing, especially in terms of estimating corrosion dynamics at fixed surfaces in the reactor (13) and, respectively, at reactor wall (17). This is because at one fixed surface or at reactor wall the

transfer of the participants to the surface electro-chemical process, respectively, the removal of the products from this surface is controlled by mass transfer. It should be added that in conceptual design of some reactors of this kind can be considered situations when on submerged surfaces or on the wall are proposed chemical reactions or other processes. And that require the knowledge of the kinetics of physical species transfer, so require the use of relationships (13) and (17). Based on transfer phenomena analogy, the relation (13) can be used to estimate the partially heat transfer coefficient from a coil in the reactor to the stirred medium. It easy to obtain, for partally heat transfer coefficient, the expression $\alpha = k_l \rho c_p \, w/w_M$, which leads to α values from 1000 to 5000 W/(m^2 K), according to many data from literature [18]. Extension of our mass transfer data to heat transfer from the wall to stirred liquid-gas dispersion finds α in the range of 100 W/(m^2 K). Our values for mass transfer coefficient for fixed particles in stirred environment are almost an order of magnitude larger than those characteristic of suspended particles [19]. We appreciate that this is due to the fact that the boundary layer formed on the fixed particles breaks, while the one formed on the suspended particles remains stable.

4. Conclusions

The present paper focuses on mass transfer analysis from a surface (particle), placed in the centre of mixing field respectively at the wall, in a reactor with mechanical mixing. The dimensional analysis applied to both cases showed which are the geometrical simplexes and the similarity criteria that determine the values of the *Sh* number, which is characteristic for mass transfer kinetics.
For each case, the experimental procedure was developed to allow, for fixed values of the process factors, the experimental determination of the mass transfer coefficients.
A procedure was developed, common to both cases, for the automatic capitalization of the primary measurements in order to highlight the dependence of *Sh* number on similitude criteria and specific geometric simplexes.
The results obtained, synthetized in relations (13) and (17), were compared with literature data. At the same time, their usefulness for a better knowledge of this type of equipment was demonstrated.

References

[1] Bratu Em. A., *Unit Operations in Chemical Engineering, Tome I, Chapter: Mixing in Liquid Media*, Technical Publishing House, Bucharest, 1983.
[2] Geankoplis C.J., *Transport Process and Unit Operations*, 3th Edition, Prentice-Hall International, Inc., Chapter: Mixing, 1993.

[3] Harriott, P., *Mass transfer to particles: Part I. Suspended particles in agitated tanks*, AIChE Journal 8, 93-101, 1962.
[4] Hughmark, *G.A., Hydrodynamics and mass transfer for suspended solid particles in a turbulent liquid.* AIChE Journal 20, 202-204, 1974.
[5] Grisafi F., Brucato A., Rizzuti L., *Solid-liquid mass transfer coefficients in gas-solid-liquid agitated vessels.* The Canadian Journal of Chemical Engineering 76, 446-455, 1998.
[6] Chisti Y., Jauregui-Haza U.J., *Oxygen transfer and mixing in mechanically agitated airlift bioreactors*, Biochemical Engineering Journal 10, 143–153, 2002.
[7] Moucha T., Linek V., Prokopova E., *Gas hold-up, mixing time and gas-liquid volumetric mass transfer coefficient of various multiple-impeller configurations: Rushton turbine, pitched blade and techmix impeller and their combinations*, Chemical Engineering Science 58, 1839–1846, 2003.
[8] Ban, W., Nikov I., Delmas H., Bascoul, A., *Gas–liquid mass transfer in a new three-phase stirred airlift reactor*, J. Chem. Technol. Biotechnol. 72, 137–142, 1998.
[9] Barker J. J.,Treybal R. E., *Mass transfer coefficients for solids suspended in agitated liquids*, AIChE Journal 6, 289-295, 1960.
[10] Brian P. L.T., Hales H.B., Sherwood T.K., *Transport of heat and mass between liquids and spherical particles in an agitated tank*, AIChE Journal 15, 727-733, 1969.
[11] Dobre T., Sandu Ohreac B.,, Parvulescu O., Danciu T., *Effects of solid carriers on oxygen mass transfer in a stirred tank bioreactor*, Rev. Chim. Bucharest, 65 (4), 489-496, 2014.
[12] Sara O.N., Icer F., Yapıcı S., Sahin B., *Effect of suspended CuO nanoparticles on mass transfer to a rotating disc electrode*, Exp. Therm. Fluid Sci., 35, 558-564, 2011.
[13] Abdel-Aziz M. H., *Solid–liquid mass transfer in relation to diffusion controlled corrosion at the outer surface of helical coils immersed in agitated vessels*, Chemical Engineering Research and Design 91, 43-50, 2013.
[14] Baday A., El-Shazly Y. M., Nosier S., *Corrosion rate determination of vessel walls agitated by double impeller and gas sparging*, Corrosion Reviews, paper 53, 2017.
[15] Zidan M.A., El-Shazly Y.M., Zaatout A. A., *Effect of the configuration of the dual impeller agitated vessel on the flow pattern and rate of mass transfer at the wall*, J. Thermo. Catal., 8, 3, 1-5, 2017.
[16] Dobre T., Sanchez J.M., *Chemical Engineering Modelling Simulation and Similitude, Chapter 5-Statistic Modelling*, Wiley VCH, 2007.
[17] Engineering ToolBox, (2014). *Sugar Solutions-Viscosities*, [online] Available at: https://www.engineerring toolbox.com/sugar-solutions-dynamic-viscosity-d_1895.html [Accessed on 02.05.2020].
[18] Debab A., Chergui N., Bekrentchir K. Bertrand J., *An investigation of heat transfer in a mechanically agitated vessel*, Journal of Applied Fluid Mechanics, 4, 2, 1, 43-50, 2011.
[19] Yawalkar A. A., Sharma M. M., Beenackers M., *Particle−Liquid mass transfer coefficient in two-/three-phases stirred tank reactors*, Ind. Eng. Chem. Res. , 41, 17, 4141-4167, 2002.

OPTIMIZATION OF AMMONIA SYNTHESIS REACTOR WITH DIRECT COOLING

Ariana IVANCIU, Cristiana Luminița GÎJIU, Raluca ISOPESCU*

Chemical and Biochemical Department, University POLITEHNICA of Bucharest, Str. Gheorghe POLIZU, nr. 1-7, sector 1, 011061, Bucharest

Abstract

The fixed, 3 vertical catalytic beds ammonia reactor with direct cooling was modeled and optimized in two distinct approaches: (i)optimization of the feed flow rate split between the three catalytic beds in order to maximize the final nitrogen conversion, and (ii) simultaneous conversion maximization and minimization of total catalytic bed length by formulating a multi-objective function. The mathematical model reflects the steady state reactor operation and consists in mass and heat balances and pressure drop equation. The modified Temkin kinetic equation was selected to model the process. Genetic algorithms were used for optimization. The numerical calculations were performed in the frame of Matlab R2015 software. The results proved that multi-objective optimization can provide a series of optimal solution where a high conversion, over 24 % can be reached with a reasonable catalyst consumption.

Key words: Ammonia synthesis, Optimization, Multi-objective function

1. Introduction

Ammonia is a chemical compound largely used in various industries. The greatest amount of synthesized ammonia is used as raw material for fertilizers, but it is also necessary in plastics or paper manufacturing. Ammonia synthesis directly from nitrogen and hydrogen, the Haber-Bosh process, represented a huge gain for the chemical industry, and had a tremendous impact on the agricultural products worldwide since large scale production of fertilizers begun. The process was implemented by various manufactures under different trademarks and was continuously improved to increase its performance.

The NH_3 synthesis occurs by the chemical reaction between N_2 and H_2 over a complex catalyst where adsorption/desorption are important steps. Iron-based catalysts were firstly studied and used while in recent years Ru based ones proved to have some favorable properties [1]. The primary raw material for ammonia synthesis is methane from which H_2 is obtained by reformation, while

* Corresponding author: Email address: r_isopescu@chim.upb.ro

N_2 is obtained by air distillation. The chemical reaction is reversible and there are no secondary products.

$$N_2 + 3H_2 \rightleftharpoons 2\,NH_3 \quad (1)$$

The thermodynamic conditions are severe: for iron-based catalyst the process occurs at high temperature, between 380 ^oC and 520 ^oC and pressure in the range of 150-250 bar [1].

As the reaction is exothermic and its equilibrium conversion is shifted towards smaller values by increasing temperature, the industrial synthesis is performed using 3 or 4 layers of catalyst operated adiabatically with cooling between layers. Two distinct approaches are generally used. The first way is the direct cooling which uses an injection of fresh, unreacted feed between the catalyst layers. This has the role of decreasing temperature, but it also decreases the conversion. This technological solution was adapted by the Kellogg converter. A second approach is the so-called indirect cooling that uses heat exchangers between the catalytic beds. A less used method is the internal cooling where cooling agent flows in tubes placed in the catalyst bed [2]. In our study, the direct cooling method considering the classical Kellog configuration with three vertical catalytic beds was chosen for modelling and optimization.

Due to the thermodynamic conditions and exothermic effect of the process, the final nitrogen conversion is rather low. For traditional Fe-magnetite catalyst 4 bed reactor, the conversion for one pass was about 15-16 % [1], requiring recirculation of unreacted raw materials. The recirculation increases the operation cost and as large quantities of ammonia are required by industries the interest for better operating the ammonia reactor encouraged many researchers to find new more favorable structures and operating ways.

Mathematical models for the ammonia synthesis reactor were proposed, starting with the early work of Annable [3]. More recent publications propose tools for proper design and simulation [4-5], analysis and optimization [6,7]. For the direct cooling technological solutions early studies are present [8], where the effect of the reactor temperature profile is analyzed. More recent papers present a comparison between different cooling system for a multi-bed ammonia reactor [2] and study the behavior of an industrial 4-beds ammonia reactor using one and two-dimensional models [9]. In these papers the operating conditions are optimized to maximize the reactor final conversion.

For a large scale chemical, even small improvement in conversion significantly affects the overall economic balance. Therefore, the maximization of the conversion seems to be a recommended approach. In the present paper the optimization of ammonia converter was performed in two situations: (i) the maximization of N_2 conversion for a given reactor design, and (ii) the maximization of conversion and minimization of total catalytic volume by formulating a multi-objective function.

2. Mathematical model

2.1 Conservation equations

The mathematical model for the ammonia reactor is one-dimensional and pseudo-homogeneous, and reflects the steady state operating conditions, ignoring axial heat and mass transfer. These assumptions are based on recent reports [9] which proved by simulation that the difference between one- and bi-dimensional models is small, and both are close to industrial data. The model basically consists in mass and heat conservation equations and pressure drop evaluation.

Mass balance equation gives the variation of a N_2 conversion along the catalytic bed:

$$\frac{dX_{N_2}}{dz} = \frac{S}{D_{M,N_2}} \cdot v_{R,N_2} \tag{2}$$

where S is the cross section of the reactor, $D_{M,\,N2}$ is the inlet molar flow rate of nitrogen and $v_{R,\,N2}$ is the reaction rate referred to N_2.

The heat balance for the adiabatic catalytic beds is expressed by the relation:

$$\frac{dT}{dz} = \frac{S}{D_m \cdot c_p} \cdot \left(-\Delta H_R\right) \cdot v_{R,N_2} \tag{3}$$

where c_p is the heat capacity of the gaseous mixture, D_m is the mass flow rate, ΔH_R is the heat of reaction calculated with the general relations:

The pressure drop along the catalytic layers is estimated by Ergün equation:

$$\frac{dp}{dz} = -f \cdot \frac{w^2 \cdot \rho}{d_p} \tag{4}$$

The friction factor f calculated as:

$$f = 4 \cdot \frac{1-\varepsilon}{\varepsilon} \cdot \left(1.75 + 150 \cdot \frac{1-\varepsilon}{Re}\right) \tag{5}$$

where ε is the void fraction in the catalyst layer and Re is the Reynolds number calculated with the apparent velocity and mean properties of the gaseous mixture.

Mass and heat balance for the mixing points with fresh feed used for intermediate cooling are expressed in terms of given split of the mass feed, D_m

(Fig 1): D_{m1} - mass flow rate on the fist catalytic layer, D_{m2} - mass flow added for cooling before the second layer, D_{m3} - mass flow added for cooling before the third layer):

$$D_m = D_{m1} + D_{m2} + D_{m3} \tag{6}$$

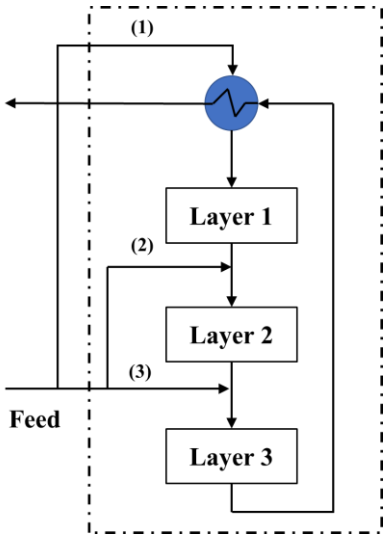

Fig 1. Split of the mass feed

The conversion corrections after cooling with fresh added flow are calculated by relations:

$$X_{A02} = \frac{X_{A1} \cdot D_{M0}^{(1)}}{D_{M0}^{(1)} + D_{M0}^{(2)}} \tag{7}$$

$$X_{A03} = \frac{X_{A2} \cdot \left(D_{M0}^{(1)} + D_{M0}^{(2)} \right)}{D_{M0}^{(1)} + D_{M0}^{(2)} + D_{M0}^{(3)}} \tag{8}$$

where $D_{M0}^{(i)}$ represents the fresh molar flow rate (cold) fed on layer '*i*'

$$D_{m1} \cdot c_{p1} \cdot T_1 + D_{m2} \cdot c_{p2} \cdot T_{cold} = (D_{m1} + D_{m2}) \cdot c_{p3} \cdot T_{03} \tag{9}$$

$$(D_{m1} + D_{m2}) \cdot c_{p4} \cdot T_2 + D_{m3} \cdot c_{p3} \cdot T_{cold} = (D_{m1} + D_{m2} + D_{m3}) \cdot c_{p5} \cdot T_{03} \tag{10}$$

where T_{0i} is the inlet temperature of quench gas flow on layer *i*, *i* = 2,3.

The specific heat mentioned in relation (9) and (10) corresponds to following conditions: c_{p1} – inlet feed on layer 1, c_{p2} – cooling gas at feed composition and cooling temperature, c_{p3} – feed conditions on layer 2 after mixing with quench gas, c_{p4} – gas exit after layer 2, c_{p5} – final product.

2.2 Reaction rate

The process takes place by a series of adsorption and dissociations steps and the kinetic parameter are complex function on surface structure. In the present work the reaction rate was estimated using the modified Temkin equation, defined for an iron-based catalyst [10]

$$v_{R,NH_3} = 2 \cdot k \cdot \left[K_a^2 \cdot a_{N_2} \cdot \left(\frac{a_{H_2}^3}{a_{NH_3}^2} \right)^{\alpha} - \left(\frac{a_{NH_3}^2}{a_{H_2}^3} \right)^{1-\alpha} \right] \tag{11}$$

According to the stoichiometry of the chemical reaction given in relation (1)

$$v_{R,N_2} = \frac{1}{2} \cdot v_{R,NH_3} \tag{12}$$

In the rate expression k is the kinetic constant for reverse reaction and is calculated with an Arrhenius type relation:

$$k = k_0 \cdot e^{-\frac{E}{R \cdot T}} \tag{13}$$

where k_0 is the Arrhenius coefficient and has the value $8.849 \cdot 10^{14}$ and E, the activation energy, equal to 40765 kcal/kmol.

In relation (2) a_i stands for the activity of component i, defined by the ratio between the fugacity and the reference fugacity:

$$a_i = \frac{f_i}{f_i^0} \tag{14}$$

The reference fugacity, f_i^0 is considered 1 atm and the definition of the component activity can be expressed as a function of molar fraction, y_i, fugacity coefficient, ϕ pressure, p:

$$a_i = \frac{f_i}{1} = f_i = y_i \cdot \phi_i \cdot p \tag{15}$$

Empirical relations for the fugacity coefficient, obtained in [9] are used:

$$\phi_{H_2} = 0.93431737 + 0.2101804 \cdot 10^{-3} \cdot T + 0.295896 \cdot 10^{-3} \cdot p - \\ - 0.2707279 \cdot 10^{-6} \cdot T^2 + 0.4775207 \cdot 10^{-6} \cdot p^2 \tag{16}$$

$$\phi_{N_2} = exp\left\{ p \cdot exp\left[-3.8402 \cdot T^{0.125} + 0.541 \right] - p^2 \cdot exp\left[-0.1263 \cdot T^{0.5} - 15.980 \right] + \right. \\ \left. + 300 \cdot \left[exp\left(-0.011901 \cdot T - 5.941 \right) \right] \cdot \left[exp\left(-p/300 \right) - 1 \right] \right\} \tag{17}$$

$$\phi_{NH_3} = 0.1438996 + 0.2028538 \cdot 10^{-2} \cdot T - 0.4487572 \cdot 10^{-3} \cdot p - \\ - 0.1142945 \cdot 10^{-5} \cdot T^2 + 0.2761216 \cdot 10^{-6} \cdot p^2 \tag{18}$$

K_a is the equilibrium constant calculated with the relation given by Gillespie and Beattie [11]:

$$lg\, K_a = -2.691122 \cdot lg\, T - 5.519265 \cdot 10^{-5} \cdot T + 1.848863 \cdot 10^{-7} \cdot T^2 + \\ + 2001.6/T + 2.6899 \tag{19}$$

2.3 Thermodynamic properties

Heat capacities and thermal effect of the chemical reaction were calculated using general relations:

$$C_p = A + B \cdot T + C \cdot T^2 + D \cdot T^3 \tag{20}$$

$$\Delta H_{R,T} = \Delta H_{R,T_0} + \int_{T_0}^{T} \Delta C_p\left(T\right) \cdot dT \tag{21}$$

$$\Delta c_p = \sum_i \nu_i \cdot c_{p,i} \tag{22}$$

$$\Delta H_{R,T_0} = \sum_i \nu_i \cdot H_{0,f,i} \tag{23}$$

where $H_{0,f,i}$ is the standard heat of formation for component i, ν_i are the stoichiometric coefficients in relation (1).

The coefficients for C_p (J/mol/K) calculation and components standard heat of formations are given in Table 1 [12].

Table 1

Component heat capacity coefficients and standard heat of formation

Component	i	A	B	C	D	H_f (J/mol/K)
N_2	1	31.15	-0.01357	0.0000268	$-1.17E\cdot10^{-8}$	0
H_2	2	27.14	0.09274	-0.00001381	$7.645\cdot10^{-8}$	0
NH_3	3	23.23	0.02383	0.00001707	$-1.19\cdot10^{-8}$	-45720

2.3 Optimization

The optimization of ammonia reactor was realized using two distinct approaches.

- The first aims to maximize the final conversion for a given reactor structure (3 catalytic layers with given section and length).

$$f = \max\left(X_{N_2}\right) \tag{24}$$

The decision variables are the split ratios for fresh feed on each layer:

$$x_i = \frac{Dm_i}{Dm}, \quad i = 1,2,3 \tag{25}$$

With the restriction:

$$x_1 + x_2 + x_3 = 1 \tag{26}$$

- The second approach is a multi-objective optimization problem [13]. The two dichotomic objectives are the maximization of the conversion and the minimization of the total catalytic bed length. By formulating this problem, we considered that the maximization of throughput is balanced by the increase of investment costs, mainly due to the catalyst required in the process. The objective function in this case must encompass the two criteria.

  A minimization problem was formulated:

$$\text{Min } F\left[f_1(x), f_2(x)\right] \tag{27}$$

  The two components of the vector function F are:

$$f_1(x) = -X_{N_2} \text{ and } f_2(x) = \sum_{i=1}^{3} l_i \tag{28}$$

where l_i is the length of the i layer, $i = 1,2,3$ and X_{N_2} is the nitrogen conversion and x is the vector of decision variables.

The decision variables in this case were the split ratios for the fresh feed and the catalytic bed lengths:

$$x_i = \frac{Dm_i}{Dm}, \quad i = 1,2,3$$
$$x_i = l_i, \quad i = 4,5,6 \tag{29}$$

Supplementary restrictions are added for both problems, referring to technically accepted temperatures ranges on each catalytic layer, *i*:

$$370\ ^oC < T_i < 525\ ^oC \tag{30}$$

2.4 Numerical methods

Numerical solution for the mathematical model and optimization problem were obtained in the frame of Matlab®R2015 software. The differential equations describing the mass and heat balance in the reactor and pressure drop (relations 2-4) are solved using *ode15s* built-in function which is a variable-step and variable order (between 1 and 5) algorithm for differential equations. The optimization was performed using genetic algorithm (GA). GA is defined by random search operating on string structures and imitating the biological selection of favorable outsprints. One of the main parameters is the population size. This population is a set of vectors that contain values, in the range indicated by the user, for the decision variables. Using specific operators (reproduction, crossover, and mutation) a new set of strings (a new population) is generated along the procedure, which finally aims to represent an optimum of the problem. The built-in functions *ga* and *gamultiobj* were used in the present work. For the first case a population size of 50 was defined, while for the second case the population size was 100.

3. Results and discussion

3.1. Maximization of the conversion

The main operating conditions and reactor characteristics considered are presented in table 2. The results obtained by applying the mathematical model and maximization of final conversion are synthetized in table 3.

Fig. 2 and 3 present the evolution of temperatures and conversion along the catalytic beds. As can be seen, the temperature is in the prescribed ranges (Fig. 2), with a maximum value at the end of the first and third catalytic layers. The comparison of reaction conversion with the equilibrium conditions (Fig. 3) shows that on the first layer the difference between these two conversions is rather big for the first bed, and this may lead to the conclusion that a more increased first layer would have been favorable.

Table 2

Operating conditions and design parameters

Operating conditions	
Inlet pressure, atm	150
Inlet temperature, °C	380
Total flowrate, kg/h	341820
Feed composition (mol. fraction)	
y_{N2}	0.22
y_{H2}	0.66
y_{NH3}	0.002
y_{CH4}	0.078
y_{Ar}	0.004
Constructive conditions	
Length of catalytic layer, m	6.5
Layer I, m	1.5
Layer II, m	2.0
Layer II, m	3.0
Diameter of the reactor, m	2.8

Table 3

Optimization results

Decision variables at optimum	
Dm_1/Dm	0.817
Dm_2/Dm	0.116
Dm_3/Dm	0.067
Objective function (final conversion), %	24.4

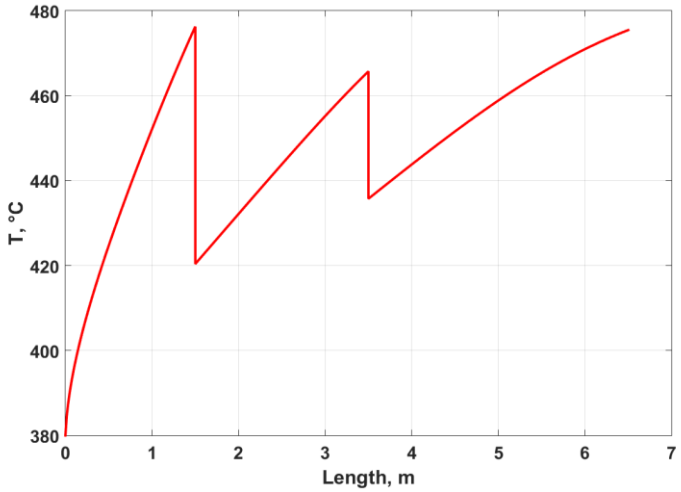

Fig. 2. Temperature profile along the catalytic beds.

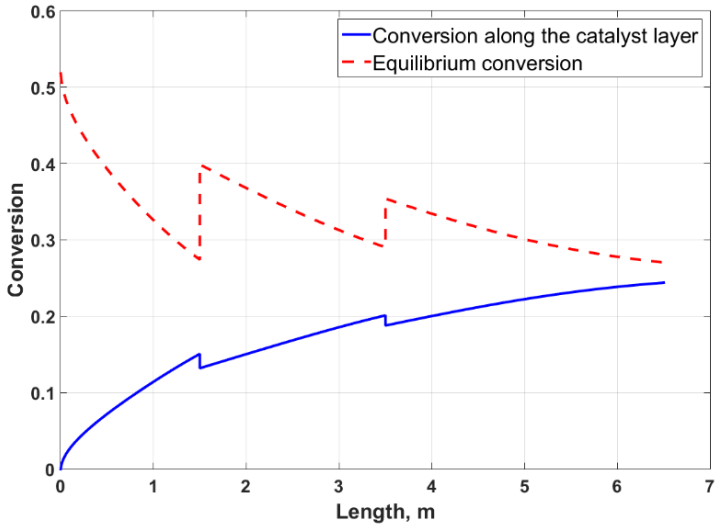

Fig. 3. Equilibrium and reaction conversion along the catalytic beds.

The representation of the equilibrium and reaction conversion together with the rate curves (Fig. 4) give a better insight of the process evolution. As it can be noticed, the operating line for all three layers is crossing the so called "line of maximum conversion" which interconnects the maximum points of the rate curves. This fact proves that the reactor with given catalytic layers length is well operated in order to obtain a good final conversion. Again, the position of the operating line of layer 1 indicates that its length could have been increased.

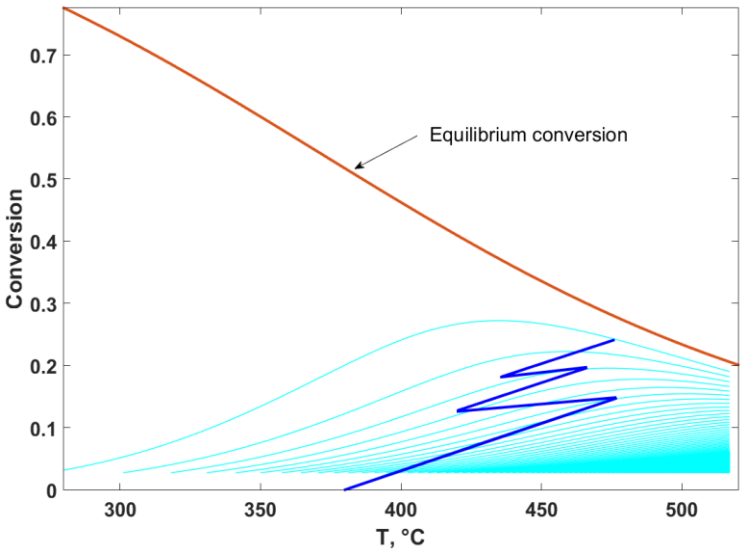

Fig. 4. Conversion and process rate curves vs. temperature

3.2 Multi-objective optimization

As the problem involves conflicting objectives (high conversion and small catalytic bed length) there is a trade-off between these objectives and there is no simultaneous optimum. There can be identified "compromised solutions" which define a so- called Pareto optimum set and where from a given selection can be made considering other technical or economical elements.

The optimization was carried out for the same operating conditions presented in Table 2 and the same diameter of the reactor. In this approach the heights of catalytic beds are decision variables together with the split ratios of the feed used for intermediate cooling.

The Pareto front is presented in Fig. 5 and shows the set of optimal solutions. This set shows possible conversion that can be realized with given heights of catalytic layers. As can be seen, smaller total heights (3-4 m) can ensure conversions up to 20-21% while a conversion of over 25% can be achieved with total length greater than 7 m. It can also be noticed that the increase in conversion with 2% can be realized if the catalyst layer increases from 4 to 5 meters while only 1% in conversion can be added for an increase of the catalyst layer from 6 to 7 m. From the Pareto front, some numerical values are presented in Table 4.

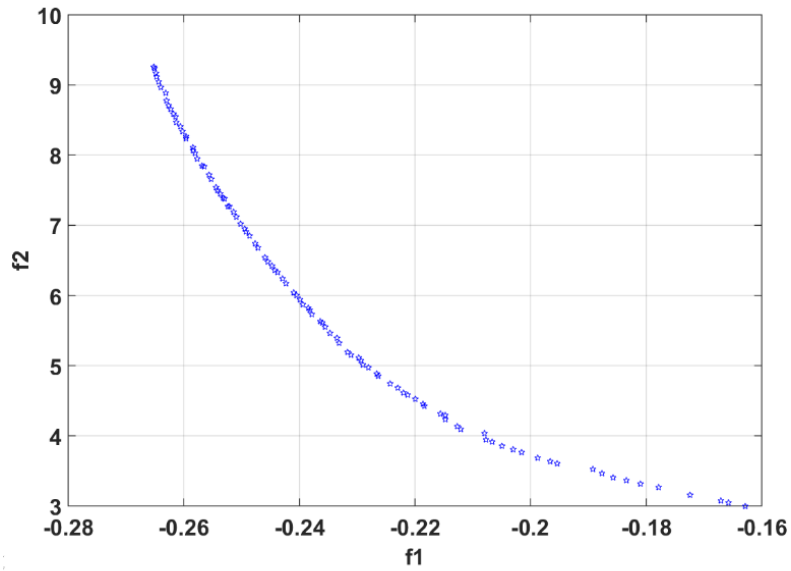

Fig 5. Pareto front for the minimization of the vector function F (rel. 27-28).

Table 4

Data selected from the Pareto front

Dm_1/Dm	Dm_2/Dm	Dm_3/Dm	L_1 (m)	L_2 (m)	L_3 (m)	Conversion (%)	Total length (m)
0.812	0.119	0.069	2.03	1.73	2.40	24.3	6.13
0.845	0.102	0.053	2.00	1.25	1.90	23.1	5.15
0.849	0.101	0.051	1.81	1.09	1.78	22.3	4.68
0.769	0.140	0.091	2.13	2.51	3.47	25.8	8.12

Analyzing the data in table 4 it can be noticed that with a better distribution of the catalyst between the layers, and practically the main distribution of fresh gas for cooling, a total length of 6.13 m can ensure practically the same conversion as a total length of 6.5, value considered for the calculations presented in section 3.1. The heights of the three catalytic layers in this case is increased for layer 1 and decreased for layer 3, compared to the data previously used. Lines 2 and 3 in Table 3 show that good conversion (over 22%) can be obtained also with lower catalyst consumption. If higher values for conversion are desired, only an important increase in total catalyst layer can provide them. We studied the process for a total catalytic length of 8 m (distribute: 2 m on the first layer, 2.6 m on the second and 3.5 on the third layer), according to information in the last line in Table 3, and the evolution of temperature and conversion along the catalytic layers are presented in Fig 6 and Fig 7. As Fig 6 shows, the temperature reaches very high values in the first layer, but still admissible in order to get closer to the equilibrium curve.

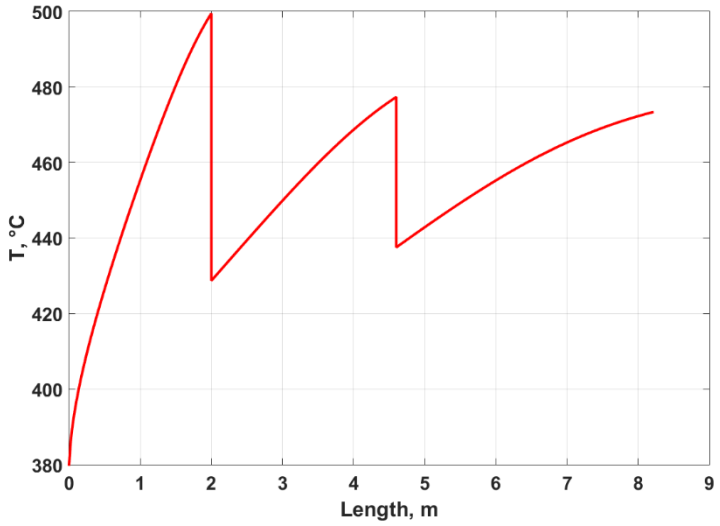

Fig 6. Temperature profile along the reactor for a total catalytic bed of 8.1 m.

The operating trajectory (Fig 7) shows a symmetric evolution around the "line f maximum conversion" and this is because conversion and the heights of catalytic layer were optimized simultaneously.

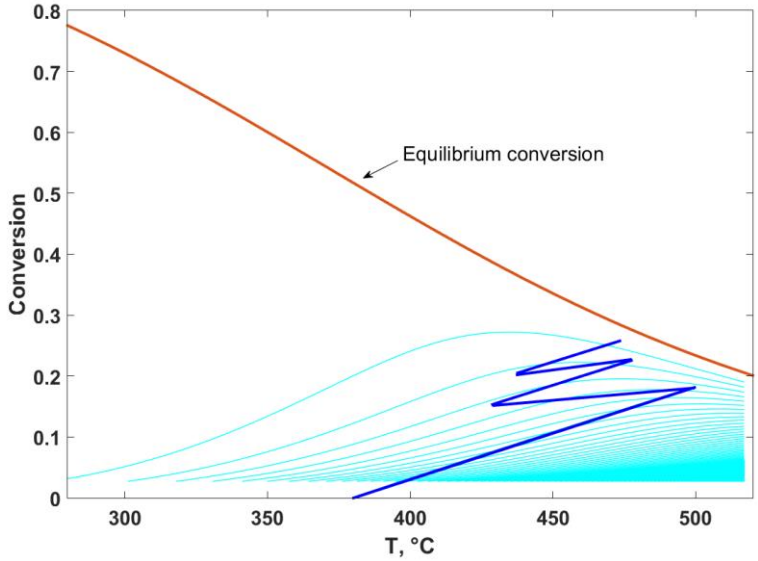

Fig 7. Operating line and rate curves vs temperature for a total catalytic length of 8.1 m.

4. Conclusions

The optimal conditions for the gas split between the catalytic layers on an ammonia reactor operated with direct cooling were determined aiming to obtain a maximum nitrogen conversion for a given design in terms of reactor cross-section and hights of catalytic layers. The temperature and conversion profiles along the catalityc beds proved to be in accordance with technical restrictions. The multi-objective optimisation considering the conversion maximisation and total catalytic hight minimisation proved to be an usuful tool for providing a set of equi-optimal solutions for the catalytic leyers distribution and inlet gas split to ensure the intermmediate cooling. From the multiple solution provided by the Pareto front some convenient ones may be chosen according to the users's needs.

REFERENCES

[1] Lin B., Wei K., Ni J., Lin J., *KOH activation of thermally modified carbon as a support of Ru catalyst for ammonia synthesis*, ChemCatChem, 5, (2013), 1941-1947.

[2] Khademi M. H., Sabbaghi R. S., *Comparison between three types of ammonia synthesis reactor configurations in terms of cooling methods*, Chemical Engineering Research and Design, 28, (2017), 306–317.

[3] Annable D., *Application of the Temkin kinetic equation to ammonia synthesis in the large-scale reactors*, Chemical Engineering Science, 1, (1952), 145-154.
[4] Murase A., Roberts H. L., and Converse A. O., *Optimal thermal design of an autothermal ammonia synthesis reactor*, Industrial and Engineering Chemistry Process Design Development, 9, (1970), 503–513.
[5] Babu B. V., Angira R., *Optimal design of an auto-thermal ammonia synthesis reactor*, Computers & Chemical Engineering, 29, (2005), 1041-1045.
[6] Dashti A., Khorsand K., Marvast M. A., Kakavand M., *Modeling and simulation of ammonia synthesis reactor*, Petroleum & Coal, 48, (2006), 15-23.
[7] Florez-Orego D., De Oliveira Junior S., *Modeling and optimization of an industrial ammonia synthesis unit: An exergy approach*, Energy, 137 (2017), 234-250.
[8] Gaines, L.D., *Optimal temperatures for ammonia synthesis converters.* Industrial & Engineering Chemistry Process Design and Development, 16, (1977), 381–389.
[9] Sadeghi, M.T., Kavianiboroujeni, A., *The optimization of an ammonia synthesis reactor using genetic algorithm*, International Journal of Chemical Reactor Engineering, 6, (2009), 1–18.
[10] Dyson, D.C., Simon, J.M., *A kinetic expression whit diffusion correction for ammonia synthesis on industrial catalyst*, Industrial & Engineering Chemistry Fundamentals, 7, (1968), 605–610.
[11] Gillespie, L. J., Beattie J. A., *The Thermodynamic Treatment of Chemical Equilibria in Systems Composed of Real Gases. I. An Approximate Equation for the Mass Action Function Applied to the Existing Data on the Haber Equilibrium*, Physical Review, 36, (1930), 743-753.
[12] Reid R. V., Prausnitz J. M., Poling B. E., *The properties of gases & liquids*, Fourth Edition, McGraw-Hill, 1977.
[13] Gunantara N., *A review of multi-objective optimization: Methods and its applications*, Cogent Engineering, 5, (2018), online https://doi.org/10.1080/23311916.2018.1502242.

EXPERIMENTAL ASSESSMENT OF WATER INJECTION DOWNSTREAM OF A TURBO-ENGINE THAT WORKS ON NATURAL GAS

Radu MIREA [1], Ene BARBU[1], Valeriu VILAG[1], Mădălin DOMBROVSCHI[1], Laurenţiu CEATRĂ[1*], Octavian BOCIAR[1]

[1]*COMOTI Romanian Research and Development Institute for Gas Turbines, 220D, Iuliu Maniu Blvd., 061126, Bucharest ROMANIA*

Abstract*. Civil and military aviation is still remaining a rapidly developing field that has a large environmental impact mainly due to acoustic and gaseous emission (CO, NO_x, CH_4) pollutants. These have a serious impact on people, animals and environment leading to stress, sleep disorder, respiratory and/or cardiac affection and even cancer. Although many protocols and agreements have been enforced internationally (Kyoto protocol 1997) and/or regionally, technical progress is still remaining the main field that has the strongest impact on environment in terms of pollutant reduction (acoustic, gaseous, etc.) by increasing energy efficiency, traffic management and new plane models. First experiments consisting of water injection within a turbo-engine have been made in 1958 and the aim was noise reduction. The water was injected within a circular collector having 6 1/2" and 6 1/4" nozzles placed downstream post-combustion. At INCDT COMOTI a research programme is undergoing, aiming to assess the influence of water injection downstream of turbo-engine. Present paper is presenting the experimental data collected on a test bench situated near a residential area in terms of NO_x emission and its dispersion within the surrounding area when water was injected downstream the turbo-engine when idling and working on natural gas.*

Keywords: gas turbine, post combustion, test bench, emissions, modelling.

1. Introduction

In our ever growing society, the economical development led to an increase of noise and gaseous pollution, having heavy impact on humans, animals, plants, etc., leading to stress, sleep disorder, respiratory and/or cardiac affection and even cancer. In the last 30 years the noise produced by air transport has been drastically reduced by combining technological innovations and international legislation for noise reduction.

EU target for aerial transport, imposes a 50% noise reduction by 2020 and 65% by 2050 by comparing with 2000 ACARE (Advisory Council for Aeronautics Research in Europe) [1]. The researches related to propulsion systems are mainly focused on improving performances and continuous weight reduction and secondary noise and gaseous emission reduction. First water injection experiment was performed in 1958 aiming the reduction of noise and injecting water within a ring-shaped collector having 6 1/2" and 6 1/4" nozzles placed downstream post-combustion [2].

*Corresponding author:laurentiu.ceatra@comoti.ro

The increased impact of aviation gaseous emissions on the atmosphere has been the catalyst for trials on gaseous and particulate matter emission reduction of a jet engine. Nevertheless nitrogen oxides (NO_x) are particularly difficult to control, therefore this type of emissions are higher than other types. Thus, a considerable effort was made to quantify these NO_x emissions [3].

In the field of natural gas based co-generative plants, water injection is often used for NO_x reduction, but in the field of aerial transport, this solution may be used during takeoff and shortly during ascension period.

The enforced limitations are more and more restrictive [4], thus, an integrated research to enclose noise and emissions is needed. At COMOTI, researches have been carried out on the post-combustion testing rig regarding the impact of water injection on TA2 turbo engine's intake working idle [5]. The testing rig's placement enforced a thorough investigation on NO_x emissions impact at the border of industrial and residential area.

TA2 turbo engine is actually a helicopter TV2-117A turbo engine modified to run on natural gas by the COMOTI scientists. There are several research projects aiming to investigate noise reduction of jet engines by integrating chevron systems along with water/air injection. It is to be expected that water injection in particular to lead to NO_x decrease. Thus, the present paper is showing the preliminary results on NO_x reduction obtained during water injection downstream the turbo engine working on idle and the impact on the residential area.

2. Experimental

COMOTI's testing rig consists of: TA2 turbo engine working on natural gas and placed horizontally, post-combustion facility placed vertically, water injection facility and command and data acquisition chamber.

Post-combustion facility (fig. 3) consists of 3 post-combustion modules and post-combustion chamber, which acts also as a chimney. During the experiments shown within current paper, post-combustion facility was turned off, so its main role was as chimney. Water injection probe (figs. 1 and 3) was placed inside post-combustion chamber after 3 module burner.

Constructive parameters of the chimney for emissions exhausting are:

- Chimney height: 5 m;
- The equivalent diameter of the chimney: 0.819 m.

Gaseous emissions have been measured to the test bench chimney (post combustion chamber) with a gas analyzer MRU type, placed as in figs. 3 and 4.

The MRU type gas analyzer allows the measurement of NO_x, CO, CH_4 and gas temperature.

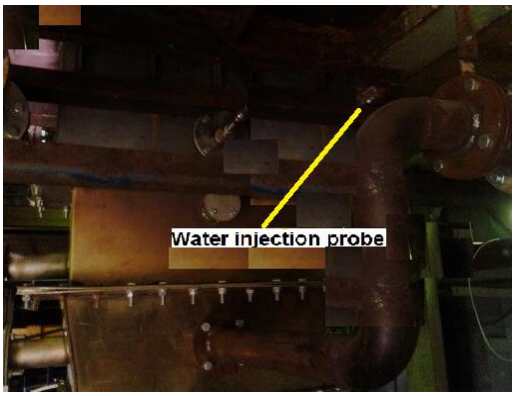

Fig. 1. Water injection probe, downstream TA2 turbo engine

Fig. 2 Testing rig

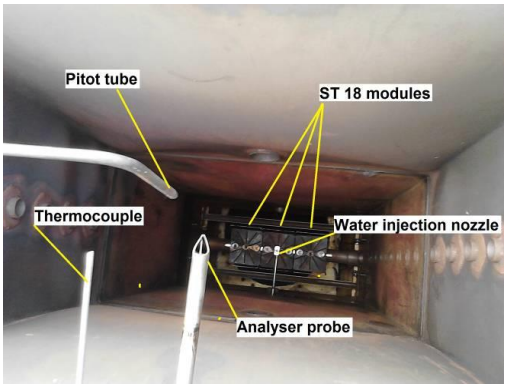

Fig. 3. Burner view with ST 18 post combustion module

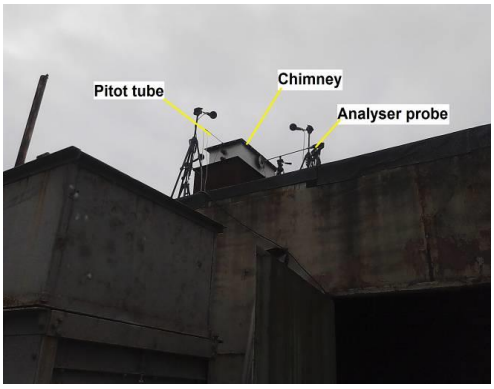

Fig. 4 The Gas analyzer at the test bench chimney

The experiments were carried out in 2 regimes:

- Regime 1 - Turbo-engine working on natural gas with (idling);
- Regime 2 - Turbo-engine on natural gas with and injected water (idling).

After switching on the turbo-engine on natural gas (Version 1) and getting a stationary regime (corresponding to a constant flow of natural gas), it was kept for 10 minutes and all the values were recorded.

After 10 minute of working, the water injection was turned on (Version 2) and kept for 10 minutes.

For each operating versions, have been recorded simultaneously the required parameters as follows:

- using the MRU analyzer, were recorded: gas temperature, NO_x, CO and CH_4 emissions at bench chimney;
- using the mobile air quality monitoring lab, NO_x concentrations were recorded and at the interface between industrial and residential area.

3. Results and discussions

The starting of the turbo-engine working on natural gas and exhausting gas led to a maximum working temperature of 342.6^0C and in the moment the water was injected, the temperature dropped almost instantly until 337.8^0C. The recorded temperature after 10 minutes of water injection was even lower: 336.1^0C, as seen in fig. 5.

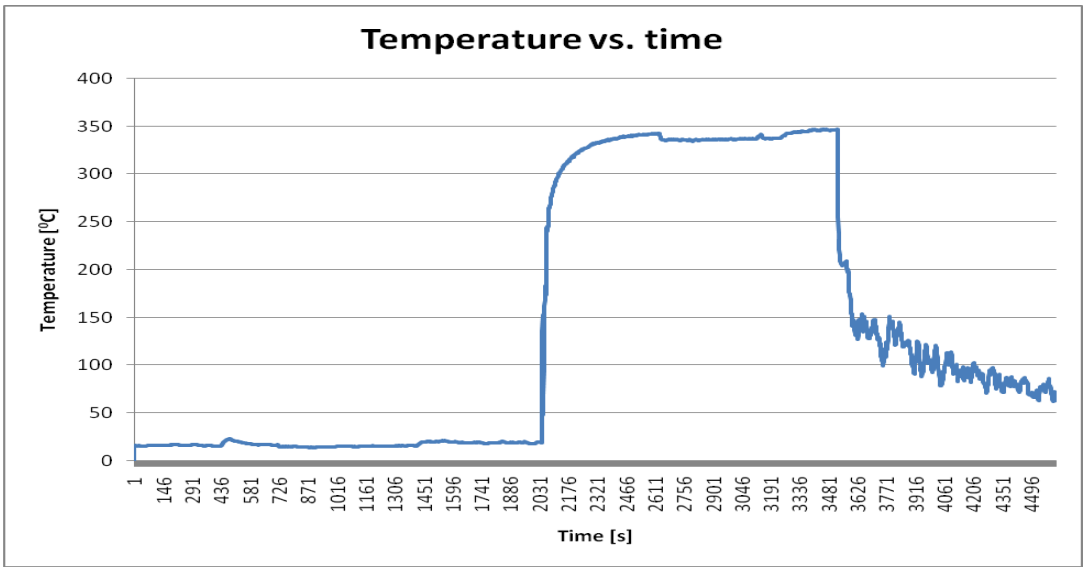

Fig. 5 Temperature variation vs. Time

After 10 minutes, the water was injected and the temperature drop was recorded. After the water injection was performed for 10 minutes, it was stopped and again, the temperature increased. In the end, the turbine was shouted down and let to cool.

The recorded temperature difference was 4.8^0C immediately after the water injection started and reached 6.5^0C at the end of injection period, meaning a drop of 1.4 - 1.9%.

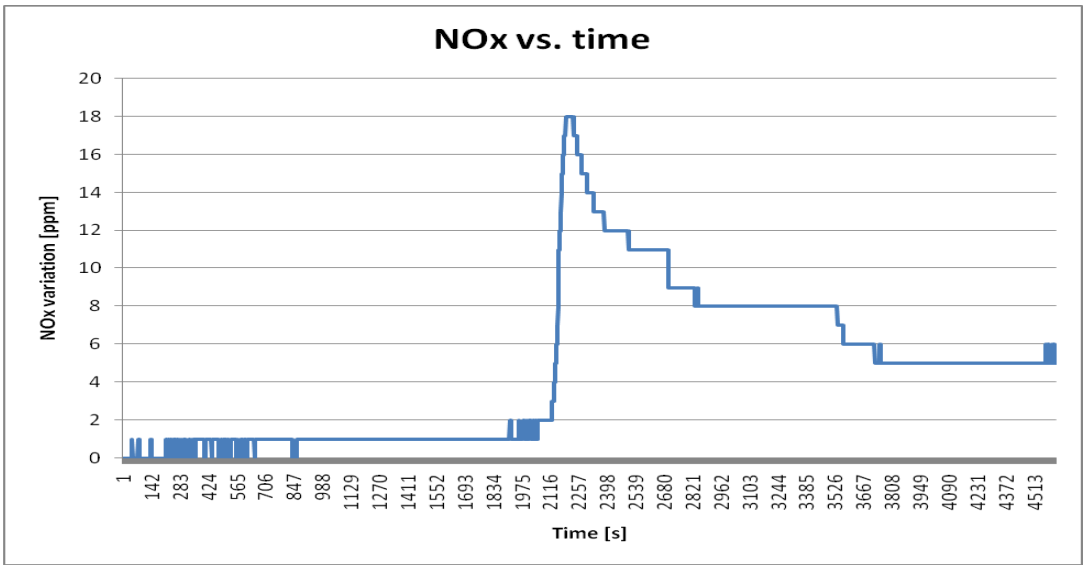

Fig. 6 NOx variation vs. time

Figure 6 is showing the NO_x variation during the testing period. When the fuel was injected and the burning started, NO_x value suddenly increased until 18 ppm and decreased slowly until 9 ppm as the engine stabilizes, but in the moment when the water was injected it dropped until 8 ppm. The recorded difference value was between 1 ppm, meaning 11% decrease and the 35-45 seconds gap between the injection time and registered value is due to the NO_x sensor lag inside MRU analyser.

Figures 7 and 8 are showing the dispersion of gaseous pollutants trough out the entire period of experimental research, meaning 10 minutes without water injection and 10 minutes with water injection.

As can be seen the NO_x concentration at the interface between the industrial and residential area decreases by almost 50%. The registered values from which the dispersion maps have been drawn are: for version 1 - 6.73 ppm and for version 2 - 5.59 ppm meaning an almost 17% decrease between the two regimes and also considerable decrease in relation with the chimney measured values, as: for regime 1 a decrease from 9 to 6.73 ppm, more than 25% and for regime 2 a decrease from 8 to 5.59 ppm meaning more than 30%.

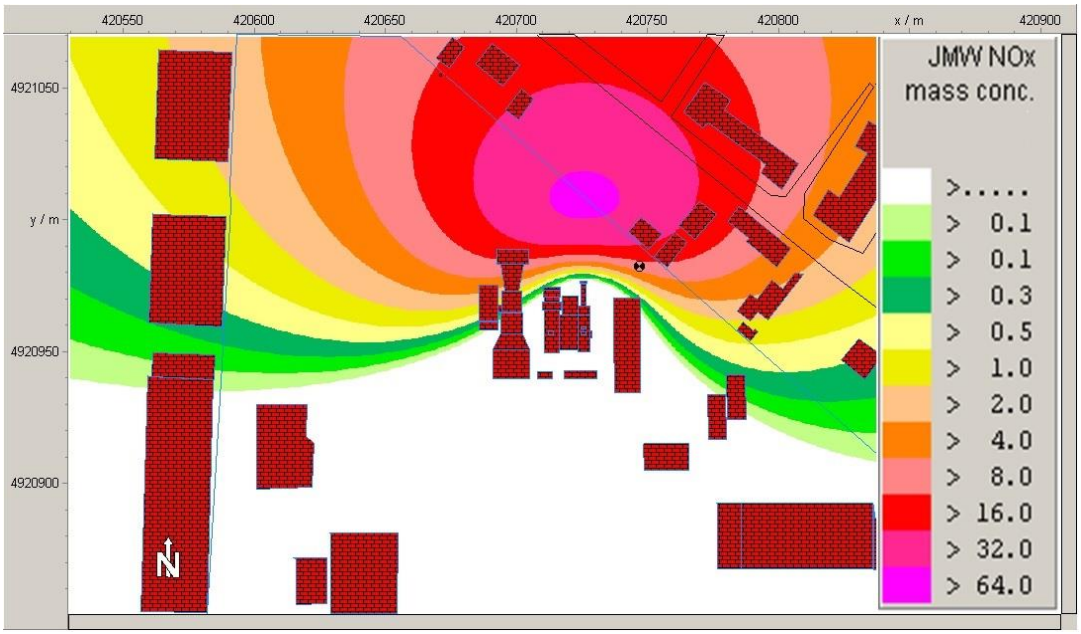

Fig. 7 NO_x dispersion in regime 1

Fig. 8 NO_x dispersion in regime 2

4. Conclusions

- The use of water injection within a post combustion facility of a gas turbine may represent a viable solution for decreasing the gaseous emissions of a co-generative plant.
- Testing a turbo-engine on the bench is usually made at nominal load. Due to the more and more restrictive environmental requirements, emissions researches were needed related to idling regime of the gas turbines group. Researches from COMOTI Romanian Research and Development Institute for Gas Turbines Bucharest focused on NO_x emissions from bench testing of a gas turbine when idling operates (in starting regime).
- The most important drop is obtained for NO_x emissions but it is to be mentioned that the significant decrease may be measured at the interface between the industrial and residential area meaning the public and environment health are in no danger while the test bench is working.
- As there is a constant attention and also the possibility to increase the test bench's load, it results that there is no danger for the set values by the in force law to be exceeded at the interface with the residential area.

REFERENCES

[1] Gely D., Leylekian L., *Civil aircraft noise reduction: Summary of recent research and overview of fortcoming effort to promote new research within European context*, Proceedings of 22nd International Congres on Acoustics, Buenos Aires, 2016.
[2] Kurbjun C. M., *Limited investigation of noise suppression by injection of water into exhaust of afterburning jet engine*, NACA RM L57L05, 1958.
[3] Yize Liu et al, *Review of modern low emissions combustion technologies for aero gas turbine engines (Accepted Manuscript)*, Process in Aerospace Sciences, Vol. 94, October 2017, 12-45.
[4] Directive 2008/50/EC of the EUROPEAN PARLIAMENT and of the COUNCIL of 21 May 2008 on ambient air quality and cleaner air for Europe
[5] Barbu E., Mirea R., Creţu M., Deaconu M., Vilag V., *The impact of water injection within a gas turbine's intake, at its starting on the test bench*, 18th International Multidisciplinary Scientific GeoConference SGEM 2018, www.sgem.org, SGEM2018 Conference Proceedings, ISBN 978-619-7408-45-4 / ISSN 1314-2704, 2 - 8 July, 2018, Vol. 18, Issue 4.2, 647-654.

PARAMETERS IDENTIFICATION FOR SHRINKING CORE MODEL IN $CaCO_3$ CALCINATION

Alexandra MOCANU[1], Sorina TEIUSANU [1], Cristian RĂDUCANU[1], TANASE DOBRE[1,2*]

[1]Faculty of Applied Chemistry and Materials Science, University POLITEHNICA of Bucharest, 1-3 Gheorghe Polizu Street, 011061, Bucharest, Romania;
[2]Technical Science Academy of Romania, 26 Dacia Boulevard, sector 1, Bucharest, Romania

Abstract

A mathematical model to predict how the dynamics of calcium carbonate calcination is influenced by the contracting core, when calcining $CaCO_3$ was developed. Experimental data, regarding the decomposition of particles of 6 mm, 4 mm and 2 mm size at temperatures over 1000 K, was used to identity the CO_2 concentration at the reaction front (C_R), the ratio (r_D) between in particle and out particle diffusion coefficients, the reaction constant (k) of decomposition rate at high conversion and the time (τ_s) for touching high conversion level, which are the model parameters. A dependence upon temperature of calcination was proposed for these parameters. More published data concerning the dynamics of $CaCO_3$ conversion are covered with the obtained model.

Key words: Calcination kinetics, mathematical model, shrinking core model, parameters identification, data correlation

1. Introduction

Carbon sequestration or CO_2 capturing, two of the most challenging anthropogenic-like issues to be solved, involve, besides establishing the causes and blame attribution, reviewing some sort of primary CO_2 formation cycle, already present in multiple globally industrial processes [1]. Among processes that claims the CO_2 capture, the $CaCO_3$ calcination is extreme important due to it large industrial implementation [2]. More points of view were considered in establishing of various kinetics models for this process. In shrinking core calcining kinetic models, the competition between surface reaction and CO_2 diffusion, through the calcium oxide resulted product, separates various models. In some models, as those here considered the temperature dependence of the CO_2 concentration at reaction front and the effective CO_2 diffusion coefficient through

* Corresponding author: Email address: tanase.dobre@upb.ro

small pores resulted calcium oxide, appears as model parameters. These mathematical model variables, implemented in a concrete model, can capitalize current exploitation or future designing of industrial reactors for calcining process [3-6].

2. Shrinking core mathematical model

Calcination of calcium carbonate is a kinetic process in which, following heating of a particle with a fixed calcium carbonate content, it decomposes (1), so that the particle is gradually covered with a layer of calcium oxide.

$$CaCO_3 \rightarrow CaO + CO_2 \quad (1)$$

For this process we analyze the calcination of some spherical particles for which a large mathematical model contains [7-10]: i) the equation of temperature field inside of particle, ii) the equation of the concentration field of calcium carbonate or carbon dioxide in particle, iii) the expression of chemical kinetics regarding the consumption of calcium carbonate, iv) the expression showing the reaction enthalpy dependence upon temperature and calcium carbonate concentration and respectively v) univocity conditions for temperature field and calcium carbonate or carbon dioxide concentration field.

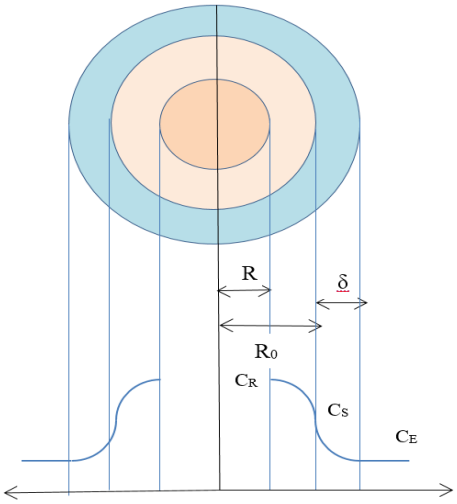

Fig. 1. Schematic presentation for the model of the contracting core with it characteristic carbon dioxide concentration profile (blue – gas boundary layer, pink – calcium oxide cylindrical layer, light brown –spherical calcium carbonate core).

Various ways were taken into account in order to produce alternatives to the above presented model, which is complicated, respect to its equations content. On one of these ways is the shrinking core model. The model of the shrinking core considers that, at constant temperature, the size of the calcium carbonate granule diminishes over time with simultaneous carbon dioxide diffusing, from its surface, through the calcium oxide layer and then through the boundary layer surrounding the particle.

The calcination process consists of three series of stages: i) the surface reaction with carbon dioxide generation with the C_R concentration level (Fig. 1); ii) diffusion of carbon dioxide from the surface, of the active core of $CaCO_3$, through the calcium oxide layer; iii) diffusion of carbon dioxide through the boundary layer surrounding the particle.

In isothermal conditions, if the diffusion rate is much faster than the rate of change of the reacting core, then the diffusion process can be characterized to be near stationary. In accordance with Fig. 1, the relation and conditions (2) and relation and conditions (3) are used to express the concentration field of carbon dioxide in the calcium oxide crust and respectively to fluid film adjacent to the particle.

$$D_1\frac{\partial}{\partial r}\left(r^2\frac{\partial C}{\partial r}\right)=0,\ \mathrm{R}\le \mathrm{r}\le \mathrm{R}_0, C(R)=C_R, C(R_0)=C_S \tag{2}$$

$$D_2\frac{\partial}{\partial r}\left(r^2\frac{\partial C}{\partial r}\right)=0,\ \mathrm{R}_0\le \mathrm{r}\le \mathrm{R}_0+\delta, C(R_0)=C_S, C(R_0+\delta)=C_E \tag{3}$$

The integration of these equations with its specified conditions, leads to equations (4) and (5), which show the state of gradient of carbon dioxide concentration in CaO crust, respectively, in particle boundary layer.

$$\frac{dC}{dr}=\frac{\mathrm{C_R}-C_S}{r^2(1/R-1/R_0)},\ \mathrm{R}\le \mathrm{r}\le \mathrm{R}_0 \tag{4}$$

$$\frac{dC}{dr}=\frac{\mathrm{C_S}-C_E}{r^2(1/R_0-1/(R_0+\delta))},\ \mathrm{R}_0\le \mathrm{r}\le \mathrm{R}_0+\delta \tag{5}$$

Relation (6) takes into account that at the boundary R_0 there must be continuity of the flow of carbon dioxide transferred. Taking into account the relations (4) and (5) in relation (6) can be obtained the relation (7). Now the concentration of carbon dioxide at the outer surface of the particle could be immediately expressed (8).

$$\left(4\pi R_0^2\right)D_1\frac{dC}{dr}_{r=R_0}=\left(4\pi R_0^2\right)D_2\frac{dC}{dr}_{r=R_0+} \tag{6}$$

$$D_1\frac{C_R-C_S}{(1/R-1/R_0)}=D_2\frac{C_S-C_E}{(1/R_0-1/(R_0+\delta))} \tag{7}$$

$$C_S=\frac{r_D C_E(1/R_0-1/(R_0+\delta))+C_E(1/R-1/R_0)}{r_D/(1/R_0-1/(R_0+\delta))+1/(1/R-1/R_0)} \tag{8}$$

In relation (8) r_D is the diffusion coefficients ratio, *i.e.* $r_D = D_2/D_1$. According to relation (1), the molar flow rate of the resulting carbon dioxide is equal to the flow of calcium carbonate consumed. Thus, can be written the relation (9), which, in combination with the relation (4), leads to the equation (10). This differential equation shows how the radius of the unreacted core, that contains calcium carbonate, changes over time.

$$\frac{d}{d\tau}\left(\frac{4\pi R^3(1-\varepsilon)\rho_s}{3M}\right)=-4\pi r^2 D_1\frac{dC}{dr} \quad R\prec r\prec R_0 \tag{9}$$

$$\left(\frac{(1-\varepsilon)\rho_s}{M}\right)R^2\frac{dR}{d\tau}=-D_1\frac{C_R-C_S}{(1/R-1/R_0)} \quad R\prec r\prec R_0 \tag{10}$$

Replacing the relation (8) in equation (10) and rearranging the terms, the differential equation (10) will take the form (11):

$$R^2\left(1+\frac{r_D(1/R-1/R_0)}{1/R_0-1/(R_0+\delta)}\right)\frac{dR}{d\tau}=-\frac{MD_1r_D(C_R-C_E)}{\rho_s(1-\varepsilon)(1/R_0+1/(R_0+\delta)} \tag{11}$$

For a given decomposition temperature C_R can be assumed to be constant. If the calcination is done in a gas stream in natural convection or in a large volume of gas, and the concentration of carbon dioxide away from the particle can be C_E, it can be considered constant and noted. It follows that equation (11) can be integrated with the initial condition shown in relation (12). Taking into account the connection between the current radius of the core, the initial radius of the particle and the definition of calcium carbonate conversion (13), the result of the integration of the differential equation (11) takes the form of equation (14). This is an implicit equation that, for a fixed time allows the calculation of the value of the calcium carbonate conversion.

$$\tau=0 \quad R=R_0 \tag{12}$$

$$X=\frac{R_0^3-R^3}{R_0^3} \tag{13}$$

$$\frac{R_0^3}{3}\left(1-\frac{r_D}{R_0(1/R_0-1/(R_0+\delta)}\right)X+\frac{r_DR_0^2}{2(1/R_0-1/(R_0+\delta))}(1-(1-X)^{\frac{2}{3}})=\frac{MD_1r_D(C_R-C_E)}{\rho_s(1-\varepsilon)(1/R_0+1/(R_0+\delta)}\tau \tag{14}$$

If experimental data are available to show the evolution of the conversion over time at a given temperature, the result obtained in relation (14) can be oriented mainly to determine the concentration of carbon dioxide, at the reaction front and the ratio of diffusion coefficients. Since the diffusion coefficient of carbon dioxide in the gas film, surrounding the particle, can be easily calculated, it follows that information can be obtained about the state of diffusion coefficient in fine porous calcium oxide crust.

A transformation after calcium carbonate conversion of relation (11) is possible by considering the connection *R vs. X*, as it is shown in relation (13). The result expressed by relation (15) is important, because it can be used as relation expressing chemical kinetics, for the reactors design, where occurs the thermal decomposition of calcium carbonate.

$$\frac{dX}{d\tau}=-\frac{3}{R_0}\left(\frac{\left(\frac{MD_1 r_D (C_R-C_E)}{\rho_s(1-\varepsilon)(1/R_0+1/(R_0+\delta)}\right)}{\left(1+\frac{1/(R_0(1-X)^{1/3}-1/R_0}{1/R_0-1/(R_0+\delta)}\right)}\right) \tag{15}$$

Taking into account the dynamics of $CaCO_3$ particle at high conversion, especially over 85%, it was established that here the conversion follows an exponential evolution [11,12]. Consequently, the relation (14) and respectively (15) will be completed. The filling out of relation (14) leads to relation (16), which shows that our model contains 4 parameters. These parameters are: c_R ($kmoli_{CO2}/m^3$) - carbon dioxide concentration at surface of active core, r_D (dimensionless) – ratio between carbon dioxide diffusion coefficient in porous calcium oxide and carbon dioxide diffusion coefficient outside of particle, k (s^{-1}) – kinetic reaction constant for $CaCO_3$ degradation at high conversion, τ_s (s) – characteristic time showing the touching of $CaCO_3$ conversion over 0.85.

$$X(\tau)=\frac{root\left(\frac{R_0^3}{3}\left(1-\frac{r_D}{R_0(1/R_0-1/(R_0+\delta)}\right)X+\frac{r_D R_0^2}{2(1/R_0-1/(R_0+\delta))}\left(1-(1-X)^{2/3}\right)=\frac{MD_1 r_D(c_R-c_E)}{\rho_s(1-\varepsilon_s)(1/R_0+1/(R_0+\delta)}\tau\right), X\le 0.85}{0.85\exp(-k(\tau-\tau_s), \ X\succ 0.85} \tag{16}$$

3. Experimental

An experimental set composed of a sensible balance (precision under 0.01 g) with computer link and a vertical cylindrical laboratory oven, equipped with temperature-controlled system, was used in experimental investigation. Spherical particles of $CaCO_3$ having the diameter of 6 mm, from Holcim Romania, were used as samples for calcination testing. The $CaCO_3$ particle is a calcite type and a SEM image of it is given in figure 2. It is expected that CaO resulted from calcining will keep this very fine porous structure, revealed by Fig.2. The sample

caught on top of a thin vertical rod is placed in the mounting bracket on the balance tray. Over the sample is lowered the cylindrical oven having the selected operating temperature (1075, 1125, 1175 and 1225 K).

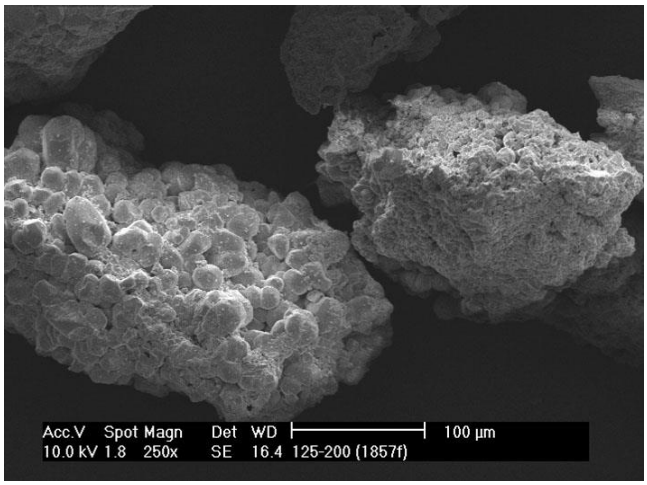

Fig.2. Microscopic image of the crystalline structure of the calcite particle

Table 1

Dynamics of calcite to calcium oxide conversion for 6 mm particles

Crt.no.	Time (min)	T=1075 K	T= 1123 K	T=1173 K	T= 1223 K
1	0	0	0	0	0
2	1	0.067	0.104	0,105	0.106
3	2	0.121	0.205	0.251	0.434
4	3	0.173	0.375	0.411	0.783
5	4	0.224	0.445	0.537	0.866
6	5	0.266	0.508	0.636	0.917
7	6	0.319	0.564	0.713	0.949
8	7	0.349	0.613	0.775	0.968
9	8	0.387	0.657	0.825	0.98
10	9	0.423	0.731	0.860	1
11	11	0.456	0.762	0.890	1
12	12	0.488	0.788	0.914	1
13	13	0.518	0.812	0.932	1
14	14	0.546	0.831	0.947	1
15	15	0.564	0.849	0.958	

The mass loss of the sample is recorded by computer connected to the balance. From mass-time file it computes the momentary conversion $X= 1-m_0/m_\tau$. In this computation the process start basic time is considered those where m_τ

becomes observable. Table 1 contains the obtained conversion dynamics for above specified temperature (1075 K, 1125 K, 1175 K, respectively, 1225 K).

4. Results and discussions

In order to obtain the temperature dependence of c_R, r_D, k and, respectively, τ_s, our model parameters, a Mathcad computation solution was developed. This solution contains the following sequences: i) equation (16) is put in numerical form as solution X_t (c_R, r_D, k, τ_s, τ), ii) for the first temperature c_R, r_D, k and τ_s are identified by minimizing the mean square deviation between the experimental dynamics of conversion and those predicted numerically; iii) the identification sequence is repeated for all other temperatures. Referring to Mathcad model solution it is specified that: a) the diffusion coefficient of carbon dioxide in air D_1 was calculated with the relation Hirschfelder-Bird-Spotsz, ii) the thickness of the boundary layer around the particle was obtained by accepting the constant value of the Sherwood number, for the transfer of carbon dioxide from the spherical particle to the neighboring air ($Sh=2$); iii) the concentration of carbon dioxide, away from the particle, was considered equal to that in the air (almost zero). Table 2 contains results of this procedure, using table 1 data.

First of all, we observe the independency of r_D upon temperature. This fact is expected taking into account that r_D depends only on solid CaO pores fraction (ε) and mean pores tortuosity (ζ), as it results from relation (17).

$$r_D = (\varepsilon D_{CO2}(\mathrm{T})/\zeta)/D_{CO2}(\mathrm{T}) = \varepsilon/\zeta \qquad (17)$$

Table 2

Identified model parameters based with experimental data from Table 1

T ^{0}K	1075	1125	1175	1225
r_D	0.125	0.123	0.115	0.116
c_R kmoli/m^3	0.002	0.005	0.025	0.08
k s^{-1}	0.001	0.002	0.004	0.0075
τ_s s	1610	781	420	239

The results showed that all the other model parameters have strong temperature dependence. Regarding the c_R dependence on T, was checked to express it, by analogy with the temperature dependence of the vapour pressure of sublimable solids and liquids [13]. Very good results were obtained with the polynomial expression (18). It is extremely important to show that there are no reasons to consider that the carbon dioxide pressure at the reaction front would depend on other factors, for example size particle.

$$c_R(T) = 55.711 - 144.917\left(\frac{T}{1000}\right) + 125.3\left(\frac{T}{1000}\right)^2 - 36\left(\frac{T}{1000}\right)^3 \qquad (18)$$

The other two parameters of the model follow a temperature dependency that highlight an almost exponential evolution with 1/T in argument, as it is indicated by the general relation (19).

$$y(T) = \exp\left(a - \frac{b}{T + c}\right) \tag{19}$$

Particularization of the relation (19) to the dependencies k vs. T and τ_s vs. T leads to relations (20) and (21). Obviously, these relationships are for particles used in experimental analysis from table 1 (d_p= 6 mm). In order to highlight the influence of particle size on these last two parameters, new experimental measurements were made, at 1125 K, with calcite particles of 4 mm and 2 mm, for which table 3 shows the process conversion dynamics. The results of these data processing showed that r_D and c_R have the values reported, for this temperature, in table 2. Table 4 shows how k and τ_s evolve at 1125 K, according to the radius of the particle subjected to calcination. Relationships (22) and (23) quantitatively show this dependence. The coupling of relations (20) and (21) with relations (22) and (23) leads to expressions that show the effect of particle size and calcination temperature on constant of calcite decomposition rate (k) respectively on time for touching a conversion over 85% (τ_s)

$$k(T) = \exp\left(9.317 - \frac{16850}{T - 39.438}\right) \tag{20}$$

$$\tau_s(T) = \exp\left(-8.359 + \frac{16750}{T - 10.95}\right) \tag{21}$$

$$k(R) = 1.498\,10^{-5} R^{-0.881} \tag{22}$$

$$\tau_s(R) = 7.1790^{5} R^{1.18} \tag{23}$$

Table 3

Calcite conversion dynamics at 1125 K for 2 and 4 mm particles [14]

Nr crt	Timp (min)	d_p=0.004 m	d_p= 0.002 m
1	0	0	0
2	0.5	0.18	0.18
3	1	0.24	0.25
4	1.5	0.33	0.40
5	2	0.41	0.50
6	2.5	0.47	0.60
7	3	0.51	0.69
8	3.5	0.57	0.77
9	4	0.62	0.83
10	4.5	0.66	0.88
11	5	0.67	0.93
12	5.5	0.73	0.96
13	6	0.77	0.98
14	6.5	0.79	1.00

Table 4

Evolution of k and τ_s with particle diameter

Crt.no.	Parameters	d_p = 0.001 m	d_p = 0.002 m	d_p = 0.003 m
1	k	0.00658	0.0038	0.0021
2	τ_s	261	403	781

With the constant value establised for r_D (r_D= 0.118) and with the expressions (18), (24) and (25) for c_R, k and τ_s any case of calcination can be simulated. In this sense, the figure 3 show that our developed model can very well simulate the experimental data published by Escadrino et all [14]. For this simulation the computed values of model parameters are given in table 5

$$k(T,R) = 7.49\,10^{-3}\exp\left(9.317 - \frac{16850}{T - 39.438}\right)R^{-0.881} \qquad (24)$$

$$\tau_s(T,R) = 9.19\ 10^{2}\exp\left(-8.359 + \frac{16750}{T - 10.95}\right)R^{1.18} \qquad (25)$$

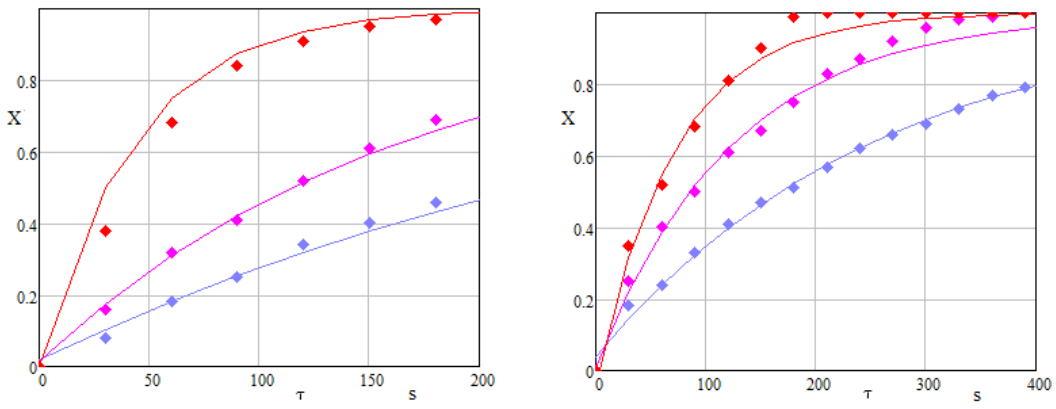

Fig. 3. Conversion dynamics for calcite particles of 0.002 (left) and 0.004 m (right) at 1125 0K (blue), 1175 0K (magenta) and 1225 0K (red) (continuous lines –shrinking core model, points – experimental data [15]

Table 5

Computation of model parameters value for simulation of experimental data [15]

Case	Parameters	T= 1125 ^{0}K	T= 1175 ^{0}K	T= 1225 ^{0}K
d_p=0.002 m	r_D	0.118	0.118	0.118
	c_R kmoli/m^3	0.005	0.025	0.038
	k s^{-1}	0.0077	0.014	0.027
	τ_s s	190	107	47
d_p=0.004 m	r_D	0.118	0.118	0.118
	c_R kmoli/m^3	0.005	0.025	0.038
	k s^{-1}	0.0039	0.0081	0.0139
	τ_s s	403	280	118

As it results from the case of simulation of experimental results of Escadrino et all [14], the developed model has the capacity to simulate almost any kind of calcium carbonate calcination experimental analysis. At the same time, the model can be used for sizing and for functional simulation of any type of CaCO3 calcination reactor, especially fluidized bed reactor, mobile bed reactor and respectively fixed bed reactor.

5. Conclusions

A mathematical model to predict how the dynamics of calcium carbonate calcination is influenced by the contracting core when calcining $CaCO_3$ was developed. For the range of high calcination conversion the shrinking core model is coupled with the exponential model. In order to identify the influence of temperature on the 4 parameters of model spherical calcite particles of 6 mm was calcined at 1075, 1125, 1175 and 1225 ^{0}K. Particle with 2 mm and 4 mm was calcined at 1125 0K with the aim to observe the influence of particle size on model parameters. The obtained expressions, showing the dependence of r_D, c_R, k and τ_s on T and R was used to simulate the experimental data reported by some papers. The model has the capacity to be used for analysis and optimization of all calcining reactors type.

REFERENCES

[1] Romsagar V., Bertran Maria-Oana, Frauzem Rebecca, Babu Ane Sarat, Rafiqul G., *Sustainable chemical processing and energy-carbon dioxide management: review of challenges and npportunities*. Chemical Engineering Research & Design, 131, 440-464, 2018.

[2] Felder-Casagrande S., H. G. Wiedemann G. H., Reller A.,*The calcination of limestone — Studies on the past, the presence and the future of a crucial industrial process***,** Journal of Thermal Analysis, 49,971-978, 1997.

[3] Kehat E., Markin A., *Calcination of limestone in a tubular reactor*, The Canadian Journal of Chemical Engineering, 45, 40- 45, 1967.

[4] Batenin M. V., Kovbasyuk I. V., Kretova G. L., Yu. V. Medvedev V, Yu., *Dust reactor for limestone calcination*, High Temperature, 53, 289-298, 2015

[5] Martínez I., Grasa G., Murillo R., Arias B., Abanades J.C., *Kinetics of Calcination of Partially Carbonated Particles in a Ca-Looping System for CO2 Capture*, Energy & Fuels, 26, 1432-1440, 2012.

[6] Mujumdar S. K., Ganesh V. K., Kulkarni B. S., Ranade V. V., *Rotary cement kiln simulator: Integrated modeling of pre-heater, calciner, kiln and clinker cooler*. Chemical Engineering Science, 62, 2590–2607, 2007.

[7] Ingraham R. J., Marier P., Kinetic *studies on the thermal decomposition of calcium carbonate*. Canadian Journal of Chemical Engineering, 41, 170– 173, 1963.

[8] Hills A.W.D., *The mechanism of the thermal decomposition of calcium carbonate*. Chem. Eng. Sci. 23, 297–320,1968.

[9] Mikulic H., von Berg E., Vujanovic M., Priesching P., Perovic L., Tatschi R., Duic N., *Numerical modeling of calcination reaction mechanism for cement production*, Chem. Eng. Sci., 69, 607-615, 2012.
[10] Garcıa-Labiano F., Abad A., Diego F. L., Gayan P., Adanez J., *Calcination of calcium-based sorbents at pressure in a broad range of CO2 concentrations*, Chemical Engineering Science, 57, 2381–2393, 2002.
[11] Ishida M. Wen Y. C., *Comparison of kinetic and diffusional models for solid-gas reactions*. AIChE Journal, 14, 311–317, 1968.
[12] Hallak B., Specht E., Herz F., Gröpler R., Warnecke G., *Simulation of lime calcination in Normal Shaft Kilns – Influence of process parameters*, Int. Journal of Cement Lime Gypsum 10, 46-50, 2015.
[13] Elder J.P., *Sublimation measurements of pharmaceutical compounds by isothermal thermogravimetry*, J. Therm. Anal., 49, 897–905, 1997.
[14] Escardino B. A., García T., Francisco J., Feliu M. C., Saburit L. A., Cantavella S.V., *Kinetic study of the thermal decomposition process of calcite particles in air and CO_2 atmosphere*, Journal of Industrial and Engineering Chemistry 19, 3, 1-25, 2013.

GUANIDINE-BASED SUPERBASE ON LIGNOCELLULOSIC RESIDUAL BIOMASS SUPPORT AS HETEROGENEOUS CATALYST FOR BIODIESEL PRODUCTION

Cristian Eugen RĂDUCANU[1], Oana Cristina PÂRVULESCU[*1], Doiniţa Roxana TÎRPAN[2], Tănase DOBRE[1,3]

[1]Faculty of Applied Chemistry and Materials Science, University POLITEHNICA of Bucharest, 1-3 Gheorghe Polizu Street, 011061, Bucharest, Romania
[2]Ovidius University of Constanta, 124 Mamaia Blvd., 900527, Constanta, Romania
[3]Technical Science Academy of Romania

Abstract

A supported alkaline catalyst was prepared by impregnating a support derived from apricot stones with a superbase obtained from guanidine and KOH. Batch transesterification runs of fresh sunflower oil with methanol (1/6 molar ratio) to fatty acid methyl esters (FAME) and glycerol were performed at 65 °C for 1.5 h in the presence of fresh and reused supported catalysts. Levels of FAME (biodiesel) yield in 11 transesterification cycles were in the range of 72-92%. Accordingly, the supported catalyst prepared from abundant and low-cost lignocellulosic residues impregnated with strong alkaline catalyst had a high catalytic activity in multiple production cycles.

Key words: biodiesel**,** guanidine, superbase, supported catalyst, transesterification

1. Introduction

There has been an obvious propensity lately to produce greener biodiesel to replace petroleum-based diesel. Biodiesel is obtained from renewable sources, generally vegetable oils, is less hazardous for the environment, and burns more cleanly than diesel fuel [1-6]. A greener biodiesel is one produced in a more economical process, *e.g.*, obtained by easy separation of the catalyst/product using a heterogeneous catalyst [7-13].

One way to obtain a heterogeneous catalyst is to impregnate a catalyst support with an alkaline or acid catalyst. Strong chemical bonds between the catalyst and support are essential for a high catalytic activity of supported catalyst.

Lignocellulosic residual materials, *e.g.*, fruit stones, could be promising precursors of catalyst supports. Thus, these materials are abundant, available, and

* Corresponding author: Email address: oana.parvulescu@yahoo.com

relatively low-cost resources as well as different catalysts can be strongly linked to their lignocellulosic matrix.

On the other hand, guanidine, a strong alkaline catalyst, could replace NaOH or KOH used in commercial biodiesel production [14]. Guanidine is a biodegradable organic chemical compound with basicity similar to that of NaOH or KOH and having two *amino* groups and an *imino* group, which can be chemically linked to different functional groups. Moreover, a superbase can be obtained by combining guanidine with another strong base, the resulting chemical compound benefiting from the characteristics of both components [15].

A new supported catalyst was prepared in this paper by impregnating a catalyst support derived from apricot stones with a superbase obtained from guanidine and KOH. The catalytic activity of fresh and reused supported catalysts was tested in 11 cycles of batch transesterification of sunflower oil to FAME.

2. Experimental

Materials

Catalyst support was prepared from apricot stones. Alcoholic guanidine solution was synthesized using dimethyl sulfate (Merck, Darmstadt, Germany), urea (Merck, Darmstadt, Germany), methanol (99.8%, Honeywell, Offenbach, Germany), 25% ammonia solution (Merck, Darmstadt, Germany), potassium hydroxide (Erba Lachema, Brno, Czech Republic), distilled water (produced by a Millipore Q-Gard A2 AFS 15E distiller) [16]. Supported catalyst was obtained by impregnating the catalyst support with alcoholic guanidine solution and KOH dissolved in methanol.

Fresh sunflower oil (ARGUS SA, Constanta) and methanol were used as reactants for biodiesel production.

Catalyst support preparation

Operation scheme for preparation of catalyst support from apricot stones is shown in Fig. 1. The apricots were cut in half and the pulp (consisting of exocarp and mesocarp) was removed. After manual removal of mesocarp residues, the stones (each consisting of kernel and endocarp) with a moisture content of 20% were dried in a thermobalance (OHAUS, Nänikon, Switzerland) at 50 °C for 5 h. Dried stones were subjected to an abrasive and then a soft polishing, for finishing the external surface, and further were chemically treated. Polished stones (15 g) were introduced into a solution of KOH (5.6 g), methanol (21 g), and distilled water (73.4 g) and a batch extraction was performed at 60 °C for 2 h in the experimental setup represented in Fig. 2. The system consisting of stones and KOH solution is shown in Fig. 3 at different values of extraction time. Chemically

treated stones were further dried in the thermobalance at 50 °C for 5 h. Catalyst support was then broken, the kernels removed, and the fragments of treated endocarp were used to prepare the supported catalyst.

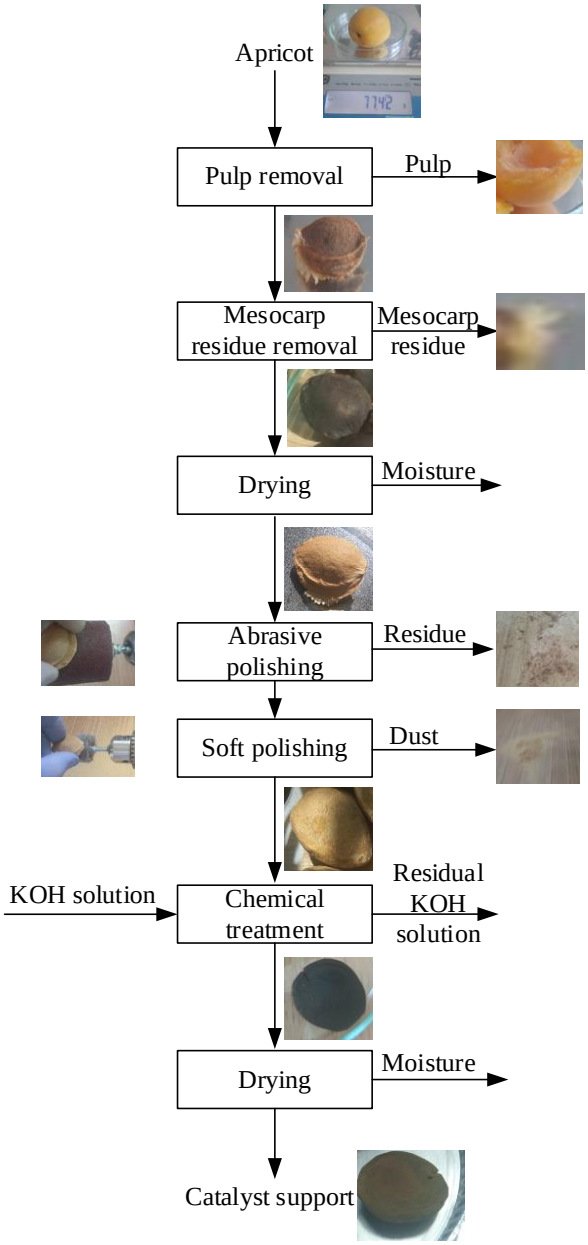

Fig.1. Operation scheme for preparation of catalyst support from apricot stones.

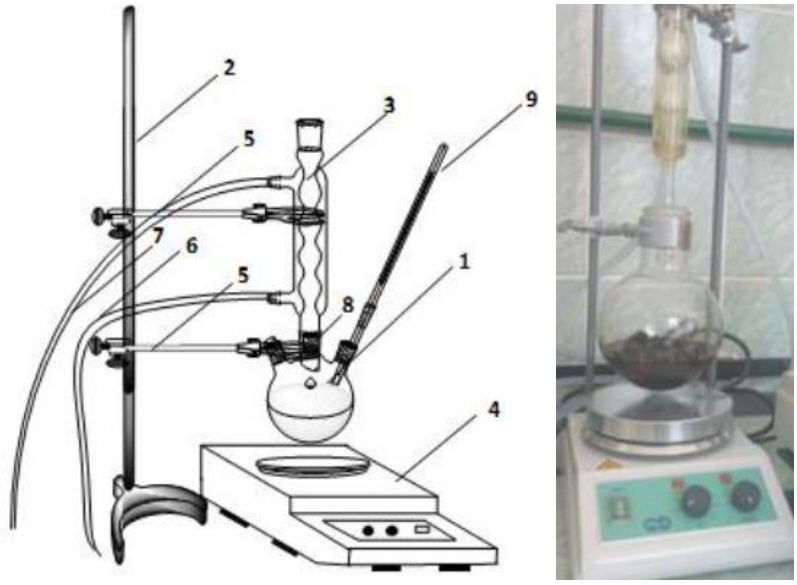

Fig. 2. Experimental setup: (1) 1 L reaction flask; (2) stand; (3) refrigerant; (4) magnetic stirrer with heating; (5) clamp; (6) water inlet; (7) water outlet; (8) reduction; (9) thermometer [16].

Fig. 3. System consisting of apricot stones and KOH solution after:
(a) 1 min; (b) 10 min; (c) 2 h [16].

Supported catalyst preparation

Broken catalyst support prepared from apricot stones (*AS*) was introduced into the reaction flask of the experimental setup (Fig. 2) and 20 mL of alcoholic guanidine (*Gu*-ROH), corresponding to 0.03 mol of guanidine, was poured over the *AS* support. An alcoholic KOH solution, *i.e.*, 0.42 g (0.0075 mol) of KOH dissolved in 10 mL of methanol, was added after 15 min. The system was left to react at 68 °C for 180 min, resulting in a *Gu/AS* base catalyst.

Supported catalyst characterization

The surface morphology of *Gu/AS* catalyst was visualized using a FEI QUANTA 200 Environmental Scanning Electron Microscope (ESEM).

Supported catalyst testing

Gu/AS was used as heterogeneous base catalyst to produce biodiesel from fresh sunflower oil under conditions as similar as possible to those used for commercial biodiesel production, *i.e*., atmospheric pressure, 60-70 °C reaction temperature, 6/1 methanol/oil ratio, 1.5-2 h reaction time.

Supported catalyst (23 g) and 0.66 mol of methanol were added into the reaction flask of the experimental setup (Fig. 2) and heated to 55 °C for 15 min to activate the catalyst. 100 g (0.11 mol) of heated (~60 °C) sunflower oil was then added and the system was kept under stirring (250 rpm) at 65 °C for 1.5 h. Supported catalyst was separated by filtration from the reaction mixture and further reused in a new experimental run. This transesterification run, which was performed using fresh catalyst (FC), was repetead 10 times reusing the catalyst, the catalyst reused in the experimental run *i* being coded as RC*i* (*i*=1..10).

3. Results and discussions

Supported catalyst characterization

ESEM images for the surface morphology of supported catalyst are shown in Fig. 4. ESEM image in Fig. 4a indicates a network of pores covered almost uniformly by the superbase obtained from guanidine and KOH, whereas superbase crystals can be seen in Fig. 4b.

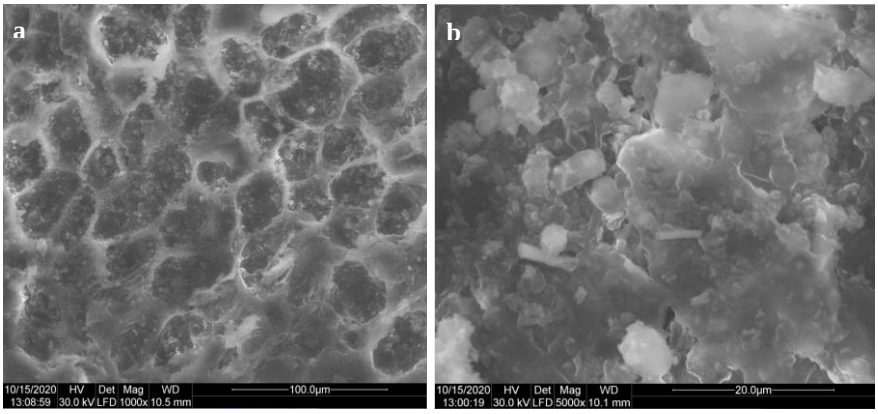

Fig. 4. ESEM images for the surface morphology of *Gu/AS* supported catalyst for scale bar of: (a) 100 µm; (b) 20 µm [16].

Supported catalyst testing

Images of reaction mixture at different values of transesterification time (τ) are shown in Fig. 5. In the image in Fig. 5a, corresponding to the reaction mixture at τ=10 min, appear 2 immiscible liquid phases, *i.e.*, a methanol top layer and a mixture of triglycerides, diglycerides, and monoglycerides, the conversion taking place at the interface between these immiscible phases. A lower layer of glycerol and a top one consisting mainly of FAME and methanol can be seen in the reaction flask at the final moment (τ_{fin}=1.5 h) of oil conversion (Fig. 5b).

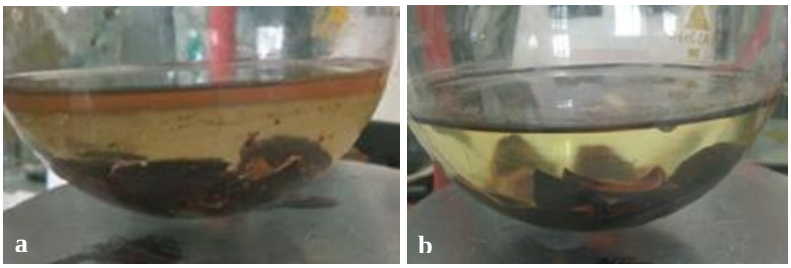

Fig. 5. Reaction mixture at different values of transesterification time: (a) 10 min; (b) 1.5 h [16].

Levels of FAME yield (Y_{FAME}) obtained by batch transesterification of fresh sunflower oil using fresh *Gu/AS* catalyst (FC) and reused *Gu/AS* catalyst (RC*i*) (*i*=1..10) are shown in Fig. 6. The values of Y_{FAME} in the presence of supported catalysts FC, RC1, and RC2 were in the range of 89.7-92.4%, whereas those corresponding to the catalysts RC3-RC10 were between 71.5% and 81.3%. While in the case of commercial homogeneous catalysis, the KOH catalyst appears in both FAME phase and glycerol phase, being separated in a subsequent purification stage, the solid catalyst used in this work was easily separated and had a high catalytic activity in multiple transesterification cycles, levels of FAME yield being in the range of 72-92%.

4. Conclusions

A lignocellulosic residual material, *i.e.*, apricot stones, was used to prepare a catalyst support (*AS*), which was impregnated with a superbase based on guanidine and KOH (*Gu*), resulting in *Gu/AS* supported catalyst. This supported catalyst was tested in batch heterogenous transesterification process of sunflower oil with methanol, producing FAME (biodiesel) and glycerol. Reaction conditions, *i.e.*, atmospheric pressure, 65 °C reaction temperature, 6/1 methanol/oil ratio, 1.5 h reaction time, were similar with those of commercial homogeneous process.

Catalytic activity of fresh and reused supported catalysts was evaluated for oil transesterification in heterogeneous catalysis. The value of FAME yield was of 92.4% for fresh catalyst, whereas for reused catalysts the levels of FAME yield

were in the range of 71.5-91.8% for 10 production cycles. These values demonstrate strong chemical bonds between lignocellulosic catalyst support and guanidine-based superbase, which resulted in a high catalytic activity.

This study showed promising results regarding the use and reuse of *Gu/AS* supported catalyst. Thus, heterogeneous catalysis in the presence of this type of material could be an interesting research perspective to approach.

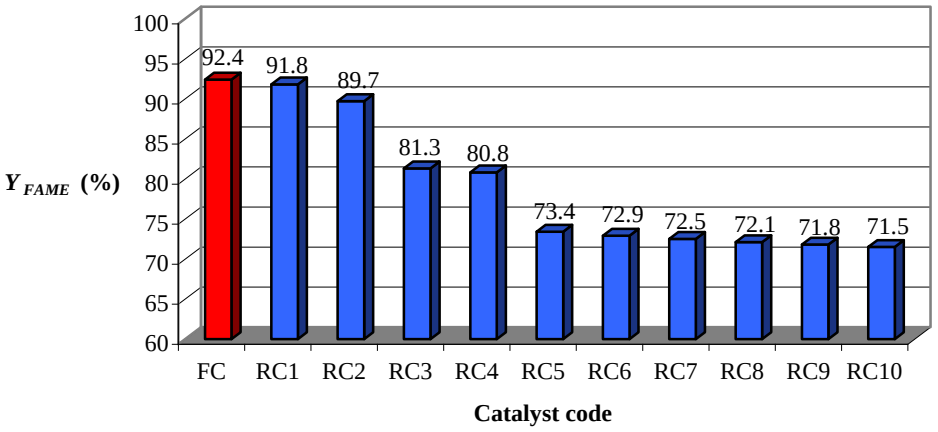

Fig. 6. Levels of FAME yield obtained for batch transesterification of fresh sunflower oil using fresh *Gu/AS* catalyst (FC) and reused *Gu/AS* catalyst (RC*i*) (*i*=1..10).

REFERENCES

[1] Lee S.L., Wong Y.C., Tan Y.P., Yew S.Y., Transesterification of palm oil to biodiesel by using waste obtuse horn shell-derived CaO catalyst, *Energy Conversion and Management*, 93, (2015), 282-288.

[2] Maneerung T., Kawi S., Dai Y., Wang C.H., Sustainable biodiesel production via transesterification of waste cooking oil by using CaO catalysts prepared from chicken manure, *Energy Conversion and Management*, 123, (2016), 487-497.

[3] Martinez S.L., Romero R., Natividad R., Gonzalez J., Optimization of biodiesel production from sunflower oil by transesterification using Na_2O/NaX and methanol, *Catalysis Today*, 220-222, (2014), 12-20.

[4] Meher L.C., Sagar D.V., Naik S.N., Technical aspects of biodiesel production by transesterification-A review, *Renewable and Sustainable Energy Reviews*, 10(3), (2006), 248-268.

[5] Muthukumaran C., Praniesh R., Navamani P., Swathi R., Sharmila G., Kumar N.M., Process optimization and kinetic modeling of biodiesel production using non-edible *Madhuca indica* oil, *Fuel*, 195, (2017), 217-225.

[6] Răducanu C.E., Pârvulescu. O.C., Dobre, T., Modelling of biodiesel synthesis: Batch and fed-batch mode with and whitout glycerol separation, *Bulletin of Romanian Chemical Engineering Society*, 4(2), (2017), 43-51.

[7] Agarwal M., Chauhan G., Chaurasia S.P., Singh K., Study of catalytic behavior of KOH as homogeneous and heterogeneous catalyst for biodiesel production, *Journal of the Taiwan Institute of Chemical Engineers*, 43(1), (2012), 89-94.
[8] Almerindo G.I., Probst L.F.D., Campos C.E.M., Almeida R.M., Meneghetti S.M.P., Meneghetti M.R., Clacens J.M., Fajardo H.V., Magnesium oxide prepared via metal–chitosan complexation method: Application as catalyst for transesterification of soybean oil and catalyst deactivation studies, *Journal of Power Sources*, 196(19), (2011), 8057-8063.
[9] Antunes W.M., Veloso C.O., Henrique C.A., Transesterification soybean oil with methanol catalyzed by basic solids, *Catalysis Today*, 133-135, (2008), 548-554.
[10] Deka D.C., Basumatary S., High quality biodiesel from yellow oleander (*Thevetia peruviana*) seed oil, *Biomass Bioenergy*, 35(5), (2011), 1797-1803.
[11] Liang M., He B., Shao Y., Li J., Cheng Y., Preparation and catalytic performance of N-[(2-Hydroxy-3-trimethylammonium)propyl] chitosan chloride/Na_2SiO_3 polymer based catalyst for biodiesel production, *Renewable Energy*, 88, (2016), 51-57.
[12] Sanjay B., Heterogeneous catalyst derived from natural resources for biodiesel production: A review, *Research Journal of Chemical Sciences*, 3(6), (2013), 95-101.
[13] Xie J., Zheng X., Dong A., Xiao Z., Zhang J., Biont shell catalyst for biodiesel production, *Green Chemistry*, 11(3), (2009) 355-364.
[14] Ishikawa T., Guanidines in organic synthesis (Chapter 4). In: Ishikawa T. (Ed.), *Superbases for Organic Synthesis: Guanidines, Amidines, Phosphazenes and Related Organocatalysts*, pp. 93-144, John Wiley & Sons, 2009, DOI:10.1002/9780470740859.
[15] Caubere P., Unimetal super bases, *Chemical Reviews*, 93(6), (1993), 2317-2334.
[16] Răducanu C.E., *New solutions regarding catalytic transesterification integration with separation in biodiesel technology*, Ph.D. Thesis, University POLITEHNICA of Bucharest, 2020.

DYNAMICS OF OIL AND PETROLEUM PRODUCTS SORPTION IN POROUS STRUCTURES

Alina-Georgiana CIUFU[1,*], Oana PÂRVULESCU [1], Cristian Eugen RĂDUCANU [1], Tănase DOBRE [1,2]

[1]Faculty of Applied Chemistry and Materials Science, University POLITEHNICA of Bucharest, 1-3 Gheorghe Polizu Street, 011061, Bucharest, Romania; [2]Technical Science Academy of Romania.

Abstract

The phenomenon of sorption by capillary action has been highlighted, a phenomenon that removes petroleum products from the affected environment. Initially, the adsorption rate is high, after which the adsorption rate begins to gradually decrease. Due to capillarity, the wool retains in its structure the analyzed oil products. The results obtained indicate that there is a rapid increase in the sorption of the various oils in the first 5 minutes after which it proceeds at a slower rate until equilibrium after 45 minutes.

The obtained results suggest that natural wool fibers can be a suitable sorbent material for spilled oil retention on marine surfaces, with performance that are competitive with the materials of synthetic origin proposed for similar applications. Wool fibers beds retain the oil due to porous structure and because fibers structure - they have an oleophilic outer cuticle that is covered by lanolin, which repels water and supports the oil suction

Key words: wool fiber, fibers bed, oil spill, capillary ascension, sorption capacity

1. Introduction

Porous media can be found almost everywhere in the environment, with few materials except fluids, that can be considered as non-porous. The main properties of porous environments are the porosity and the permeability. Sometimes we need to take into account experiences more or less complicated, which target at least one characteristic of the porous. And that is imperious when it uses the porous body as sorbent for gasses or liquids as in the case of this paper.

The dynamics of the liquid mass ratio retained in the porous structure of identical capillaries, with h_s characteristic length in sense of liquid asscension, is given by equation (1). When the porous structure reaches saturation then the capillary lift rate becomes zero. As a consequence of (1), the relation (2) is obtained for the maximum liquid loading ratio of the porous structure [1].

* Corresponding author: Email address: alinag.ciufu@gmail.com

$$\frac{d\Omega}{d\tau} = \frac{r_p^2}{8\eta_l}\left(\frac{\rho_l \varepsilon}{\rho_s(1-\varepsilon)}\right)^2 \frac{1}{h_s \Omega}\left(\frac{2\sigma\cos(\theta)}{r_p} - \rho_s g h_s \frac{1-\varepsilon}{\varepsilon}\Omega\right) \quad (1)$$

$$\Omega_{\max} = \frac{2\sigma\cos(\theta)}{\rho_s g h_s r_p}\frac{\varepsilon}{1-\varepsilon} \quad (2)$$

The relations obtained, even though they very well highlight the influence of the factors that take into account the fluid that rises in the capillary structure (σ, η_l, ρ_l), the properties of the porous structure (r_p, ε, h_s, ρ_s) and the interaction between the liquid and the structure (liquid solid contact angle, θ), are very hard to be found in the experimental measurements. The one model of real porous body is more complicated in that it has accumulation holes which are fed by capillary pumping from pores with transport capacity below that those given by maximum capillary lifting height; from each hole other pores can transport liquid to other holes.

As many experimental data show, an analysis of the relation (2) leads to the conclusion that it is very difficult for Ω_{max} to have high values as, example over 1 kg_{oil}/kg_s when oil is adsorbed into this porous body type. As shows relation (2) the pore fraction of the porous body (porosity) and the pore radius establish, form the point of view of porous body, the values of the mass saturation ratio (Ω_{max}). In Fig. 1 it is shown how it depends on the two factors, when the material of the porous body is watered by oil. It is obvious that the model considered in establishing the relation (1) cannot realistically allow saturation mass ratios greater than 0.5 - 1 kg_{oil}/kg_s. See in the sense of this statement that a porous body with a pore fraction over 0.7 m^3/ m^3 and pores no larger than 0.0003 m is something extremely fine. Compared to the above, it should be noted that: i) capillary phenomena are determined by the interaction forces between a liquid and a solid body; ii) these phenomena are more obvious in the case of tubes of small sections, called capillaries; iii) in relation to the value of the angle θ the liquid rises in the capillary when it wets its walls ($0 < \theta < \pi/2$).

The phenomenon of capillarity plays an important role in nature and in technique. Water penetration into the soil and various porous materials occurs due to capillarity. Capillarity also plays an important role in feeding plants. The use of wicks, the absorption of water by hydrophilic wool, the cooling of microchips in electronic assemblies, etc. are based on the capillarity phenomenon. Let us add that most of the fluid circulation in the body of animals and humans is based on capillary pumping. Last but not least, capillarity, through capillary pumping, is also particularly important in the retention by adsorbent materials of oil or petroleum products that pollute the surface of the water by deliberate or accidental discharge [2-6].

2. Modeling and Experimental
The dynamics of oil saturation of the porous body with holes

As it have been shown with disscusion reffreing to figure 2 it is obvious that the model above considered (body with small pores diameter) cannot realistically allow saturation mass ratios greater than 0.5– 1 kg_{oil}/kg_s [6,7]. So, considering the experimental observations that show values of the mass saturation ratio more over 1 kg_{oil} /kg_s it is obvious that other model of the porous body, which can explain these values of the mass saturation ratio, as well as its dynamics during saturation must be considered [7,8].

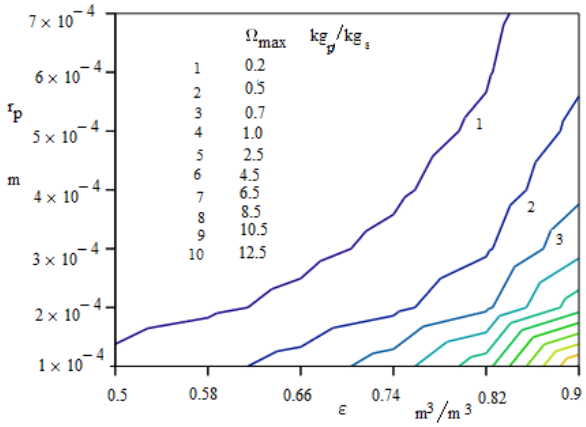

Fig. 1 Evolution of porosity and pore radius on oil maximum saturation ratio of a porous body (ρ_s=800 kg/m^3, θ=40 grd, σ=0.025 N/m, h_s=0.05 m)

Thus, it was considered that the structure of the porous body, which can meet the requirement to explain high values of Ω_{max}, is that of a porous body with holes, where the following hypotheses are accepted:

a) the porous body consists of large holes and small pores that connect, pass through its; we also have pore that pass near to holes;

b) pores are branched and their characteristic dimension (pore radius) follows a normal distribution, as shown by the relation (3), where r_{pm} is the average pore radius and σ_{rp} is the pore radius dispersion around the average radius;

c) the holes in the porous body do not have a completely defined shape (they can be assumed to be spherical but that is not abssoluytely requested) with the random variable volume normally distributed with the parameters V_m and σ_V ; that is shown by relation (4);

d) the volume of the voids (holes) in the porous body is greater than the volume of the pores so that the total porosity of the porous body satisfies the

relation (5), where α represents the participation of the voids in its formation and β is the pore fraction in it;

e) in a void (hole), the pores that bring liquid through capillary pumping are active pores; their number being proportional to the volume of the void, as shown by the relation (6), where V_{min} is the smallest volume of void that binds a pore;

f) pores that do not bring liquid into the gaps (holes), begin as capillary pump and remove liquid from the gaps as it fills; as in the case of active pores, the number of this type of pores is proportional to the volume of the gaps (7);

g) the flow through an active pore that brings liquid into a gap corresponds to the laminar flow so that it is calculable by expressing the velocity through it according to the relation (8) in which for h the value $h_{max}/2$ will be taken;

h) any hole (gap) is filled and remains filled as long as the capillary adhesion force on its walls remains over the weight of the liquid in the pores;

i) viewed on the height of the porous layer with gaps, the process of filling the gaps probably follows the following sequence: a) when the porous structure gets in contact with the oil layer all the gaps below a given h_1 begin to fill; b) as they are filled, the pores that do not bring liquid into the pores below h_1 are activated and the pumping into the pores between the levels h_1 and 2 h_1 begins; c) the process is repeated in this fractal propagation mode between levels 2 h_1 and 3 h_1 etc.

Figure 2 shows the dynamics of the state of saturation with oil in the porous body with holes corresponding to the description in the above model, in which the filling of a gap between 0 and h_{max} evolves as described in points e, f, g and h. As shown in relations (3) and (4), usually there are accepted normal distributions of the pore radius and volume of the void in the porous media. In the functioning of the model, the number of pores that contribute to the filling of a void is expressed according to the relation (6) and the number of pores that become active by filling the void follows the expression from the relation (7).

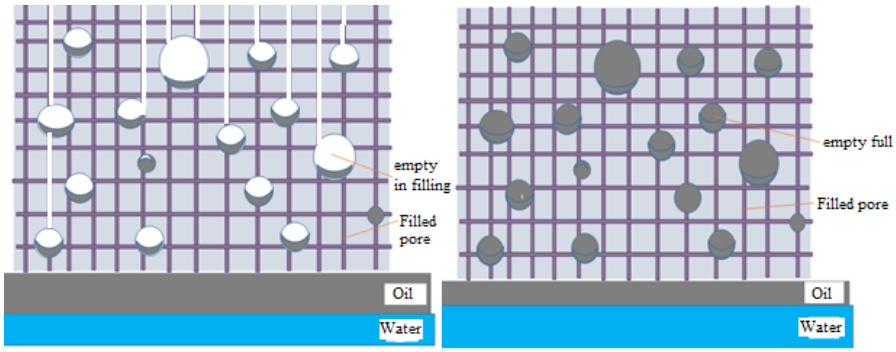

Fig. 2 A mechanism regarding the dynamics of oil saturation of the porous body with holes. (left: at one point, right: at the end of saturation)

$$f(r_p)=\frac{1}{\sigma_{rP}\sqrt{2\pi}}\exp\left(\frac{(r_p-r_m)^2}{2\sigma_{rp}^2}\right) \quad (3)$$

$$f(V)=\frac{1}{\sigma_V\sqrt{2\pi}}\exp\left(\frac{(V-V_m)^2}{2\sigma_V^2}\right) \quad (4)$$

$$\frac{\varepsilon}{\varepsilon_G}=\alpha,\ \frac{\varepsilon}{\varepsilon_p}=\beta \quad (5)$$

$$n_a=1+\frac{\mathrm{V}}{\mathrm{V}_{\min}} \quad (6)$$

$$n_{p,pc}=\begin{array}{l}0\ \text{pentru}\ \mathrm{V}(\tau)\prec\frac{\mathrm{V}}{2}\\ 1+\frac{\mathrm{V}(\tau)}{\mathrm{V}_{\min}}\ \text{pentru}\ \mathrm{V}\succ\frac{\mathrm{V}}{2}\end{array} \quad (7)$$

$$\frac{dh}{d\tau}=\frac{r_p^2}{8\eta_l h}\left(\frac{2\sigma\cos(\theta)}{r_p}-\rho_l gh\right) \quad (8)$$

Particularly important in the functioning of the model is the filling of one empty (gap). In this case, starting from the flow through an active radius r_p (9), the particularization of the non-stationary balance to a volume gap V leads to the relation (10). If each active pore or passive in the capillary pumping is associated with a pore radius from their normal distribution then the relation (11) is modified accordingly.

$$G_{vp}=\pi\mathrm{r}_{\mathrm{p}}^2 w(h_{\max}/2)=\pi r_p^2\left(\frac{r_p^2}{4\eta_l h_{\max}}\left(\frac{2\sigma\cos(\theta)}{r_p}-\frac{\rho_l gh_{\max}}{2}\right)\right) \quad (9)$$

$$\frac{dV}{d\tau}=(n_a-n_{p,pc})G_{vp} \quad (10)$$

$$\Omega(\tau)=\left(\frac{(n_{p\max}-\sum_i n_{ai})\rho_l h_{\max}Sh_s+\rho_l\sum_{i=1}^{n_{G\max}}V_i(\tau)}{Sh_s\rho_{vrac}}\right) \quad (11)$$

The model brings as new the fact that the capillary motion of the liquid in its pores can be described phenomenologically by a system of ordinary differential equations, in which each differential equation can be individually integrated when the topology of the supply and discharge of liquid from the pores of the porous body is fixed. An example of its numerical implementation is shows in Table1.

Table 1

Mathcad implementation of the dynamics of suction of a liquid in a porous body with accumulating holes

N.c.	The calculation action
1	**It is specified:** Porosity of the porous body: ε=0.7 m^3/m^3; The participation fraction of the gaps in porosity: a = 0.5; The surface tension value of the capillary suction fluid: σ=0.021 N/m; The value of the watering angle θ= 40 grade; Density of capillary rising fluid: ρ_l = 820 kg/m3; The viscosity of the liquid that rises in the capillary η_l = 0.01 Pa; The value of the acceleration of the gravitational field g = 10 m/s2; The size of the characteristic section of the porous body; S= 10-4 m2; The height on the suction direction of the porous body: h_s = 0.09 m: The pore participation at the total porosity: b = 0.5
2	**It is obtained**: Pore fraction of the porous body: ε_p = 0.35 m^3/m^3; The fraction of voids in the porous body: ε_G= 0.35 m^3/m^3
3	**It is chosen**: Medium pore radius: r_{pm} = 0.0001 m; Pore dispersion around the middle radius: σ_p = 0.00001 m; A tortuosity coefficient is chosen for the pores: ξ = 1.3
4	**It is written**:The repartition and distribution functions of the pore radius of porous body: $f(r_p)=\frac{1}{\sigma_{rp}\sqrt{2\pi}}\exp\left(\frac{(r_p-r_m)^2}{2\sigma_{rp}^2}\right)$ $\Psi(r_p) := \int_0^{r_p} f(r_p)\,dr_p$
5	**It is chosen**: The average volume characteristic of a void (d_mx=0.003 m): V_m = 1.414 10^{-8} m^3; The dispersion of the pore volume around the average volume: σ_V=0.28 10^{-8} m^3
6	**It is computed**: The maximum number of gaps in the characteristic volume of porous body is calculated: $n_{Gmax} := \text{round}\left(\frac{\varepsilon_G \cdot S \cdot h_s}{V_m}\right)$, n_{Gmax} = 223
7	**It is computed**: The maximum height of capillary lift, the number of sections disposed on the height of the porous body and the maximum number of holes per section: $h_{max} := \frac{2\cdot\sigma\cdot\cos\left(\frac{\theta}{\pi}\right)}{\rho_l \cdot g_r \cdot r_{pm}}$ $n_s := \text{round}\left(\frac{h_s}{h_{max}}\right)$ $n_{Gmaxs} := \text{round}\left(\frac{n_{Gmax}}{n_s}\right)$ n_{Gmaxs} = 74
8	**The building of topology**: It is found that in a section of 0.03 m, 74 gaps must be introduced, which are fed by a part of the 223 pores. Thus, 9 gaps (empties) can be arranged in 8 planes with a distance of 0.004 m between them. They are chosen according to the representation Ψ (V_g) vs. V_g, three representative volumes for goals: v_1= 1 10^{-8} m^3, v_2= 1.5 10^{-8} m^3 and respectively v_3 = 2 10^{-8} m^3
9	**The building of topology**: The selected volumes are distributed, by circular exchange (permutation), to all 74 goals in the first section: i= 1,2…9 $V_{G1}=v_1, V_{G2}=v_2, V_{G3} = v_3$, ..$V_{G8} = v_2$, $V_{G9} = v_3$; ….i = 64,65….72 $V_{G\,i} = V_{G\,i-64}$
10	**The building of topology**: The average flow through a pore feeding a gap it is given by:

	$r_p = r_{pm}$; $G_{vp} = \pi r_p^2 w(h_{max}/2) = \pi r_p^2 \left(\frac{r_p^2}{4\eta_l h_{max}} \left(\frac{2\sigma\cos(\theta)}{r_p} - \frac{\rho_l g h_{max}}{2} \right) \right)$, $G_{vp}=3.38\ 10^{-10}$ m^3/s
11	**The building of topology**: The distribution of the pores that feeds each gap is chosen (here 2 pores per gap): i = 1,2…72, $n_{a\,i} = 2$
12	**The building of topology**: A function that describes the capillary transport of the pores that start from each void is chosen: $n_{pc}(V) = 0$ if $V<V_{G\,i}/2$; 1 if $V_{G\,i}/2, V<V_{G\,i}/1.01$; $n_{a\,i}$ otherwise
15	**The computation of holes filling:** It begins with integration of the 9 differential equations for the first plane of 0.004 m from the 8 planes of h_{max}. First gap (hole) : $n_{pc}(V) = 0$ if $V<V_{G\,1}/2$; 1 if $V_{G\,1}/2, V<V_{G\,1}/1.01$; $n_{a\,i}$ otherwise; $f_1(\tau, V_1) := \left(n_{a_1} - n_{pc}(V_1)\right) \cdot G_{vp}$ $\tau_0 := 0$ $V_{10} := 0$ $\tau_1 := 100$ $N := 100$ Given $V_1'(\tau) = f_1(\tau, V_1(\tau))$ $V_1(\tau_0) = V_{10}$ $V_1 := \text{Odesolve}(\tau, \tau_1)$ The second gap…. …The ninth gap: $n_{pc}(V) = 0$ if $V<V_{G\,9}/2$; 1 if $V_{G\,9}/2, V<V_{G\,9}/1.01$; $n_{a\,9}$ It is calculated the average flow that flows through a supply pore of the gap: $r_p=r_{pm}/1.2$ $G_{vp} = \pi r_p^2 w(h_{max}/2) = \pi r_p^2 \left(\frac{r_p^2}{4\eta_l h_{max}} \left(\frac{2\sigma\cos(\theta)}{r_p} - \frac{\rho_l g h_{max}}{2} \right) \right)$ $G_{vp} = 2.282 \times 10^{-10}$ $f_1(\tau, V_9) := \left(n_{a_1} - n_{pc}(V_9)\right) \cdot G_{vp}$ $\tau_0 := 0$ $V_{10} := 0$ $\tau_1 := 100$ $N := 100$ Given $V_9'(\tau) = f_1(\tau, V_9(\tau))$ $V_9(\tau_0) = V_{10}$ $V_9 := \text{Odesolve}(\tau, \tau_1)$
16	**The computation of holes filling**: On the basis of step, it is started the integration of the 9 differential equations for the second plane of 0.004 m from the 8 planes from h_{max}. Following this procedure, the integration is continued until the last of the 223 gaps (holes, empties), established in step 6, is filled.

3. Results and discussions

Based on the facts presented in Table 1 and in Fig. 3 it is shown how the filling of the first and second level gaps (holes) out of the 8 available after h_s evolves. It is observed that we have to deal with a quite differentiated process, in the sense that each of the 18 gaps considered in the representation are filled individually. Thus, from the first level, the gaps V_1 and V_4 are filled in about 10 seconds, those coded V_2, V_3, V_6, V_8 and V_9 reach filling between 20 and 22 seconds while the gap V_5 needs 35 seconds until filling. After 10 seconds, more precisely between 12 and 15 seconds, most of the second level gaps in the h_s begin to fill. Here the gaps V_{11} (linked, according to the topology considered in the calculation program, with V_2 from the first level) and V_{14} (linked with V_5 from the first level) start filling after 25 seconds and are the last ones to fill (50 seconds - V_{11}, respectively 60 sec. - V_{14}).

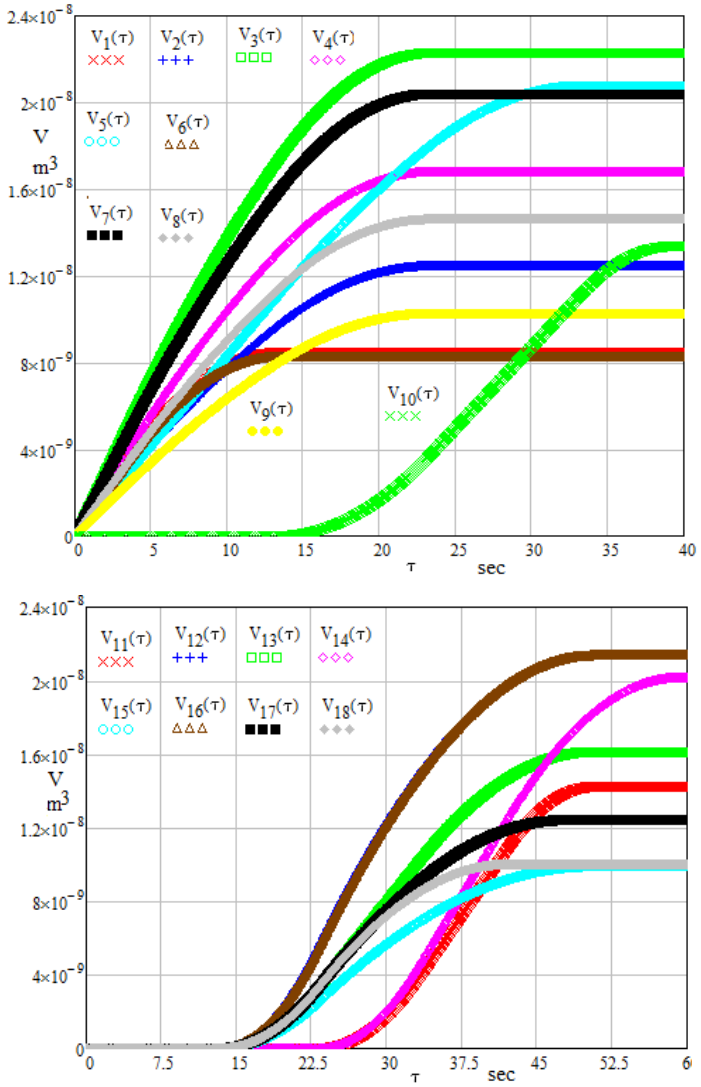

Fig. 3. Dynamics of filling with a petroleum product of pores positioned in first and second levels form h_s in a porous body with ε_p=0.35 m^3/m^3,ε_G=0.35 m^3/m^3,r_{pm}=0.00018 m, V_m=1.414 10^{-8} m^3.

Those observed in connection with the filling of the gaps lead to the idea that, if the capillary rise in such a body were to be followed visually, the upper level of the elevation should be highly fragmented. In figure 4, images from the capillary lift of the Azeri crude oil in a 20 mm glass tube, filled with 8 grams of merino wool with a total height of 170 mm (ρ_{vrac} = 0.15 g/cm^3, ε = 0.81 m^3/m^3) and under a pressure of 800 Pa, which supports this observation.

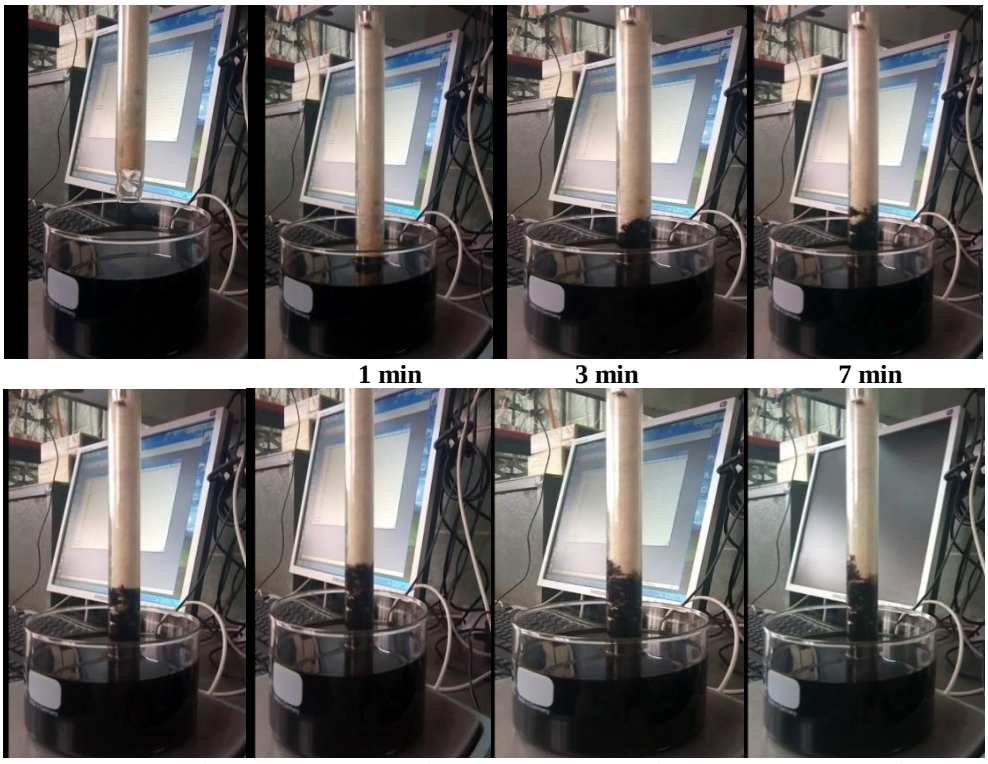

Fig. 4 Images regarding the dynamics of the capillary rise of Azeri oil in wool fiber porous body (d_{fir}= 0.00015 m, ρ_{vrac}=0.15 g/cm^3, ε=0.81 m^3/m^3, ρ_l =890 kg/m^3, σ=0.027 N/m)

The dynamics of the evolution in time of the retained mass oil ratio is obtained mainly by summing the volumes of the gaps that have been filled until the τ moment, to which the liquid rising in the pores is added. The relation (11), in which it was considered that in free pores (not bound by gaps) the rise reaches h_s, extremely quickly, can be used in this way.

4. Conclusions

In this study, the role of the capillaries was taken by the wool fibers on which Azeri crude oil rises due to the capillarity. Meeting a two or more fibers create a space for the accumulation of capillary transported crude oil. Fibers leaving the storage space carrying oil product, through capillary mechanism, to a new storage space. It is obvious that the storage spaces in which the weight of the crude oil accumulated exceeds the capillary force will lose the crude oil collected until the two forces equalize. Specifically, the advance of the Azeri crude oil

absorbed in such a structure appears to be the advance of a fractal that develops from accumulation spaces. This fact was highlighted by sequential shooting.

REFERENCES

[1] Rodríguez M. A., Tirado V., Tirado María Miranda, *Derivation of Jurin law revisited,* Eur. J. Phys., 32**,** 49- 53, 2010.
[2] Babel S., Kurniawan T. A., *Low-cost adsorbent for heavy metal uptake from contaminated water: a review*, Journal of Hazardous Materials 97, 1-3, 219–243, 2003.
[3] Bailey S. E., Olin T. J., Bricka R. M., Adrian D. D., *A review of potentially low cost sorbents for heavy metals*, Water Research, 33, 2469–2479, 1999.
[4] Bazargan A., Tan J., McKay G., *Standardization of Oil Sorbent Performance Testing*, Journal of Testing and Evaluation, 43(6), 1–8, 2015.
[5] Igwe J. C., Abia A. A., *Review: A bioseparation process for removing heavy metals from wastewater using biosorbents*, African Journal of Biotechnol, 5, 1167–1179, 2006.
[6] Fulekar M. H., *Bioremediation Technology-Recent Advances*, Department of Life Sciences, University of Mumbai, India, Ed. Springer, 35-53, 2012.
[7] Joekar-Niasar V., Hassanizadeh S. M., Leijnse A., *Insights into the Relationships Among Capillary Pressure, Saturation, Interfacial Area and Relative Permeability Using Pore-Network Modeling*, Transport in Porous Media, 74, 201–219, 2008.
[8] Takeuchi K., Kitazawa, H., Fujishige, M., Akuzawa, N.,Ortiz, J. et al., *Oil removing properties of exfoliated graphite in actual produced water treatment*, Journal of Water Process Engineering, 20, 226-231, 2017.

ON SOME ASPECTS FROM OPERATION OF A LARGE WASTEWATER TREATMENT PLANTS

Claudia Ana Maria PATRICHI[1,*] Tănase DOBRE[1]

[1]University POLITEHNICA of Bucharest, Department of Chemical and Biochemical Engineering, Str. Gh. Polizu 1-7, RO-011061, Bucharest Romania

Abstract

The most efficient and economical method of removing organic substances from wastewater is the use of biological treatment processes. Large wastewater treatment plants contain many phases of hydrodynamic processing of heterogeneous systems and have as their core the aerobic fermenters for wastewater and anaerobic fermenters for the biogas transformation of the active sludge produced in the plant. The role of gradually feeding anaerobic fermenters with low doses is to facilitate the controlled development of methane-producing bacteria. The aim of the paper is to present data about the commissioning of an aerobic fermenter and analysis by experimental measurements of the functioning of the biogas fermenter.

Key words: Aerobic fermentation, Anaerobic fermentation, Wastewater treatment, Active sludge, Biogas

1. Introduction

Wastewater treatment, also called sewage treatment, the removal of impurities from wastewater, or sewage, before it reaches aquifers or natural bodies of water such as rivers, lakes, estuaries, and oceans. Since pure water is not found in nature (i.e., outside chemical laboratories), any distinction between clean water and polluted water depends on the type and concentration of impurities found in the water as well as on its intended use. In broad terms, water is said to be polluted when it contains enough impurities to make it unfit for a particular use, such as drinking, swimming, or fishing.

Wastewater treatment is a process used to remove contaminants from wastewater or sewage and convert it into an effluent that can be returned to the water cycle with minimum impact on the environment, or directly reused.

A raw material that quickly qualifies for biogas production is anaerobic sewage sludge from municipal water processing. The amount of sludge generated by municipal wastewater treatment plants in Romania was 123460 tSU in 2011 [1]. This sludge contains both organic materials, nutrients such as nitrogen,

* Corresponding author: Email address: patrichi.claudia@gmail.com

phosphorus, potassium, sulfur, magnesium and small amounts of calcium, as well as pollutants - heavy metals, toxic organic substances and pathogens.

Biomass used for the production of biogas includes: domestic and industrial waste water, solid and liquid urban waste, manure and plant mass. Obtaining biogas from raw materials involves its collection, transport, storage and processing. The basic method applied for biogas production is anaerobic fermentation of biomass. Anaerobic fermentation is a microbiological process of decomposition of organic matter in the absence of air. The optimum temperature for this process is between 20-45°C. As a result of anaerobic fermentation, a gaseous product (mainly composed of methane and carbon dioxide) and a residual mass that can no longer be fermented are obtained. This mass is usually used as a soil fertilizer. Anaerobic fermentation in the world is seen as a very beneficial solution from two points of view: solving the problem of waste and energy production.

On average, at a fermentation station, approximately 400–600 m^3 of biogas can be obtained from a tone of waste mixture, of which 50–70% can be methane [2-4]. The entire fermentation process involves four main phases of biomass decomposition:

1. Hydrolysis: Hydrolytic microorganisms convert heavy organic molecules into smaller particles such as sugars, fatty acids, amino acids, water.
2. Acidogenesis: the particles formed in the first phase are decomposed into organic acids, ammonia, hydrogen sulphite and carbon dioxide.
3. Acetogenesis: the formation of hydrogen and carbon dioxide as a result of the transformation of the complex mixture of fatty acids into acetic acid.
4. Methanogenesis: the formation of methane, carbon dioxide and water.

The methane formation process accelerates at the beginning of fermentation and practically reduces in intensity at the end of it. Anaerobic fermentation is considered to be one of the most attractive solutions for the production of renewable energy from biomass.

Wastewater purification may be more or less complex, depending on the physico-chemical and microbiological characteristics of processed water. Thus, waste water, having a predominantly inorganic character, can be treated by physico-chemical processes in which the elimination of impurifying substances is done by chemical and physical processes such as: sedimentation, neutralization, precipitation, coagulation, adsorption on activated charcoal, ion exchange, etc. Wastewater with a pronounced organic character can be treated by physico-chemical and/or biological processes, in the latter case, the elimination of organic pollutants substances are done by biochemical processes, the metabolic processes of microorganisms. Till present days, water purification specialists consider that the most efficient and economical method of removing organic substances from

waste water is the use of biological treatment processes. These processes are based on the metabolic reactions of a mixed population of bacteria, fungi and other microorganisms (especially protozoas and some lower metazoans), which operate in certain hydrotechnical constructions, treatment plants. In the practice of purification, this population (biocenosis) is called biomass. The composition of biocenosis and the efficiency of removal of organic substances depend on the environmental conditions: the composition of the waste water and the concentration of impurities, the temperature, the mixing conditions, and the operation mode of the treatment plant. The different species of biomass coexist in dynamic equilibrium, their frequency can be changed by the factors listed above. The temporal fluctuations of environmental factors are compensated by the population dynamics of microorganisms which has a good ability to adapt, thus the quality of the purified water varies slightly.

Household wastewater is a non-homogeneous mixture of dozens of simple and complex organic compounds that are assimilated by microorganisms, mainly carbohydrates, amino acids, fatty acid esters. Biological purification procedures use one of two physiologically different groups of microorganisms: aerobic or anaerobic. Anaerobic microorganisms are used for the fermentation of sludge and the fermentation of concentrated industrial wastewater. Aerobic microorganisms are commonly used in the majority treatment of predominantly organic wastewater, and more recently also for the fermentation of organic sludge. For aerobic water purification the most used processes are: active sludge, biofilters and oxidation ponds respectively. Variants of the active sludge treatment process differ mainly in the way of the introduction of waste water and the ratio between the substrate and microorganisms. Of particular importance in biological purification is the mass transfer, especially oxygen to oxidize pollutants from wastewater and biological multiplication into biomass. A good interfacial contact air - wastewater is essential. In the process of wastewater purification, the concentration of organic substances is expressed globally, directly by determining organic carbon or indirectly by determining chemical oxygen consumption. Large wastewater treatment plants are designed and made so that they can distribute treated water in a river or even form a river. In case of damage large installations must be able to return water to the waste water supply box. The plants contain many phases of hydrodynamic processing of heterogeneous systems and have as their core the aerobic fermenters for wastewater and anaerobic fermenters for the biogas transformation of the active sludge produced in the plant.

2. Experimental

In a complex and high-capacity for wastewater treatment, as is the case in the plant from the below schema, an extremely large number of experimental data can

be obtained. We will present here two situations, but not before of a brief presentation of the wastewater treatment plant related to a big city (figure 1).

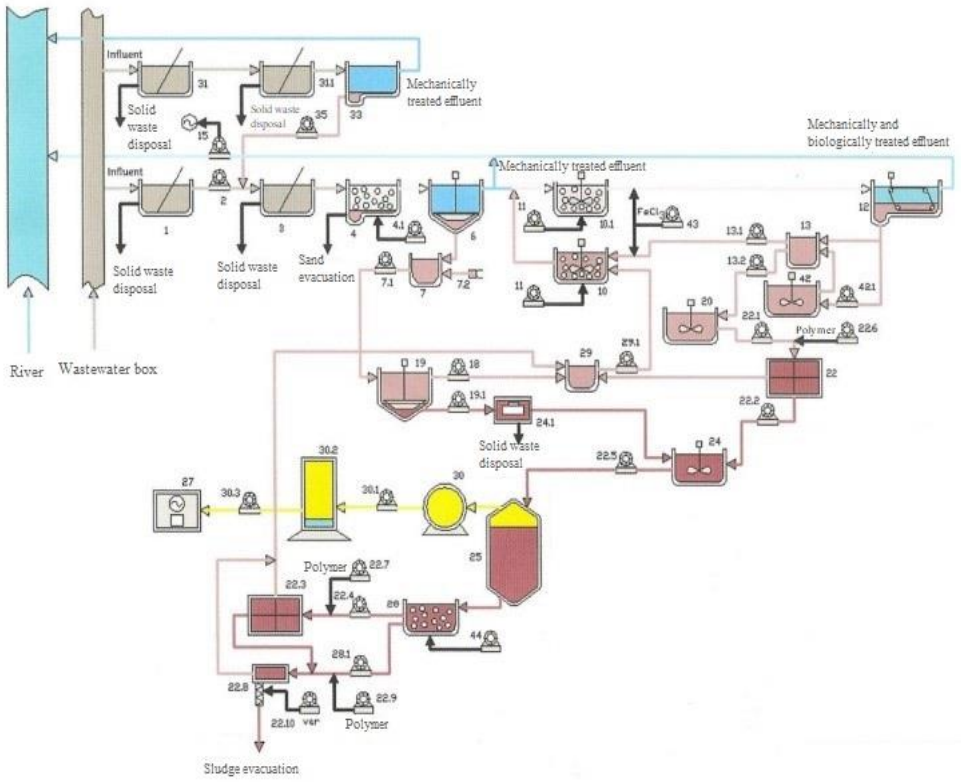

Fig. 1. Flowsheet for wastewater treatment with activated sludge (1- screens; 2- wastewater pumping station; 3- dense screens; 4- desnisipators; 4.1- desnisipation air blower station; 6- primary decanters; 7- primary sludge collector path; 7.1- primary sludge pumping station; 7.2- macerator for drained sludge; 10- activated sludge recirculation tanks; 10.1- activated sludge tanks; 11- sludge blower air station; 12- secondary decanters; 13- primary sludge collector path; 13.1- active sludge pumping station; 13.2- excess active sludge pumping station; 15- micro hydropower plant; 18- primary thickener supernatant pumping station; 19- thickener primary sludge; 19.1- thickened primary sludge pumping station; 20- excess active sludge mixing tanks; 22- thickening mass; 22.1- excess sludge pumping station to the thickening mass; 22.2- thickened sludge pumping station; 22.3- dehydration mass; 22.4- digested sludge pumping station; 22.5- digestion sludge pumping station; 22.6- thickening polymer pumping station; 22.7- polymer dehydration pumping station; 22.8- centrifuges for dehydration; 22.9- centrifugal polymer pumping station; 22.10- lime powder dispensers; 24- thickened primary sludge and excess thickened sludge mixing tanks; 24.1- fiber separators; 25- anaerobic digesters; 27- cogeneration building; 28- digested sludge tanks; 28.1- digested sludge pumping station for centrifugation; 29- supernatant collector path; 30- gasometers; 30.1- gas compressors; 30.2- biogas desulphurization unit; 30.3- gas compressors to supply the cogeneration building; 31- rare screens - rain station; 31.1- dense screens – rain station; 33- retention tanks; 35- sludge pumping station in retention

tanks; 42- anaerobic tanks, Bio-P; 42.1- sludge pumping station in tanks; 43- ferric chloride pumping station; 44- air blower station in digested sludge tanks)

The purpose of the treatment plant is to purify household, rain and industrial waste water from urban agglomeration. The treatment line for these waters is in accordance with the flow sheet from figure 1 and includes the following sequences:

- Mechanical treatment by dense-rare screens (the rare screens (10 units) with opening between 6 mm bars are intended to retain solid waste from the water for collected and discharged from the station) and dense screens
- Desnisipation
- Aerobic fermentation
- Primary and secondary decanting: Primary decanters consist of 2 batteries of 4 radial units 55 m in diameter retain fine and colloidal suspensions by sedimentation. The primary sludge scraped from the base of these decanters is sent to the sludge line for thickening and then biogas.

The sludge line contains the following steps:

- stabilization of sludge by thickening;
- anaerobic fermentation with biogas production;
- dehydration of stabilized sludge.

Technological flow; Operating installation

Around of 520800 m^3/day of wastewater enters in the mechanical water treatment step. These waters are first introduced into a separation plant of large solid bodies, which is made with the help of dense screens. Then, with the help of pumps the water is sent to the installation of dense screens, where it also separates solid bodies that have not been separated in the previous stage.

The separation of sand in the desnisipation plant follows. Aeration desnisipators, equipped with 5 units of fat separators, are used to collect gravel and sand from wastewater (separate sand and gravel is washed and evacuated from the station). The retained fats are introduced into the sludge line for recovery, taking into account their energy potential in biogas.

After desnisipation the water is sent to the decanting plant where the decantable materials are separated. From here the current of water entered separates into two parts. The first part is disposed of only as decanted water in the natural environment. In this sense, this part is directed to some of the secondary decanters, numbering 48 units, which ensure their final clearing and then discharge to the river through a bypass channel. The sludge resulting from this part of the water shall be recirculated for activation and part of the system shall be extracted under the name of excess sludge. Excess sludge is thickened in thickening units (80 m^3 per unit) in which cationic polymer additions are made. Data on operating of mechanical processing of wastewater from a big plant are given in table 1.

The second part of waste water is completely purified in the biological step. In other words, organic matter, nitrogen and phosphorus are removed from this stream. Biological purification with bacterial biomass leads to the mineralization of colloidal and dissolved carbon-based organic substances and to the retention of nutrients, nitrogen and phosphorus. The addition of ferric chloride contributes to a more efficient removal of phosphorus and to the improvement of the secondary sedimentation process. The sludge resulting from this step is called the primary sludge, approximately 4400 m^3/day, enters in the primary thickeners where it is thickened and is obtained the primary sludge thickened with a flow rate of approximately 990 m^3/day.

Part of the primary thickened sludge called and supernatat is recirculated to activate the mechanically treated water load.

With reference to the active sludge treatment line, it is shown that it has 14 units, of which 8 active sludge basins in the works, 4 active sludge regeneration (priming) basins and 2 BIO-P anaerobic basins.

Biogas technology flow; Start a digester

The thickened primary sludge and the excess thickened sludge are mixed in a buffer basin resulting in a flow rate of approximately 1900 m^3/day. The primary thickeners in the number of 4 units reduce the volume of sludge discharged from the primary decanters, gravitationally, by increasing the concentration of dry matter to about 6%.

Then it is pumped and distributed in the 5 digesters where anaerobic fermentation takes place, from which biogas is produced. Always one of the digesters is in the decolmation reserve, and four digesters are working.

The sludge fermentation tanks (digesters), numbering 5 units of 8000 m^3, are the place where the thickened mixture sludge is stabilized anaerobically by fermentation under the conditions of permanent mixing and recirculation at 36°C–37°C. The digesters are internally blended, continuously supplied and evacuated, and externally recirculated with fermented sludge.

To prevent foaming of the digestate, the digesters are equipped with an internal sprinkler-type water sprinkling system. It follows from the above that a digester in working mode is designed to process 475 m^3/day of sludge. Respect to this volume of 8000 m^3 it results a hydraulic stationary time of 17 days.

Start digestor

The initiation phase begins with the initial water supply of the digester, which has been heated in an external heat exchanger. Then start feeding with small amounts of raw sludge (primary sludge or excess). During the first 4-5 days it is supplied by about 25 m^3/day, then gradually increase the amount of food to 50 m^3/day, 80 m^3/day, 100 m^3/day up to 380-480 m^3/day everything over the course of 42 to 45 days. During this period, the first quantities of biogas begin to

be obtained from the fermentation process. In the third week (days 14 to 21) gas-producing bacteria are formed. In week four to five (days 28 to 35) the first biogas productions appear. At eight to ten weeks (days 56 to 70) from point 0 (zero) sludge production is reached, the concentration of the active sludge is reached and the normal operating flow is reached. The role of gradual feeding at low doses is to facilitate the controlled development of methane-producing bacteria. Throughout the start, the sludge in the digester is recirculated and passed through a heat exchanger outside the digester to ensure and maintain the required temperature of the digester (36°C).

Table 1

Experimental data. Mechanical waste water treatment part

Date	Raw water temperature	Influent flow rate wastewater treatment plant	Effluent flow rate wastewater treatment plant	Biological stage input flow rate + supernatant + carbon intake	Consumption of Ferric Chloride (sol 5%)	Polymer supply of thickening (sol 3%)
	°C	mc/day	mc/day	mc/day	mc	mc/day
10.09	22.73	554320.20	542210.30	436721.514	7.13	101.59
11.09	22.84	555432.10	543874.20	437481.642	7.24	100.79
12.09	23.21	554241.50	545741.30	451438.758	11.46	107.45
13.09	23.42	551268.30	543426.20	448581.954	9.56	106.64
14.09	24.10	522827.40	515264.10	464871.842	8.87	105.54
15.09	24.78	543764.30	535421.20	475198.746	9.57	107.34
16.09	25.07	553335.60	540482.30	450498.738	12.47	108.66
17.09	25.00	565425.80	552556.20	451286.469	10.99	110.42
18.09	24.96	549550.90	536718.40	449995.353	9.41	108.89
19.09	24.66	532971.90	520366.20	442388.590	11.40	112.57
20.09	24.48	514602.80	502064.10	440081.239	10.96	108.97
21.09	24.50	559495.60	546996.30	438344.105	7.36	108.46
22.09	24.20	562351.60	549939.40	435333.689	9.92	109.34
23.09	24.00	565200.10	552694.20	438588.355	8.34	110.55
24.09	23.80	580066.30	567533.40	439364.400	8.46	108.96
25.09	24.00	567724.40	555170.80	440024.409	10.81	110.02
26.09	24.20	552461.40	539961.60	438548.870	12.24	104.35
27.09	23.80	571093.90	558688.60	435057.530	10.42	98.62
28.09	23.84	550861.50	538436.80	435937.181	6.30	100.41
29.09	23.63	560232.10	547812.70	435839.798	7.57	104.16
30.09	23.24	547070.60	534846.20	428610.726	8.97	101.60
01.10	22.83	558185.80	545683.20	438398.818	7.40	100.79

02.10	22.74	553018.10	540590.20	435819.943	6.72	100.69
03.10	22.82	556546.40	544366.00	427089.142	10.01	102.69
04.10	22.83	534920.70	522536.10	434682.788	11.21	99.78
05.10	23.01	592003.30	579722.50	430269.336	8.73	101.43
06.10	23.14	570170.40	558217.20	418106.952	10.90	96.23
07.10	22.72	606854.30	595095.50	412643.908	8.87	101.93

Table 2

Experimental data. Feed and removal from digestor

	TOTAL PUMPED INTO METHANE TANK				**QUANTITY REMOVED FROM METHANE TANK MIX 25**			
Date	SAS	Flow rate	Dry substance	Volatile substance	Flow rate	Dry substance	Volatile substance	Removed from fermenters
	%	mc/day	T/day	T/day	mc/day	T/day	T/day	kg org./mc/day
10.09	73.74	1733.38	91.88	63.20	1733.38	68.31	37.25	1.58
11.09	69.62	1622.95	84.51	59.40	1622.95	64.74	35.02	1.48
12.09	51.34	1901.05	94.49	69.11	1901.05	74.83	40.76	1.73
13.09	47.79	2557.04	129.64	91.40	2557.04	101.20	53.50	2.28
14.09	51.24	2312.19	118.20	84.87	2312.19	89.07	47.89	2.12
15.09	63.71	2217.68	114.48	81.74	2217.68	84.91	45.62	2.04
16.09	57.71	1956.51	101.54	70.88	1956.51	74.60	40.18	1.77
17.09	55.49	2251.64	116.75	80.23	2251.64	85.79	45.99	2.01
18.09	54.41	2574.15	124.07	88.13	2574.15	96.63	52.00	2.20
19.09	59.80	2478.56	118.97	85.66	2478.56	92.23	49.87	2.14
20.09	63.24	2243.81	110.84	81.80	2243.81	86.05	46.04	2.05
21.09	58.06	2012.81	104.04	74.47	2012.81	76.55	40.58	1.86
22.09	56.02	2188.78	117.54	82.73	2188.78	83.92	45.67	2.07
23.09	55.27	2106.24	112.24	80.06	2106.24	80.75	44.25	2.00
24.09	53.66	1918.43	104.94	75.63	1918.43	73.69	40.23	1.89
25.09	51.32	1913.91	106.68	75.66	1913.91	73.86	40.23	1.89
26.09	48.71	2020.53	110.83	79.09	2020.53	77.97	42.64	1.98
27.09	46.17	2116.89	118.33	82.77	2116.89	81.29	44.07	2.07

28.09	53.70	2168.84	113.86	82.67	2168.84	82.37	45.35	2.07
29.09	54.66	2011.63	108.23	78.46	2011.63	75.13	41.41	1.96
30.09	54.38	1864.90	101.64	74.50	1864.90	68.44	38.13	1.86
01.10	52.87	1986.73	106.29	77.49	1986.73	73.71	41.22	1.94
02.10	56.45	1874.80	101.99	74.25	1874.80	68.43	38.80	1.86
03.10	52.74	1849.54	100.80	73.79	1849.54	67.64	38.62	1.84
04.10	54.80	1866.70	106.46	75.79	1866.70	69.74	39.72	1.89
05.10	53.11	1962.38	111.03	79.52	1962.38	73.96	41.95	1.99
06.10	45.54	2149.45	118.93	85.21	2149.45	78.78	44.13	2.13
07.10	53.84	2215.50	117.98	82.64	2215.50	76.89	43.86	2.05

Table 3

Experimental data. Biogas production

Date	Fermentation yield of organic substance	Calculated biogas production (laboratory)	Production of registered biogas (raw, gas, wet)	Registered consumed biogas (sulphurated gas, dry)	Biogas lost on valves	Global yield biogas production	Electricity produced
	%	Nmc/day	Nmc/day	Nmc/day	Nmc/day	%	kWh
10.09	41.07	23358	22569.35	21593.09	788.62	35.76	4670
11.09	41.03	21934	21347.97	20681.48	586.26	35.88	4680
12.09	41.02	25517	21234.00	19723.77	4283.06	35.64	4640
13.09	41.46	34105	29150.40	27868.10	4954.78	35.42	4720
14.09	43.57	33279	31260.52	30032.00	2018.28	35.29	4680
15.09	44.19	32508	30430.53	29388.53	2077.47	35.56	4720
16.09	43.31	27627	26851.81	26299.33	774.98	35.30	4790
17.09	42.68	30814	27910.97	25868.34	2903.44	35.95	4830
18.09	41.00	32518	31040.83	30134.55	1477.29	35.34	4690
19.09	41.78	32213	31008.58	30205.13	1204.02	35.81	4540
20.09	43.72	32190	30995.53	30119.05	1194.07	35.80	4510
21.09	45.51	30506	28553.17	27278.51	1952.96	35.80	4720
22.09	44.80	33360	30031.38	28818.58	3328.52	35.45	4620
23.09	44.73	32228	30486.17	27995.26	1742.03	35.84	4720
24.09	46.80	31856	30127.51	28764.15	1728.76	35.34	4190
25.09	46.83	31885	29595.84	28833.26	2289.42	35.44	4780
26.09	46.08	32798	30001.39	28923.64	2796.82	35.32	4730

27.09	46.76	34837	32888.37	31830.46	1949.01	36.08	4690
28.09	45.14	33587	32944.25	31786.26	643.08	36.07	4760
29.09	47.22	33345	33250.25	32575.03	94.35	35.55	4350
30.09	48.82	32734	32180.50	31608.96	553.41	35.55	4500
01.10	46.81	32641	31925.62	31222.80	715.68	35.82	4690
02.10	47.74	31903	31216.65	30427.09	686.69	35.66	4690
03.10	47.66	31648	30544.26	29577.77	1103.73	35.89	4680
04.10	47.59	32457	31017.76	29589.16	1439.41	35.37	4550
05.10	47.24	33812	31428.13	30071.96	2384.35	35.80	4740
06.10	48.21	36973	34844.44	33644.44	2129.01	35.77	4730
07.10	47.97	36852	32497.81	31005.79	2276.47	35.48	5050

3. Results and discussions

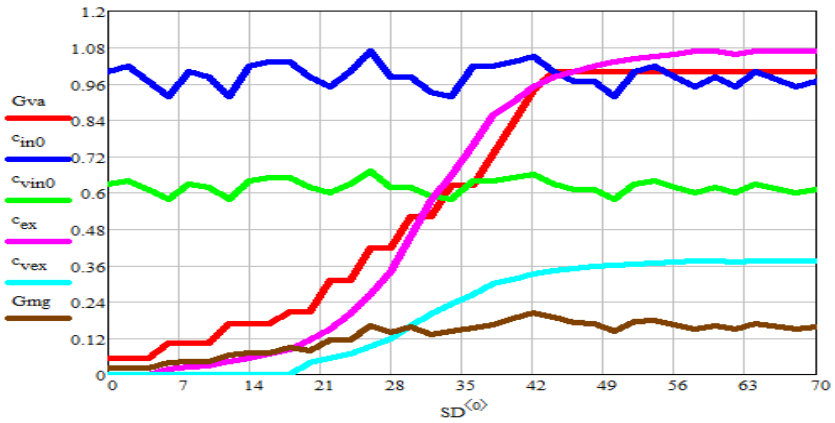

Fig. 2 Dynamics of starting an active mud digester from wastewater treatment in a large city (Gva= Gvam/480, c_{in0} =c_{inm}/60, c_{vin0}=c_{inm}/60, c_{ex} =c_{exm}/60, c_{vex}=c_{vexm}/60, Gmg=Gmgm/2.88x10^4, concentrations in g/L, flows in kg/day)

Throughout the start-up of the digester, the flow to be supplied, the total solid concentration at the entry and exit into and out of the bioreactor, the total volatile concentration (fermentable) at the entry and exit of the fermenter and the gas flow produced by the fermenter shall be measured. Figure 2 concentrates these measurements for a period of 70 days. It is noticeable a complex dynamic of the process of starting a digester, as described above. Since the bioreactor is full, i.e. it operates without volume variation, its operation during this period can be described mathematically, simplified, as shown by relationships (1) and (2). A global kinetic for volatiles (c_{ve}) and biomass (c_x) is recognized here. Noting that

the experimental data come from only one type of experimental measurement, whether industrial as is the case with Figure 2, it is not advisable to identify the parameters of the model [5].

$$\frac{dc_{ve}}{d\tau} = \alpha \frac{v_{max} c_{ve}}{K_m + c_{ve}} c_x + \beta \frac{v_{max} c_{ve}}{K_m + c_{ve}} + G_{Vg} (c_{vin} - c_{ve}) \quad (1)$$

$$\frac{dc_x}{d\tau} = \alpha \frac{v_{max} c_{ve}}{K_m + c_{ve}} c_x + + G_{Vg} (c_{xin} - c_{vex}) \quad (2)$$

Now that 4 of the 5 digesters are in nominal operating mode, it is found that they are supplied with about 2000 m^3/day of sludge and that the digested sludge is continuously discharged. Figure 3, where it uses data from table 2 and 3, focuses the operating data of the biogas line in the household water processing plant of a large city. It is thus found that the fresh substrate and the level as required by the normal operating regime of the biogas phase are maintained in the digesters.

The normal evolution of sludge is towards an acidic pH (pH=6-7). The pH value is periodically checked and its control is done by adding quick lime, $Ca(OH)_2$, to keep the pH value around 7. The value of volatile acid it needs to be ≤ 500 mg/L, if higher, shall also be corrected by the addition of $Ca(OH)_2$. CO_2 evolution in digestor should also be monitored as a value of more than 30 % affects combustion capacity and increases the level of crust in the digester.

Biogas from the fermentation process is captured and stored in gas tanks (gasometers). The resulting biogas is analyzed by the gas analyzers to determine its chemical composition.

It is noted from Figure 3 that from 1900 m^3/day sludge fed in digesters produces 24000 m^3/day of biogas. It shall be stored in biogas storage tanks, two gasometers of 3000 m^3 each, from which samples are taken to analyze the presence of sulphur in the form of H_2S.

Hydrogen sulfide has corrosive properties so that it attacks the generators of the power generation unit, as well as other components, such as gas and exhaust pipes. For this reason, it becomes necessary to desulphurize and dry the biogas. The methods used for desulphurization are varied and the processes can be biological or chemical in nature, taking place inside or outside the digester. Desulphurization depends on the H_2S content and the rate of gas flow through the desulphurization system. This rate can fluctuate significantly, depending on the process.

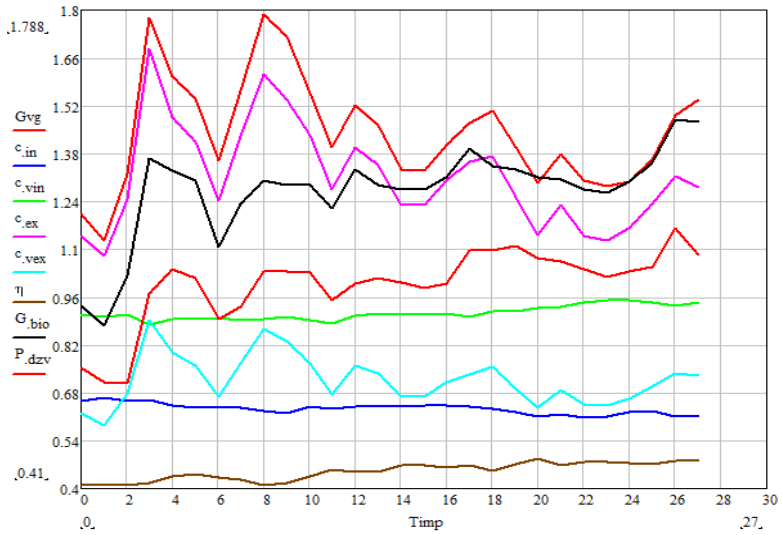

Fig. 3. Data on the nominal operation of the biogas fermentation station of the active sludge in a large city-associated plant (Gvg= Gvam/2000, c_{in0} =c_{inm}/60, c_{vin0}=c_{in0}/c_{vin}, c_{ex} =c_{exm}/60, c_{vex}=c_{exm}/c_{vexm}, G_{bio}=G_{biom}/2.88x10^4 , P_{dzv}=P_{dzvm}/2000, concentrations in g/L, flows in kg/day respectively m^3/day, P_{dzvm} in kW)

The combustion properties must be guaranteed in order to prevent generator failure. From the 24 000 m^3/day biogas, as shown in Figure 3, cogeneration produces electricity at the nominal power of 2 MWh.

Digested sludge is evacuated and stored in a basin where it is advanced dehydrates by centrifugation. In the dehydrating station of all sludge in the plant, the fermented sludge is dehydrated on press filters (7 units) and centrifuges (3 units) with added polymer and lime, up to a concentration of up to 35 % dry matter, allowing storage in the nearby ecological landfill.

From all these processes, a daily result of 1800 m^3 of waste, water mixed with solid substance that enters various stages of processing and finally, when they become inert, is stored in perfect safety at an ecological dump.

Anaerobic fermentation results in a biogas in which the carbon dioxide content does not exceed 38% vol.

The summary shows that from 1900 m^3/day sludge fed in digesters produces 24000 m^3/day of biogas. The cogeneration station powered by two 1000 m^3 gasometers operates with two 2 MWh gas engines each, which produce electricity and heat.

6. Conclusions

An ideal raw material for biogas production is sludge from the aerobic treatment of municipal wastewater. This sludge contains both organic materials, nutrients such as nitrogen, phosphorus, potassium, sulfur, magnesium and small amounts of calcium, as well as pollutants - heavy metals, toxic organic substances and pathogens.

Technological aspects of the production of activated sludge from the biological treatment of domestic waste water and its use for a cogeneration biogas plant characteristic of a large city shall be dealt with. It has been studied how the bacterial system of methanogenesis occurs when only the addition of inocul is necessary because the fermentation mass already has the bacteria needed for fermentation. The experimental part of this article concerns the commissioning of a biogas fermenter (figure 2) and the long-term tracking of the operation of the biogas line coupled with the electric current cogeneration line and hot water for the process (figure 3).

REFERENCES

[1] * * * Plan de Implementare pentru Directiva 91/271/CEE privind epurarea apelor uzate orășenești, Guvernul Romaniei, 204, Actualizare, 2012.
[2] Turoviskiy, S. I., Mathai K. P., *Wastewater Sludge Processing, Chapter 2*, John Wiley & Sons, Hoboken, NJ, USA, 2006.
[3]. Rapport, J., Zhang, R., Jenkins, M. B., Williams, B R., *Current Anaerobic Digestion Technologies Used for Treatment of Municipal Organic Solid Waste*, Biomass and Bioenergy, 35, 3, 1263 -1272, 2011.
[4] Verstraete, W., Morgan, S., Aiyuk S., Waweru, M., Rabaey., K., Lissens G., *Anaerobic digestion as a core technology in sustainable management of organic matter*, Water Science Technology, 52, 1-2, 59-68, 2005.
[5]. Dobre, T., Sanchez, J.M., *Chemical Engineering Modeling, Simulation and Similitude*, Chapter 5, Wiley VCH, 2007.

A VERSATILE MATERIAL OF THE XXIST CENTURY: APATITIC COMPOUNDS WITH MULTIFUNCTIONAL PROPERTIES

Toma FISTOS[1], Anda M. BAROI[1], Roxana I. BRAZDIS[1*], Irina FIERASCU[1,2], Irina E. CHICAN[1], Radu C. FIERASCU[1,3]

[1]National Institute for Research and Development in Chemistry and Petrochemistry – ICECHIM, 202 Splaiul Independentei, Bucharest, Romania
[2]University of Agronomic Sciences and Veterinary Medicine of Bucharest; 59 Mărăști Blvd., Bucharest, Romania
[3]University Politehnica of Bucharest, 313 Splaiul Independentei, Bucharest, Romania

Abstract

In the field of material development, apatitic compounds are the most probably studied in this century, due to their multifunctional properties. They can be used in environmental applications, for air, water and soil pollution control, in biomedical applications or cultural heritage protection. In order to enhance potential properties of these materials, changing its architecture can be an alternative to the use of toxic substances. For each final application the apatitic structure presents a particular importance. In this context, the present work focuses on synthesis and characterization methods and final applications of apatitic materials in environmental domain and cultural heritage protection. Also, this paper summarizes different aspects related the correlation of material's morphology related to final application. The literature review was conducted using different databases (Scopus, Web of Science, ScienceDirect, SpringerLink) using as keywords "hydroxyapatite", "apatitic materials", "phosphatic compounds", or multiple keywords "apatitic materials for environment", "apatitic materials for cultural heritage protection".

Key words: hydroxyapatite, apatitic materials, environmental protection, cultural heritage.

1. Introduction

With the development of nanotechnology, a new generation of innovative materials and technologies were developed, with tremendous implications for several industrial sectors. One of these materials is represented by hydroxyapatite (HAP), a calcium phosphate, which stands out for its capacity of accepting a large number of anionic and cationic substituents [1].

*Corresponding author: roxana.brazdis@icechim.ro

For the last past decades, apatitic materials have been playing an important role in various fields due to their potential applications, especially in environmental protection and cultural heritage conservation. Over the time, depending on the desired properties, which are mainly influenced by the reaction parameters, the scientific area developed several methods of obtaining these materials, the final products obtained having different morphologies, stoichiometry and crystallinity [2]. Also, it has been demonstrated that, in order to enhance the properties of hydroxyapatite, it can be doped with other compounds such as heavy metals or zeolites [3]. Moreover, besides their appropriate properties, apatitic materials are also characterized by low costs involved in their synthesis and application.

The current review aims to emphasize the importance of hydroxyapatite and its composites, by providing the most encountered methods of synthesis and properly methods of materials characterization. Also, it is described the potential application of these materials in various fields, by adsorbing organic and inorganic pollutants or by serving as a consolidant in cultural heritage conservation.

2. Synthesis and characterization of apatitic materials

Over time, a wide range of methods for the synthesis of HAP have been studied and developed, such as: sol-gel synthesis [4], hydrothermal reactions [5], ultrasound-microwave method [6], co-precipitation method [7] and sono-chemical method [8] the obtaining being in different forms such as powder or granules [9].

Phatai et al. synthesized through a sol-gel method, a “green” composite material using glutinous rice (GR) and hydroxyapatite [4]. The authors used GR seeds aqueous extract and specific reagents for classical obtaining of HAP: $Ca(NO_3)_2 \cdot 4H_2O$ and $(NH_4)_2HPO_4$, maintaining pH constant during the reaction.

In another study, HAP was synthesized by the microwave hydrothermal method using the same basic reagents, and solutions with different amounts of amino acids to see the effect of HAP crystal growth in the study of biomineralization [5]. After completion of the synthesis, the mixture was put in teflon reactors and placed in a digestive system where it was irradiated in the microwave. The product obtained after irradiation was centrifuged, washed and lyophilized.

Banerjee and his group used the co-precipitation method to synthesize HAP starting from $Ca(NO_3)_2 \cdot 4H_2O$ and $(NH_4)_2HPO_4$, but in addition to the basic ingredients they also used cysteine as a chelating agent [7].

Guesmi and his partners has also used the co-precipitation method to synthesize HAP starting from an aqueous solution of $(NH_4)_2HPO_4$ and an aqueous solution of $Ca(NO_3)_2 \cdot 4H_2O$ under nitrogen atmosphere [10].

HAP/Fe_3O_4 microspheres were synthesized by Wu and his co-workers using the hydrothermal method. In the first stage they dissolved in a solution of ethylene glycol, $FeCl_3$ and CH_3COONa separately and then the 2 solutions were mixed and autoclaved. The synthetic product obtained was magnetically separated and then washed with ethanol and water and to remove excess water it was dried by freezing. In the second stage to obtain HAP, there were used $Ca(NO_3)_2 \cdot 4H_2O$ and $(NH_4)_2HPO_4$. In the $Ca(NO_3)_2 \cdot 4H_2O$ solution was added the Fe_3O_4 solution obtained in the previous stage, then $(NH_4)_2HPO_4$ and $NH_3 \cdot H_2O$ to maintain the pH of the reaction constant. The mixture was placed in an autoclave for one day and then washed with water and alcohol and dried by freezing [11].

Apatitic materials can be characterized through modern analytical methods such as: X-ray diffraction (XRD) [12], X-ray fluorescence (XRF) [13], Fourier-transform infrared spectroscopy (FTIR) [14], Transmission electron microscopy (TEM) [15], thermal analysis [16], obtaining information regarding the morphology of the synthesized materials and their particle size.

XRD is usually used to characterize crystalline materials being a non-destructive technique and provides multiple information about the structure, phase, orientation of the crystal, texture, average grain size and crystallinity [17]. Chen and his partners, after studying the different peaks in the diffractograms provided by XRD, found that the sample is a hexagonal phase of hydroxyapatite [5].

XRF is a nondestructive technique that uses X-ray excitation in order to obtain inorganic elemental analyzes of the synthesized materials and information regarding the impurities. This is a technique that provides both qualitative and quantitative information and can be applied to solids, liquids and powders [18]. Fierascu et al. synthesized HAP with different concentrations of Ag and through XRF they noticed that all samples had no impurities and the variation of the silver peaks corresponded to the silver concentrations used in the samples [19].

FTIR gives us information about the chemical bonds that occur between different functional groups and the molecular structures of organic compounds and inorganic materials. [20]. The presence of different functional groups, such as hydroxyl, carbonyl and phosphate groups were observed by Vahdat et al. in FTIR analyses, which increased the properties of synthesized HAP [21].

TEM is a microscopique technique that uses an electron beam to imagine a sample. The principle of operation is represented by a high-energy electron beam is sent through a very thin sample, interacting with the sample as it passes, allowing angstrom-level imaging to be obtained [22]. Fierascu and his colleagues used TEM to study the morphology of the various synthesized HAP-Ag samples

and observed that bare HAP showed the classical rode shape form and Ag appears as dark spots [19].

Thermogravimetric analysis provides information about the composition of the material and its thermal stability at high temperatures. The technique consists in the quantitative measurement of the rate of change of the weight of a material depending on the temperature or time in an atmosphere of nitrogen, helium, air or vacuum. Through the processes that take place during the analysis, such as decomposition, oxidation or dehydration, it can be said if the sample loses or gains mass at various temperatures [23]. After studying the TGA curve offered by the thermal analysis, Ma et al. noticed a decrease in the mass of the sample between 626 - 770ºC corresponding to the decomposition of the calcite in the marble sample [24].

3. Application of apatitic materials

One of the major problems that the entire world is facing in the last centuries is the pollution. Various industries such as pharmaceutical, plastic, cosmetics and textile generate pollutants that are therefore found in the environment, especially in soil and water [25]. These pollutants are divided into two categories: organic substances, such as phenols [26, 27] and dyes [28, 29] and inorganic substances, mainly heavy metals [30-32].

Hydroxyapatite and its composites have been studied as adsorbents for environmental applications [9].

Phenolic compounds discharge into waters and soils represent a health threat, due to their carcinogenic influences on aquatic organisms [30]. Although they are hard to degrade, there are several studies that demonstrate the capacity of apatitic materials of removing phenolic compounds.

Ekka et al. studied the degradation of phenol, 4-clorophenol and 4-nitrophenol using the ratio 1:1hydroxyapatite-zirconia nanocomposite obtained by sono-chemical synthesis [33]. In order to explore the proposed materials in the water purification field, the authors have also tested their toxicity, using THP-1 cell, resulting that the cell morphology was normal after 3-days of exposure. The photocatalytic activity of the obtained material was evaluated under UV light irradiation, in comparison with the pure hydroxyapatite and zirconia nanoparticles. They obtained the best results for the hydroxyapatite-zirconia nanocomposites, where the removal rates were 95-98% for all phenol compounds, while, for the bare hydroxyapatite and zirconia particles, the range of removal rate was 15-36%.

In another study, Bouiahya and co-workers synthesized Al_2O_3-HAP composites, by a re-precipitation method of natural phosphate ore in the presence of Al (III) ions, varying the amount of Al-precursor added [26]. Therefore, they

obtained final Al_2O_3-HAP weight ratios of 5, 10 and 20%. The authors evaluated the adsorption capacity using 0.2 g of each sample and phenol solutions with concentrations ranging from 5 to 100g/L. They concluded that the Al (III) content in the materials influences proportionally the phenol adsorption, due to the chemical nature of alumina. Also, the study included three cycles of "adsorption-desorption" in order to regenerate the adsorbents, which demonstrated that there are eco-friendly composites, with low costs included.

Our group have also investigated the removal of phenols using non-substituted and substituted apatites (Sr and Ba) [27]. It was observed that phenol amount adsorbed is higher at pH 3, in comparison with an adsorption conducted at basic pH. The BaHAP adsorbent presented the maximum amount of phenol uptake. Moreover, the obtained materials showed biocide features.

Synthetic dyes are usually generated by petroleum products, and then used to color materials in order to maintain that coloring even after washing them, Methylene Blue, Direct Yellow 4, Congo Red and Eriochrome Black T are just few examples of synthetic dyes which are mainly used in the leather and textile industries in a proportion of 70% [34]. Over time, apatitic adsorbents have been studied also for the removal of such dyes.

Magnetic hydroxyapatite, obtained by a chemical co-precipitation method, was reported by Sahoo et al. to show good results in the removal of Eriochrome Black T, an azo dye, from aqueous solutions [29]. They have shown that the maximum EBT dye removal efficiency depended on the amount of adsorbent dosage, due to the availability of more active binding sites. Thus, at a dosage of 100 mg magnetic hydroxyapatite nanocomposite, they obtained a 97.2 % removal efficiency.

The removal of three anionic dyes, namely Reactive Orange 5, Reactive Orange 16 and Congo Red, from aqueous solutions, was studied by Piri et al., who used a magnetic/zeolite hydroxyapatite (MZeo-HAP), obtained by co-precipitation method [35]. At pH 2, the maximum adsorption capacity is reached for all three samples. The best results are obtained for Congo Red adsorption, approximatively 104.05 mg/g, while, for Reactive Orange 16, the maximum adsorption capacity is approximatively 88.31 mg/g.

Beside phenolic compounds and synthetic dyes, heavy metals are reported to cause toxicity and ecological problems, due to their accumulation in the environment [36]. For the past decades, nanomaterials have been used to remove a variety of heavy metals such as arsenic [37], cadmium [38], chromium [39], copper [30], lead [21], and nickel [30], etc. Apatitic materials seems to be much more promising in terms of water and soil depollution. Vahdat et al. used a magnetic nanocomposite of HAP for the removal of lead ions from aqueous solutions, but in this case, de HAP phase was obtained from chicken thighbones, which were washed, carbonized completely, calcinated at 1000ºC and powdered

via the milling process [21]. The maximum adsorption capacity of HAP/Fe_3O_4 was approximatively 109.89 mg/g, obtained at pH 6 and 25°C. Also, after the FTIR tests, they concluded that the presence of the functional groups, such as hydroxyl, carbonyl and phosphate groups, is the reason of the efficiency of recovery/adsorption of the metal ions.

In another study, Thanh et al. removed copper and nickel from aqueous solutions also using a synthesized magnetic hydroxyapatite nanocomposite [30]. They obtained a 48.78 mg/g adsorption capacity for Cu (II), respectively 29.07 mg/g for Ni (II).

Preservation of cultural heritage is a problem of utmost importance today because environmental conditions (rain, frost, heat) are becoming more aggressive which leads to damaging the art objects (sculptures, historic buildings). For this reason, it is necessary to find solutions as quickly and efficiently possible for removing the damage of the artifacts. In the case of carbonated stones, the existing solutions on the market for preventing and stopping the meteorological processes that affect these stones were unsatisfactory. The desired result from the material needed to preserve the carbonate stones is that it forms a hydrophobic layer with the stone or a surface layer with low solubility. Hydroxyapatite comes as a solution to the problem for the preservation of carbonaceous stones and later tried for the preservation of additional substrates: sandstone, concrete, gypsum and sulfated stones [40].

The synthesis of hydroxyapatite can take place in the laboratory or *in situ*. Sassoni et al. tried to treat the marble with TiO_2 nanoparticles but he noticed that due to the rain they were washing off the surface of the stone [41]. They came up with an innovative solution to combine TiO_2 nanoparticles with hydroxyapatite. Following this combination, it was observed that TiO_2 nanoparticles are no longer washed from the rock after rain and its photocatalytic activity is not affected. To test the efficiency of the combination between TiO_2 and HAP they did three tests: in the first sample they treated marble only with TiO_2 nanoparticles, in the second sample they treated marble with sequential application of the HAP and TiO_2 and in the third sample they treated marble with TiO_2-HAP combination. They observed that the sequential application and that of the TiO_2-HAP combination goes beyond the simple application of TiO_2 nanoparticles, the main advantage being that the material does not wash off the stone after rain. Moreover, the combination offers marble a high capacity for self-cleaning and high durability.

Gong and his parteners synthesized by the hydrothermal method an aqueous colloidal HAP in order to consolidate the ancient ivory from the site of the Jinsha ruins [42]. It was observed that a compact layer of HAP nanoparticles is formed on the original surface of the ivory. They concluded that after treating ivory with synthesized HAP, the mechanical properties (hardness, elastic modulus and anti-scratch) are significantly improved.

Another group tried to consolidate a Hellenistic-Roman burial chamber in Cyprus by synthesizing HAP in situ starting from diammonium hydrogen phosphate (DAP) [24]. To synthesize HAP they treated 3 distinct places in the tomb with DAP solution, which will react with the calcium carbonate in the stones to form HAP needed to strengthen the stones. Desalination of the treated areas was performed to see if it influences the formation of HAP and if significant changes occur. To see if this treatment has a positive effect on the treated areas, they performed compositional and microstructural tests immediately after applying the DAP solution and a year later. The limestone was transformed into a HAP network that helped strengthen the substrates of the treated areas. No difference was observed between the three treated areas and no difference was observed between the desalinated and non-desalinated areas. They concluded that this treatment with the *in situ* formation of HAP has a great potential to strengthen the powdery archaeological limestone surfaces.

Like the other sources mentioned, Fierascu et al. synthesized apatitic materials with antimicrobial properties that can be used as potential materials for consolidating carbon stones [19]. To demonstrate the antimicrobial properties, they performed both quantitative and qualitative tests on different strains of pathogenic bacteria and on strains of filamentous fungi.

4. Conclusions

The present article outlines the insights of HAP and its composites. Even we are talking of different applications, such as removal of hazardous pollutants from waters, or protection of cultural heritage, apatitic materials are promising materials with potential to use. As a future perspective, there is a large possibility to propose solutions for the enhancement of materials' properties related to final applications.

Acknowledgements: This work was supported by a grant of the Romanian National Authority for Scientific Research and Innovation, CNCS/CCCDI – UEFISCDI, project number PN-III-P1-1.2-PCCDI-2017-0413, contract 50PCCDI/2018, within PNCDI III and by the Romanian Ministry of Research and Innovation - MCI (Ministry of Education and Research – MEC) through INCDCP-ICECHIM Bucharest 2019-2022 Core Program PN. 19.23 - Chem-Ergent, Project No.19.23.03.

REFERENCES

[1] Fihri A., Len C., Varma R. S., Solhy A., Hydroxyapatite: *A review of synthesis, structure and applications in heterogeneous catalysis*. Coordination Chemistry Reviews, 347, (2017), 48-76

[2] Sadat-Shojai M., Khorasani M. T., Dinpanah-Khoshdargi E., Jamshidi A., *Synthesis methods for nanosized hydroxyapatite in diver structure*. Acta Biomaterialia, 2680, (2013), 7591-7621

[3] Fierascu I., Fierascu R. C., Popa O., Babeanu N., *Synthesized materials for decontamination of heavy metals polluted aqueous solutions*, Romanian Biotechnological Letters, 19, (2014), 9196-9202.

[4] Phatai P., Futalan C.M., Kamonwannasit S., Khemthong P., *Structural characterization and antibacterial activity of hydroxyapatite synthesized via sol-gel method using glutinous rice as a template*, Journal of Sol-Gel Science and Technology, 89, (2019), 764-775.

[5] Chen J., Liu J., Deng H., Yao S., Wang Y., *Regulatory synthesis and characterization of hydroxyapatite nanocrystals by a microwave-assisted hydrothermal method*, Ceramics International, 46, (2020), 2185–2193.

[6] Nyoo J., Handoyo N., Kristiani V., Adi S., *Pomacea sp shell to hydroxyapatite using the ultrasound – microwave method (U – m)*, Ceramics International, 40, (2014), 11453–11456.

[7] Banerjee S., Bagchi B., Bhandary S., Kool A., *A facile vacuum assisted synthesis of nanoparticle impregnated hydroxyapatite composites having excellent antimicrobial properties and biocompatibility*, Ceramics International, 44, (2018), 1066–1077.

[8] Utara S., Klinkaewnarong J., *Sonochemical synthesis of nano-hydroxyapatite using natural rubber latex as a templating agent*, Ceramics International, 41, (2015), 14860–14867.

[9] Pai S., Kini S. M., Selvaraj R., Pugazhendhi A., *A review on the synthesis of hydroxyapatite, its composites and adsorptive removal of pollutants from wastewater*, Journal of Water Process Engineering, 38, (2020), 101574.

[10] Guesmi Y., Agougui H., Lafi R., Jabli M., Hafiane A., *Synthesis of hydroxyapatite-sodium alginate via a co-precipitation technique for efficient adsorption of Methylene Blue dye*, Journal of Molecular Liquids, 249, (2018), 912-920.

[11] Wu Y., Chen J., Chen G., Zhu P., *Convenient synthesis of hydroxyapatite-coated ferroferric oxide microspheres by hydrothermal method*, Materials Letters, 253, (2019), 218-221.

[12] Robinson I.K., Vartanyants I.A., Williams G.J., Pfeifer M.A., Pitney J.A., *Reconstruction of the Shapes of Gold Nanocrystals Using Coherent X-Ray Diffraction*, Physical Review Letters, 87, (2001), 195505-1.

[13] Lawryk N.J., Feng H.A., Chen B.T., *Laboratory Evaluation of a Field-Portable Sealed Source X-Ray Fluorescence Spectrometer for Determination of Metals in Air Filter Samples*, Journal of Occupational and Environmental Hygiene, 6, (2009), 433.

[14] Huth F., Govyadinov A., Amarie S., Nuansing W., Keilmann F., Hillenbrand R., *Nano-FTIR Absorption Spectroscopy of Molecular Fingerprints at 20 nm Spatial Resolution*, Nano Letters, 12, (2012), 3973.

[15] Van Renterghem W., Miller B. D., Leenaers A., Van den Berghe S., Gan J., Madden J.W., Keiser Jr. D.D., *Transmission Electron Microscopy Investigation of Neutron Irradiated Si and ZrN Coated UMo Particles Prepared Using FIB*, Journal of Nuclear Materials, 498, (2018), 60.

[16] Joliff Y., Belec L., Chailan J. F., *Finite Element Analysis of the Material's Area Affected During a Micro Thermal Analysis Applied to Homogeneous Materials*, Journal of Surface Engineered Materials and Advanced Technology, 1, (2011), 1.

[17] Jiang H., Song C., Chen C. C., Xu R., Raines K.S., Fahimian B. P., Lu C. H., Lee T. K., Nakashima A., Urano J., Ishikawa T., Tamanoi F., Miao J., *Quantitative 3D Imaging of*

Whole, Unstained Cells by Using X-Ray Diffraction Microscopy, Proceedings of the National Academy of Sciences USA, 107, (2010), 11234.

[18] West M., Ellis A. T., Potts P. J., Streli C., Vanhoof C., Wegrzynek D., Wobrauschek P., *Atomic Spectrometry Update – X-Ray Fluorescence Spectrometry*, Journal of Analytical Atomic Spectrometry, 25, (2010), 1503.

[19] Fierascu I., Fierascu R.C., Somoghi R., Ion R.M., Moanta A., Avramescu S.M., Damian C.M., Ditu L.M., *Tuned apatitic materials: Synthesis, characterization and potential antimicrobial applications*, Applied Surface Science, 438, (2018), 127–135.

[20] Johnson C. M., Bohmler M., *Nano-FTIR Microscopy and Spectroscopy Studies of Atmospheric Corrosion with a Spatial Resolution of 20 nm*, Corrosion Science, 108, (2016), 60.

[21] Vahdat A., Ghasemi B., Yousefpour M., *Synthesis of hydroxyapatite and hydroxyapatite/Fe3O4 nanocomposite for removal of heavy metals*, Environmental Nanotechnology, Monitoring & Management, 12, (2019), 100233.

[22] Kim B. H., Yang J., Lee D., Choi D. B. K., Hyeon T., Park J., *Liquid-Phase TransmissionElectron Microscopy for Studying Colloidal Inorganic Nanoparticles*, Advanced Materials, 30, (2018), 1703316.

[23] Price D.M., Reading M., Hammiche A., Pollock H.M., *New Adventures in Thermal Analysis*, Journal of Thermal Analysis and Calorimetry, 60, (2000), 723.

[24] Ma X., Balonis M., Pasco H., Toumazou M., Counts D., Kakoulli I., *Evaluation of hydroxyapatite effects for the consolidation of a Hellenistic-Roman rock-cut chamber tomb at Athienou-Malloura in Cyprus*, Construction and Building Materials, 150, (2017), 333–344.

[25] Piccirillo C., Moreira I. S., Novais R. M., Fernandes A. J. S., Pullar R. C., Castro P. M. L., *Biphasic apatite-carbon materials derived from pyrolysed fish bones for effective adsorption of persistent pollutants and heavy metals*, Journal of Environmental Chemical Engineering, 5, (2017), 4884-4894.

[26] Bouiahya K., Es-saidi I., El Bekkali C., Laghzizil A., Robert D., Nunzi J.M., Saoiabi A., *Synthesis and properties of alumina-hydroxyapatite composites from natural phosphate for phenol removal from water*, Colloid and Interface Science Communications, 31, (2019), 100-188.

[27] Fierascu I., Avramescu S. A., Petreanu I., Marinoiu A., Soare A., Nica A., Fierascu R. C., *Efficient removal of phenol from aqueous solutions using hydroxyapatite and substituted hydroxyapatites*, Reaction Kinetics, Mechanisms and Catalysis, 122, (2017), 155-175.

[28] Fierascu I., Raditoiu V., Nicolae C. A., Raditoiu A., Somoghi R., Raduly M., Ditu, L. M., *Analytical Characterization and Potential Antimicrobial and Photocatalytic Applications of Metal-Substituted Hydroxyapatite Materials*. Analytical Letters, 2016, 52, (2018), 1-16.

[29] Sahoo J. K., Konar M., Rath j., Kumar D., Sahoo H., *Magnetic hydroxyapatite nanocomposite: Impact on eriochrome black-T removal and antibacterial activity*, Journal of Molecular Liquids, 294, (2019), 111596.

[30] Thanh D. N., Novak P., Vejpravova J., Vu H. N., Lederer J., Munshi T., *Removal of copper and nickel from water using nanocomposite of magnetic hydroxyapatite nanorods*, Journal of Magnetism and Magnetic Materials, 456, (2018), 451-460.

[31] Rebelo A. H. S., Ferreira J. M. F., *Comparison of the cadmium removal efficiency by two calcium phosphate powders*, Journal of Environmental Chemical Engineering, 5, (2017), 1475-1483.

[32] Fierascu I., Fierascu R.C., Popa O., Babeanu N., *Synthesized materials for decontamination of heavy metals polluted aqueous solutions*, Romanian Biotechnological Letters, 19, (2014), 9196-9202.

[33] Ekka B., Nayak S. R., Achary L. S. K., Sarita, Kumar A., Mawatwal S., Dhiman R., Dash P., Patel R. K., *Synthesis of hydroxyapatite-zirconia nanocomposite through sonochemical route: A potential catalyst for degradation of phenolic compounds*, Journal of Environmental Chemical Engineering, 6, (2018), 6504-6515.
[34] Benkhaya S., El Harfi S., El Harfi A., *Classifications, properties and applications of textile dyes: a review*, Applied Journal of Environmental Engineering Science, 3, (2017), 311-320.
[35] Piri F., Mollahosseini A., Khadir A., Hosseini M. M., *Enhanced adsorption of dyes on microwave-assisted synthesized magnetic zeolite-hydroxyapatite nanocomposite*, Journal of Environmental Chemical Engineering, 7, (2019), 1033-1038.
[36] Cui H., Shi Y., Zhou J., Chu H., Cang L., Zhou D., *Effect of different grain sizes of hydroxyapatite on soil heavy metal bioavailability and microbial community composition*, Agriculture, Ecosystems & Environment, 267, (2018), 165-173.
[37] Mirhosseini M., Biazar E., Saeb K., *Removal of arsenic from drinking water by hydroxyapatite nanoparticles*, Current World Environment, 9, (2014), 331-338.
[38] Kazeminezhad I., Ahmadizadeh S., Babaie A.A., *Application of magnetic hydroxyapatite nanoparticles for removal of Cd^{2+} from aqueous solutions*, Journal of Environmental Studies, 40, (2014), 739-750.
[39] Hokkanen S., Bhatnagar A., Repo E., Lou S., Sillanpaa M., *Calcium hydroxyapatite microfibrillated cellulose composite as a potential adsorbent for the removal of Cr(VI) from aqueous solution*, Chemical Engineering Journal, 283, (2016), 445-452.
[40] Serafini I., Ciccola A., Nanotechnologies and Nanomaterials for Diagnostic, Conservation and Restoration of Cultural Heritage, Elsevier, 2018.
[41] Sassoni E., D'Amen E., Roveri N., Scherer G.W., Franzoni E., *Photocatalytic hydroxyapatite-titania nanocomposites for preventive conservation of marble*, Materials Science and Engineering, 364, (2018), 012073.
[42] Gong W., Yang S., Zheng L., Xiao H., Zheng J., Wu B., Zhou Z., *Consolidating effect of hydroxyapatite on the ancient ivories from Jinsha ruins site: Surface morphology and mechanical properties study*, Journal of Cultural Heritage, 35, (2019), 116–122.

MODELING OF SOME CASES OF METAL PICKLING

Ciprian ILIE[1,2], Cristian RADUCANU[1 *], Tanase DOBRE [1, 3], Timur CHIS [4]

[1]Faculty of Applied Chemistry and Materials Science, University Politehnica of Bucharest, 1-3 Gheorghe Polizu Street, 011061, Bucharest, Romania;
[2]Total Romania SA, 3-4 Vasile Alexandri Street, Bucharest;
[3]Technical Science Academy Romania;
[4] University Ovidius Constanta, Romania

Abstract: *Mathematical models for metal pickling by immersion and by spraying techniques can be developed by simultaneously solving the flow and species diffusion equations. In this paper we insist on the case of pickling by immersion for which the theoretical relationship, which characterize kinetics of process. Copper pickling (etching) by immersion in ammonium persulfate - sulfuric acid solutions is used to customize the kinetics of this process.*

Keywords: metal, surface pickling, mass transfer, process modelling, boundary layer,

1. Introduction

In metals processing for pieces of any kind, the cleaning of theirs surfaces, by degreasing and pickling, is mandatory before theirs next treatments. Chemical surface treatment has two main purposes; the first and perhaps most important is to give them good corrosion resistance; the second and perhaps just as important as the first is to change or ennoble their aesthetic appearance. Electrochemical anticorrosive or decorative depositions, super finished polymer coatings and paintings, etc., are current examples in this regard

All processes used for this purpose of metals surface treatment includes, in their development, as elementary processes, cases of transport, of one or more components, to or from surface subjected to processing. From this point of view all these processes are specific to chemical engineering [1]. So high speed operation in these procedures is ensured by: i) operation with relatively concentrated solutions in the consumable species, ii) using temperatures as close as possible to boiling of working solutions if this does not disturb the compounds formed on the surface, iii) stirring or pumping of working solutions.

Two major aspects can be considered from engineering point of view regarding this big problem of wet chemical processing of metal surfaces [1-3]. First aspect consists in theoretical approach of concrete process in the sense of establishing expressions and correlations through which to explain the connection between effects and causes (model which predicts surface etching rate versus process

*Corresponding author: cristian.raducanu@upb.ro

factors). The second aspect contains the descriptive presentation of process with complete know-how accomplishment (recipes of solutions, working procedure, etc.) so that they can be taken over for practical application.
Ennoblement and/or corrosion protection of the metal surface by oxidation (browning), phosphating, coloring, electrochemical deposits, cementation, etc., is always preceded by pickling. Also, the picking of steel is one basic process in steel factories. In this sense it uses the chemical attack of component surface by components immersion or spraying with various pickling solutions. The commonly used pickling solution are aqueous mixtures containing HNO_3 (3 to 6 M) and HF (0.5 to 2 M), which could also be used to pick other non metals such as silicon [1]. In steel factory the pickling solution are formed with hydrochloric acid. The rate of the pickling and the state of the surface of the alloys after treatment are strongly conditioned by the pickling solution composition, by pickling temperature and by picking flow around the processed components. The aim of this paper is to propose models for rate of pickling for the bath picking procedures.

2. Model and experimental investigation

For pickling by immersion, the basic phenomena occur inside of natural convection boundary layer formed on the surface of metallic piece. In this situation a mathematical model can be developed by simultaneously solving the flow and species diffusion equations [4]. At surface of pickling material, the chemical reaction characterizing the process generates the species A, who becomes responsible for pickling kinetic evolution. Figure 1 shows the development of boundary layer at pickling surface and that flow and species A transfer evolve here. If it considers a steady state evolution of pickling then the mathematical model of process is given by the system of equations (1).

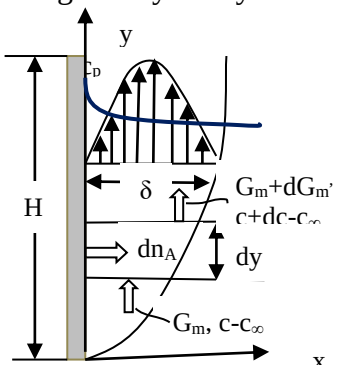

Fig. 1. Phenomenological processes at surface in pickling by immersion in working solution.

It contains the equation of flow produced by concentration gradient (c-c_∞) and the equation of diffusion of species, who have c_p concentration at pickling surface. To be active the mathematical model requests the univocity conditions. At current y these conditions are expressed by relations (2) and (3).

$$\begin{cases} \nu \dfrac{\partial^2 w_y}{\partial x^2} + g\beta_c (c - c_\infty) = 0 \\ w_y \dfrac{\partial c}{\partial y} = D \dfrac{\partial^2 c}{\partial x^2} \end{cases} \tag{1}$$

$$x = 0 \ , \quad c = c_p \quad , \quad w_y = 0 \tag{2}$$

$$x = \delta \ , \quad c = c_\infty \quad , \quad \left(\frac{\partial c}{\partial x} = 0 \right) \ , \quad w_y = 0 \tag{3}$$

A simplified method can be used for analytical solving of our mathematical model. In this sense it considers that the dimensionless concentration profile of diffusion species, inside of boundary layer from pickling surface, depends only on x, and follows the equation (4). The constraints for c from (2) and (3) particularize the dimensionless concentration of diffusive species to (5). From definition expression of species mass transfer coefficient (6) it observes that the solving of flow equation must produces a relation for boundary layer thickness, δ.

$$\Gamma_A = \frac{c - c_\infty}{c_p - c_\infty} = a + bx + cx^2 \tag{4}$$

$$\Gamma_A = \left(1 - \frac{x}{\delta} \right)^2 \tag{5}$$

$$k = \frac{-D \dfrac{dc}{dx}\Big|_{x=0}}{c_p - c_\infty} = -D \frac{\partial \Gamma_A}{\partial x}\Big|_{x=0} = \frac{2D}{\delta} \tag{6}$$

Bellow it shows the solving of flow equation for pickling model. It obtains that the mean flow velocity expression is given by relation (13)

$$\frac{d^2 w_y}{dx^2} = -A\Gamma_A \tag{7}$$

$$A = \frac{g\beta_c (c_p - c_\infty)}{\nu} \tag{8}$$

$$\frac{d^2 w_y}{dx^2} = -A\left(1 - 2\frac{x}{\delta} + \frac{x^2}{\delta^2}\right) \tag{9}$$

$$w_y = -A\left(\frac{1}{2}x^2 - \frac{1}{3\delta}x^3 + \frac{1}{12\delta^2}x^4\right) + C_1 x + C_2 \tag{10}$$

$$x = 0\ ,\ x = \delta \quad w_y = 0 \Rightarrow C_2 = 0\ ,\ C_1 = \frac{A\delta}{4} \tag{11}$$

$$w_y = -A\left(\frac{\delta}{4}x - \frac{1}{2}x^2 + \frac{1}{3\delta}x^3 - \frac{1}{12\delta^2}x^4\right) \tag{12}$$

$$\overline{w}_y = \frac{1}{\delta}\int_0^{\delta} w_y dx = \frac{A\delta^2}{40} = \frac{g\beta_c\delta^2}{40\nu}(c_p - c_\infty) \tag{13}$$

The species A balance, referring to control volume from figure 1, which have *dy* height and unitary width, goes to equations (14). Taking into account the mass flow rate on unitary width of immersed surface (15), the relation (14) becomes to (16). With $\delta = 0$ at $y = 0$ from (16) it obtains successively, the local values of mass transfer coefficient and its mean value ((17) and, respectively, (18)).

$$dn_A = (\overline{c} - c_\infty)dG_m = k(c_p - c_\infty)dy \cdot 1 \tag{14}$$

$$\frac{3\rho g\beta_c(c_p - c_\infty)\delta^2 d\delta}{40\nu} = \frac{4D}{\delta}dy \tag{16}$$

$$k = \frac{2D}{\delta} = 0{,}74\left(\frac{gD^3\beta_c(c_p - c_\infty)}{\nu y}\right)^{0{,}25} \tag{17}$$

$$k = \frac{1}{H}\int_0^H k dy = 0{,}99\left(\frac{gD^3\beta_c(c_p - c_\infty)}{\nu H}\right)^{0{,}25} \tag{18}$$

If the expression c_p - c_∞ = α c_{pa} is accepted, simultaneously with a slow dependence of β_c on concentration of interface diffusion species, then the use of *k* in expression of the pickling flow rate (N_p) leads, for it to the relation (19). Here $c = 0{,}99(\alpha\beta_c)^{0{,}25}$ and c_{pa} represents the active components concentration in the pickling media.

$$N_p = c\left(\frac{D^3}{\nu H}\right)^{0{,}25} c_{pa}^{1{,}25} \tag{19}$$

In order to validate the presented model, the experimental investigation of copper pickling using acid ammonium persulphate solutions was developed. An experimental plan 2^3, where the process factors are temperature, ammonium

persulphate concentration and respectively sulphuric acid concentration in the pickling solution was selected for the best data collection. Copper samples with 10 cm length (H= 0.1 m) and 2 cm width, was immersed, with vertical position, for a determined time, in 1.5 l of pickling solution. The pickling flux was computed, from experimental data, with relation (20) where m_τ - $m_{\tau+\Delta\tau}$ represents the mass of copper dissolved (pickled) during time period $\Delta\tau$.

$$N_{Cu,ex} = \frac{m_\tau - m_{\tau+\Delta\tau}}{S\Delta\tau} \tag{20}$$

3. Results and discussion

The chemical reactions occurring at copper pickling surface, when it uses acid persulfate solution as pickling media, are given by equations (21)- (22). The presence of sulfuric acid in pickling media prevents the decomposition of Caro acid, so that it is active only for the reaction with copper.

$$(NH_4)_2S_2O_8 + H_2O = H_2SO_5 + (NH_4)_2SO_4 \tag{21}$$

$$H_2SO_5 + Cu = CuSO_4 + H_2O \tag{22}$$

It observes that copper sulphate is the species whose diffusion controls the pickling flow. From literature data, the diffusion coefficient of Cu^{+2} (so the Cu_2SO_4 diffusion coefficient) in 0.1 M $CuSO_4$/0.2-0.8 M H_2SO_4 electrolyte, was found to be 5.23 10^{-10} m^2/sec, at 25 ^{0}C [5]. This value was accepted in our model. For each pickling solution the viscosity was experimentally established. Table 1 contains experimental conditions and measured pickling flow rate. In the same table are reported the measured cinematic viscosity of pickling solutions and the copper sulphate diffusion coefficient obtained by correction upon temperature of the above-mentioned value. The last column from table 1 contains computed values for constant <c> of relation (19).

Table 1

Experimental copper pickling flux and computed values of *c* constant (19)

Nc	t ^{0}C	c_{aps} g/l	c_{as} g/l	$N_{Cu,ex}$ kg/m^{2}s	ν m^2/s	D m^2/s	c, rel (19)
1	40	150	15	2.075 10^{-4}	6.79 10^{-7}	7.66 10^{-10}	0.039
2	40	150	7.5	1.813 10^{-4}	6.69 10^{-7}	7.81 10^{-10}	0.035
3	40	75	15	1.196 10^{-4}	6.61 10^{-7}	7.88 10^{-10}	0.045
4	40	75	7.5	1.031 10^{-4}	6.59 10^{-7}	8.02 10^{-10}	0.043
5	20	150	15	9.85210^{-5}	1.13 10^{-6}	5.05 10^{-10}	0.029
6	20	150	7.5	9.689 10^{-5}	1.11 10^{-6}	5.11 10^{-10}	0.029
7	20	75	15	6.438 10^{-5}	1.08 10^{-6}	5.22 10^{-10}	0.039

8	20	75	7.5	$5.998\ 10^{-5}$	$1.04\ 10^{-6}$	$5.29\ 10^{-10}$	0.039
9	30	112	11.2	$8.167\ 10^{-5}$	$8.07\ 10^{-7}$	$6.51\ 10^{-10}$	0.026
10	30	112	11.2	$7.987\ 10^{-5}$	$8.07\ 10^{-7}$	$6.51\ 10^{-10}$	0.025
11	30	112	11.2	$8.453\ 10^{-5}$	$8.07\ 10^{-7}$	$6.51\ 10^{-10}$	0.027

It is to specify that in computing of *c* values was considered that active species concentration in pickling solution c_{pa} is the sum of ammonium persulfate (c_{aps}) and sulphuric acid (c_{as}) concentrations. The mean value of constant c from relation (19) is 0.035, whereas their standard deviation has the value 0.0007.

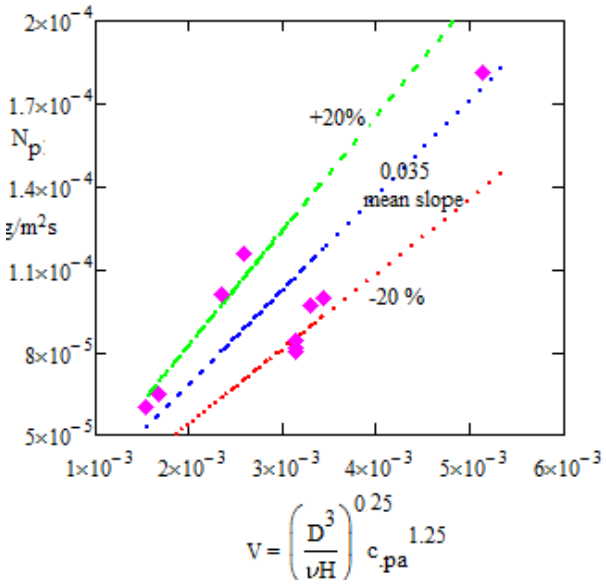

Fig. 2. Dependence of copper pickling flow rate upon term $\left(\frac{D^3}{\nu H}\right)^{0.25} c_{pa}^{1.25}$

Figure 12, where it shows the evolution of copper pickling flow rate upon the characteristic term from relation (19), find that the best value of *c* constant in this relation is 0.035. At the same time this figure cam ne considered a comparison between pickling experimental values and those according to the model with c = 0.035. With an accuracy of ± 20% we find out that the model has an acceptable answer respect to experiment data.

4. Conclusion

A mathematical model was developed in order to describe the pickling kinetics. The obtained model covers, in normal limits, the experimental data when it is

particularized to copper pickling with ammonium persulphate and sulphuric acid solutions.

References:

[1] Dustou B., Latapie L., Chauvet F., Bergerat, J.-M., Tzedakis T., *Analytical Method to Monitor Industrial Pickling Baths Initially Constituted by HF, HNO3*. Journal of Analytical Sciences, Methods and Instrumentation, 7, 116-135, 2017.
[2] Bing T., Wen Su, JiangW., Fenglian Fu, Guojun Yu, Jianyian Zh., *Minimizing the creation of spent pickling liquiors in a pickling process with high concentration hydrochloric acid solutions: Mechanismand evaluation method*, Journal of Environmental Management,98, 147-154, 2012.
[3] Alireza Bahdori, *Surface Preparation for Coating, Painting, and Lining (Chapter 1)* in Alireza Bahdori Essentials for Coating, Painting nd Lining for the Oil,Gas and Petrochemical Industriers, Elsevier, 2015.
[4] Dobre T., Floarea O., *Engineering Elements of Chemical Surfaces Processing, Chapter 3,* Matrix Rom, Bucharest, 1998.
[5] Milora Carmen, Henrickson F.G.,Hahn C. W., *Diffusion Coefficients and Kinetic Parameters in Copper Sulfate Electrolytes and in Copper Fluoborate Electrolytes Containing Organic Addition Agents*, J. Electrochem. Soc.: Electrochem. Sci. and Techn., 120, 4, 488-492, 1973.

OBTAINING ACTIVATED CHARCOAL SUPPORT STARTING FROM VEGETAL WASTES

Andreea COZEA[1], Elena BUCUR[1], Mihaela NEAGU[2], Tănase DOBRE[3], Mariana POPESCU* [1,4]

[1] *National Research and Development Institute for Industrial Ecology ECOIND, 71-73 Drumul Podul Dambovitei Street, code 060652, Bucharest, Romania*
[2] *S.C. HOFIGAL EXPORT-IMPORT S.A., Str. Intr. Serelor, no.2, 042124, Bucharest, Romania*
[3] *Chemical and Biochemical Engineering Department, University POLITEHNICA of Bucharest, 1-3 Gheorghe Polizu, 011061, Bucharest, Romania*
[4] *Titu Maiorescu University of Medicine and Pharmacy, Faculty of Pharmacy, 22 Dambovnicului Str., 040441, Bucharest, Romania*

Abstract

The purpose of this paper was to use and add value of some vegetal cellulosic wastes, rich in carbon, useful raw material for obtaining the active charcoal. The modern techniques of investigation, promoted by scientists and supported by studies, sustain the development of new useful products as filler for air filters. This plant wastes were from Hyppophae rhammnoides, Ribes nigrum, Aloe arborescens. Sprigs and cakes, remaining after plant exploit, were pyrolyzed and turned into charcoal to be used on air filters, as support for fixing noxious compounds. To achieve experimental investigation "The pyrolysis in fixed flow" was applied using plant material samples. The experimental pyrolytic system used was a modern one, and mass loss of the layer of pyrolytic oil accumulation and temperature field in different areas of the facility were online monitored. The plant material and charcoal obtained in that study were analyzed morphologically and structurally, by fast laboratory techniques: Scanning Electronic Microscopy (SEM) and Fourier Transform Infrared Spectroscopy (FT-IR). As a result of the production of activated charcoal from plant material wastes and considering its morphological and structural analysis, the following conclusion can be mentioned: FT-IR spectra obtained from plant wastes material prior to the pyrolysis process, reveal large amounts of cellulose, hemicellulose and lignin, and the presence of specific oils especially for Hyppophae rhammnoides wastes compared with the others wastes. From the SEM images, the porosity of the active charcoal was obtained. The wastes ware carbonized at high temperatures in the presence of vapors, forming internal porous structure with variable particle diameters between 10 and 120 μm. This charcoal has good features to be used to make filling for air filters.

Key words: vegetal cellulosic wastes, active charcoal, Scanning Electronic Microscopy, Infrared Spectroscopy

*Corresponding author: mari.popescu@yahoo.com

1. Introduction

Vegetal cellulosic wastes resulting from food supplements industry after a selection process can be exploited by their use after a pyrolysis process, producing charcoal, with multiple beneficial properties.

The resulting product is called activated charcoal or is also known as "carbo activatus" or adsorbent coal and is a type of amorphous carbon obtained by the strong distillation of some cellulosic materials [1].

This study brings in the foreground the necessity of reuse plant residues in a proper and efficient way and sustains the development of new useful products as filler for air filters.

It was demonstrated that activated charcoal has special properties that allow it to remove volatile organic compounds (VOCs), odours, and other gaseous pollutants from the air. It was accomplishing this in a way that is different from other air purifiers like HEPA that only maintain just particles from the air. Carbon air filters trap gas molecules on a bed of charcoal by adsorption. By this way the pollutants are fixed inside the structure itself, which acts as support for noxious compounds, dangerous for human health. This results in cleaner, fresher smell air [2].

For this purpose, we have developed a new type of charcoal and, after obtaining it, we have characterized the resulting products. Further testing methods needs to be performed before all the reported applications and benefits of activated charcoal to be applied [3].

2. Materials and methods

The plant material consisted of *Hyppophae rhammnoides, Ribes nigrum* - sprigs and *Aloe arborescens* cakes.

Experimental equipment

For the experimental study, we have used fixed-layer pyrolysis equipment using carbon dioxide as entraining gas. The experimental pyrolysis equipment used for this purpose has been described in a previous researche study [4]. The experimental laboratory pyrolysys system is conducted by a software working program, which allows the determination of the global activation energy of the pyrolytic process. The primary data processing software allows the elevation of all pyrolysis curves, as: the total mass dynamics, pyrolytic oil mass dynamics, and temperature dynamics.

a) SEM characterization was performed with a Vega Tescan LMU II equipment, with a tungsten filament. For SEM analyses, the analyzed samples

were captured in the double-sided carbon band (which assures the conductivity of the sample), and then were mixed with nitrogen sulphate [5].

b) IR spectra of the solids were obtained by using a prestigious FT-IR spectrometer (Shimadzu, Japan) with the range of 500-4000 cm^{-1}. For IR spectra the KBr powder (IR grade) was used which was mixed with the sample to obtain a transparent lozenge. Approximately 50 mg of the sample (charcoal) was mixed with 200 mg vacuum-dried IR grade KBr and pressed at a pressure of 8 t.

3. Results and discussions

For pyrolytic process, initially the column was weighed, then the column was loaded with the vegetal material and weighed it again, the thermal regime was fixed (800°C), and get start monitoring program for pyrolysis process [6].

The chemical reactions and their reporting to the main reactant (cellulose, hemicellulose and lignin) as well as the conditions of their unfolding (heterogeneous high temperature reactions) do not allow for an exhaustive investigation of each kinetic process. As a result, the pyrolysis process was analyzed using the formal kinetics applied to some kinetic schemes. The decomposition of the plant material took place through three parallel reactions that led to three global products: gases, liquid (tar) and solid (charcoal). The separation of the pyrolytic oil from the gases results from the reactor by gas-liquid interphase contact, was done by spraying cold pyrolytic oil into the gas (quench system) [6].

Depending on the degree of crushing of the vegetal material, three sizes of active charcoal pellets were obtained: 12x40, 8x30, 10x20 (U.S. Mesh).

3.1. SEM and FT-IR characterization of the active charcoal obtained

From the SEM images, it was possible to estimate the active carbon porosity as well as adsorption surface of active carbon. Activated carbon has a high specific surface area and superior adsorption characteristics, obtained only with a special gasification process [5].

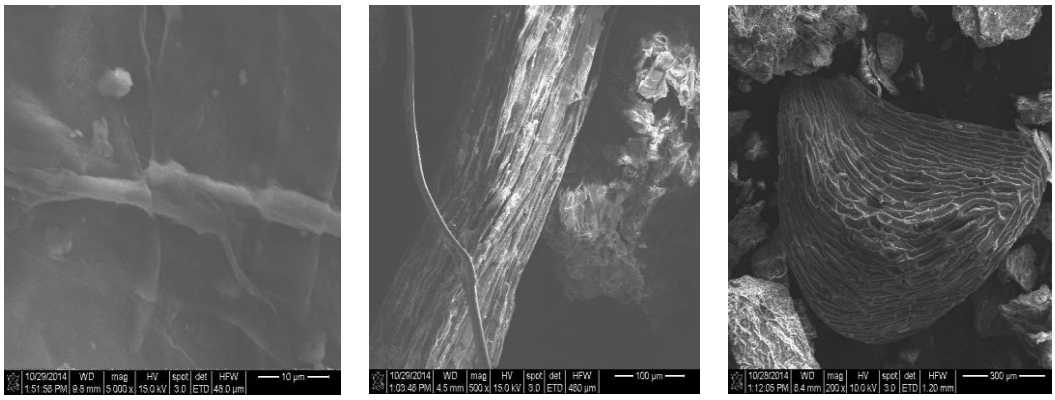

a) b) c)

Fig. 1 – SEM images of charcol types obtained from
a) *Hyppophae rhammnoides*, b) *Ribes nigrum* and c) *Aloe arborescens*

From the SEM images (Fig. 1), the porosity of the active carchoal could be observed. The wastes carbonized at high temperatures, were forming internal porous structure with variable particle diameters between 10 and 120 μm. Active charcoal made from *Hyppophae rhammnoides* - sprigs has a small pore size - 10 μm and has a high specific surface area and superior adsorption characteristics compared to other charcoal types that have a larger pore size (100-120 μm) and nonhomogeneous dispersion in the case of *Aloe arborescens* charcoal.

Analysis of the active carbon sample composition was performed using the IR Spectrum shown in Fig. 2.

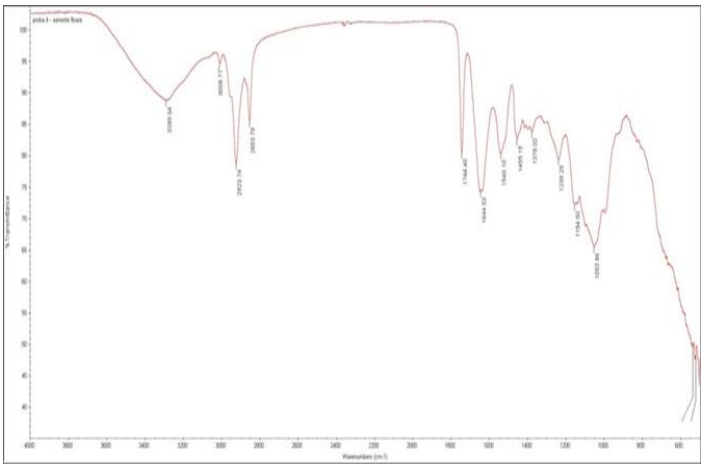

Fig. 2. IR spectrum for micrometric powder with active charcoal obtained

The obtained FT-IR spectrum reveals the absence of cellulose, hemicellulose and lignin from the samples and the presence of C in the main quantity, demonstrating that the pyrolysis process has been complete. Also, one can observe the presence of some residual oils (esters) and water less than 1% in all charcoal types.

6. **Conclusions**

The waste plant material selected for this study: *Hyppophae rhammnoides*, *Ribes nigrum* - sprigs and *Aloe arborescens* cakes, has been utilized after a pyrolysis processes for obtaining activated charcoal. The charcoal has been structurally and morphologically analyzed by various laboratory techniques: scanning electron microscopy (SEM) and infrared spectroscopy (FT-IR).

By electronic scanning microscopy (SEM), the shape and size of the charcoal pores were observed, confirming the possibility to have a good adsorbent material.

It is known that micropores and mesopores are the most efficient in the adsorption phenomenon. For the obtained material these pores represent 80-90 % in the case of *Hyppophae rhammnoides* charcoal and 70 % for *Ribes nigrum* and *Aloe arborescens* charcoal.

Thus, the following aspects could be underlined:

-the pores are placed in connected layers with pore sizes around 10 μm for *Hyppophae rhammnoides* charcoal and 120 μm for *Aloe arborescens* charcoal;

-differences between active charcoals obtained were the dimensions and the distribution of pores (uniformity) and shape (cylindrical or lamellar).

Due to the structure, the surface area of all the voids, can reach 800 m^2/g for *Aloe* charcoal, 1200 m^2/g for *Ribes* charcoal and 1300 m^2/g for *Hyppophae*, which means good surface area values. It is well known that activated charcoals with large surface adsorption present also good adsorption properties.

So, active charcoal resulting from *Hyppophae rhammnoides*-sprigs, after the pyrolysis process, followed by charcoal activation technology, presents an excellent development of pores in terms of temperature and activation time and a good ultramicroporosity. All these aspects entitle us to state that this charcoal has good features to be used as filling for air filters.

REFERENCES

[1] Cozea A., Gruia, R., Neagu, M., *Applications of popular medicine in the actual context of scientific knowledge and health care*, 3 rd North and East European NEEFood Congress on Food „Global and local Challenges in Food Science and Technology, Brasov, Romania, 20 to 23 May 2015, BTN 18 - p.39, 2015.

[2] Bucur, E., Danet, A.F., *Particulate matter and polycyclic aromatic hydrocarbon air pollution in areas of Bucharest with heavy road traffic*. Rev. Chim. 67(4):621-625, 2016.
[3] Alkhatib, A. J., Zailaey, K. A., *Medical and environmental applications of activated charcoal*. European Scientific Journal January edition vol.11, No.3 ISSN: 1857 – 7881 2015.
[4] Dobre T., Parvulescu O.C., Ramos Rodriguez I., Ceatra L., Stroescu, M., Stoica A., Mirea R., *Global Reaction Kinetics and Enthalpy in Slow Pyrolysis of Vegetal Materials*. Rev. Chim., 63(1), 54-59, 2012.
[5] Innes, R.W., Fryer, J.R., Stoeckli, H.F., *On the correlation between micropore distribution obtained from molecular probes and from high resolution electron microscopy.* Carbon, 27, 71–76, 1989.
[6] Yang Juan and Qiu Ke-qiang *Preparation of Activated Carbon by Chemical Activation under Vacuum Environ*. Sci. Technol., 43 (9), pp 3385–3390, 2009
[7] Helbig, W. A., *Activated carbon* J. Chem. Educ., 1942, 19 (4), p 194 DOI: 10.1021/ed019p194, 1942.